

Electronic Supplementary Material (ESI) for Chemical Science.
This journal is © The Royal Society of Chemistry 2018

Supplementary Information

Comparative Genome Mining and Heterologous Expression of an Orphan NRPS Gene Cluster Directs the Production of Ashimides

Jing Shi,^[a] Ying Jie Zeng,^[a] Bo Zhang,^[a] Fen Li Shao,^[a] Yan Chi Chen,^[a] Xiang Xu,^[a] Yang Sun,^[a] Qiang Xu,^[a] Ren Xiang Tan^{*(a,b)} and Hui Ming Ge^{*[a]}

Table of Contents

Experimental procedures:

General experimental procedures.

Strain isolation and identification.

Construction of cosmid library.

Heterologous Expression and HPLC detection.

Fermentation and extraction.

Isolation and structure elucidation of metabolites from *S.lividans* SBT18/pHG4001 and mutant strains.

Crystal data for ashimide A (**1**)

Construction of in-frame deletion in cosmid pHG4001.

Stable isotope labeling experiment.

Adenylation activities of A domains.

Chemical synthesis of compound **11**.

Chemical synthesis of compound **12**.

Chemical synthesis of compound **13**.

Chemical synthesis of compound **15**.

Chemical synthesis of compound **16**.

Chemical complementation of compound **10** into $\Delta asmH$ mutant, $\Delta asmJ$ mutant and $\Delta asmR$ mutant.

Chemical complementation of compound **11-14** into $\Delta asmO$ mutant and $\Delta asmP$ mutant.

Chemical complementation of compounds **17-18** into $\Delta asmS$ mutant.

Protein Expression and Purification.

In vitro assay of AsmD.

In vitro assay of AsmI.

Cytotoxicity assay.

Apoptosis analysis.

Supplementary tables:

Table S1. Bacterial plasmids and strains.

Table S2. Primers used in this study.

Table S3. Deduced functions of ORFs in the *asm* gene cluster.

Table S4. ^1H NMR (600 MHz) and ^{13}C NMR (150 MHz) data of **1** in DMSO- d_6 .

Table S5. ^1H NMR (600 MHz) and ^{13}C NMR (150 MHz) data of **2** in DMSO- d_6 .

Table S6. ^1H NMR (600 MHz) and ^{13}C NMR (150 MHz) data of **3** in DMSO- d_6 .

Table S7. ^1H NMR (600 MHz) and ^{13}C NMR (150 MHz) data of **4** in DMSO- d_6 .

Table S8. ^1H NMR (600 MHz) and ^{13}C NMR (150 MHz) data of **5** in DMSO- d_6 .

Table S9. ^1H NMR (600 MHz) and ^{13}C NMR (150 MHz) data of **6** in DMSO- d_6 .

Table S10. ^1H NMR (600 MHz) and ^{13}C NMR (150 MHz) data of **7** in DMSO- d_6 .

Table S11. ^1H NMR (600 MHz) and ^{13}C NMR (150 MHz) data of **8** in DMSO- d_6 .

Table S12. ^1H NMR (600 MHz) and ^{13}C NMR (150 MHz) data of **9** in DMSO- d_6 .

Table S13. ^1H NMR (600 MHz) and ^{13}C NMR (150 MHz) data of **10** in DMSO- d_6 .

Table S14. ^1H NMR (400 MHz) data of **11-13** in D_2O .

Table S15. ^1H NMR (600 MHz) and ^{13}C NMR (150 MHz) data of **15** in D_2O .

Table S16. ^1H NMR (400 MHz) and ^{13}C NMR (100 MHz) data of **16** in D_2O .

Table S17. ^1H NMR (600 MHz) and ^{13}C NMR (150 MHz) data of **17** in DMSO- d_6 .

Table S18. ^1H NMR (600 MHz) and ^{13}C NMR (150 MHz) data of **18** in DMSO- d_6 .

Table S19. ^1H NMR (600 MHz) and ^{13}C NMR (150 MHz) data of **19** in DMSO- d_6 .

Table S20. Substrate specificity predictions for the adenylation domains of the NRPSs encoded in the *asm* gene cluster.

Supplementary figures:

Figure S1. Verification of cosmid pHG4001.

Figure S2. HR-ESIMS spectrum of **2**.

Figure S3. Structures of compounds **1-10** and **17-19**.

Figure S4. X-ray crystal structure of **1**.

Figure S5. Comparison of ECD spectrum of **1** and **2**.

Figure S6. Apoptosis of MCF-7 cell was detected through flow cytometry after treated with different concentration of compound **2** contrasted with DMSO.

Figure S7. Construction of in-frame deletion in cosmid pHG4001.

Figure S8. HPLC contour plot of metabolic extracts.

Figure S9. Chemical complementation of compounds into mutants.

Figure S10. SDS-PAGE analysis of proteins.

Figure S11. ^1H - ^{15}N HMBC correlations of **2** feeding with ^{15}N -alanine.

Figure S12. Pathway of L-serine to phosphoenolpyruvic acid (PEP) and the pathway of chorismic acid to **10**.

Figure S13. HRESIMS spectrum of **20**.

Figure S14. HRESIMS spectrum of **21**.

Figure S15. Pseudo-first order kinetic studies of AsmI toward the formation of **1** from **17**.

Figure S16. Pseudo-first order kinetic studies of AsmI toward the formation of **2** from **18**.

Figure S17. *In vitro* assays of AsmI using **10** as substrate.

Figure S18-S23. 1D and 2D NMR spectrum of **1** in DMSO-*d*₆.

Figure S24-S30. 1D and 2D NMR spectrum of **2** in DMSO-*d*₆.

Figure S31-S36. 1D and 2D NMR spectrum of **3** in DMSO-*d*₆.

Figure S37-S42. 1D and 2D NMR spectrum of **4** in DMSO-*d*₆.

Figure S43-S48. 1D and 2D NMR spectrum of **5** in DMSO-*d*₆.

Figure S49-S54. 1D and 2D NMR spectrum of **6** in DMSO-*d*₆.

Figure S55-S60. 1D and 2D NMR spectrum of **7** in DMSO-*d*₆.

Figure S61-S66. 1D and 2D NMR spectrum of **8** in DMSO-*d*₆.

Figure S67-S72. 1D and 2D NMR spectrum of **9** in DMSO-*d*₆.

Figure S73-S78. 1D and 2D NMR spectrum of **10** in DMSO-*d*₆.

Figure S79. ¹H NMR spectrum of **12** in D₂O at 400 MHz.

Figure S80. ¹H NMR spectrum of **13** in D₂O at 400 MHz.

Figure S81. ¹H NMR spectrum of **15** in D₂O at 400 MHz.

Figure S82. ¹³C NMR spectrum of **15** in D₂O at 400 MHz.

Figure S83. ¹H NMR spectrum of **16** in D₂O at 400 MHz.

Figure S84. ¹³C NMR spectrum of **16** in D₂O at 400 MHz.

Figure S85-S90. 1D and 2D NMR spectrum of **17** in DMSO-*d*₆.

Figure S91-S97. 1D and 2D NMR spectrum of **18** in DMSO-*d*₆.

Figure S98-S103. 1D and 2D NMR spectrum of **19** in DMSO-*d*₆.

References

Experimental Procedures

General experimental procedures.

All NMR spectra were collected on a Bruker Avance 600 at 600 MHz for ^1H and 150 MHz for ^{13}C nuclei. HRESIMS data were performed on an Agilent 6530 TOF LC/MS mass spectrometer. X-ray single crystal diffraction data were collected on a Bruker APEX-II CCD diffractometer. UV absorbance was measured on a Nanodrop 2000c spectrometer with a 10 mm cuvette. CD spectra were collected on a Jasco J-710 circular dichroism spectropolarimeter. The semipreparative RP-HPLC was performed on an Agilent 1200 HPLC with an Agilent Eclipse XDB-C18 column (5 μ , 250 \times 9.4 mm). Sephadex LH-20 was purchased from GE Biotechnology. All chemicals used in the study were of analytical grade.

Strain isolation and identification.

Strain NA03103 was isolated from root sample collected in a mangrove forest of Hainan province, China. 16S rDNA gene was amplified with general primers [27F and 1492R] by using standard DNA extraction and PCR protocols. A BLAST (<http://blast.ncbi.nlm.nih.gov>) search of the partial 16S rRNA sequenced revealed 100% identity match with a *Streptomyces* sp. BCG23 strain (gene accession number KJ018714.1).

Construction of cosmid library.

The cosmid library of *S. sp.* NA03103 was constructed using an established protocol.¹ For the generation of a cosmid library, high quality chromosomal DNA (>150 kb) was isolated by salting-out procedure and partially digested with *Mbo*I, dephosphorylated with Alkaline Phosphatase (Thermo), and size-fractionated in low-melting temperature agarose by using pulsed-field gel electrophoresis (PFGE). The chromosome DNA fragments around 40 kb were recovered from the low-melting agarose gel that was digested by *b*-agarase (New England Biolabs). The recovered DNA was ligated with linearized cosmid vector pJTU2554 in a 1:1 molar ratio. After an overnight ligation at 16 $^{\circ}\text{C}$, the mixture was packaged using MaxPlax™ Lambda Packaging Extracts and transfected into *E. coli* EPI300 cell. The apramycin resistant colonies were picked individually and inoculated in LB (100 μL) that was supplied with apramycin in each well of 96-well plates. These plates were grown at 37 $^{\circ}\text{C}$ for 20 h, and then 50% glycerol (100 μL) was added into each well for storage at -80 $^{\circ}\text{C}$. Finally, The cosmid library of *Streptomyces* sp. NA3103 consisted of 5, 376 colonies with an average insert size of 40 kb.

Heterologous Expression and HPLC detection.

The cosmid pHG4001 was transferred into the *E. coli*/ET12567 (pUZ8002) strain, and further introduced into *S. lividans* SBT18 by conjugation.² The recombinant strain was grown on ISP4 agar medium supplemented with 50 $\mu\text{g}/\text{mL}$ of apramycin for sporulation. The seed culture was prepared by inoculating fresh spores into 250-mL baffled flasks containing 50 mL of TSB medium (17.0 g tryptone, 3.0 g soytone, 2.5 g glucose, 5.0 g sodium chloride, 2.5 g Na_2HPO_4 in 1 L water, pH7.0) for 2 days at 28 $^{\circ}\text{C}$ and 250 rpm. Subsequently, 20 mL seed cultures were inoculated into 1 L baffled flasks containing 400 mL of the fermentation medium (10 g soluble starch, 4 g yeast extract, 2 g peptone, 1 g CaCO_3 , 40 mg $\text{Fe}_2(\text{SO}_4)_3$, 0.1 g KBr, 27 g sea salt in 1 L water), and incubated for 10 days at 160 rpm and 28 $^{\circ}\text{C}$. Finally, the fermentation broth was filtered and absorbed with XAD-16 resin. The resin was washed with water and eluted with methanol. The afforded methanol extract was directly used for HPLC analysis. Each sample (10 μL) was injected into the column and first eluted with a linear gradient of 10% methanol to 90% methanol in water for 13 min, and finally with 100% methanol for 3 min at a flow rate of 0.5 mL/min.

Fermentation and extraction.

A fresh spore solution of *S. lividans* SBT18/pHG4001 was inoculated into 1-L flasks containing 200 mL of TSB medium. After growing at 28 $^{\circ}\text{C}$ and 160 rpm for 2 days, 20 mL of seed culture were transferred to 50 flasks each containing 200 mL of fermentation medium (10 g soluble starch, 4 g yeast extract, 2 g peptone, 1 g CaCO_3 , 40 mg $\text{Fe}_2(\text{SO}_4)_3$, 0.1 g KBr, 27 g sea salt in 1 L water, pH 7.0) and incubated at 28 $^{\circ}\text{C}$ on rotary shakers (160 rpm) for 10 days. Then, XAD-16 resin (600 g) was added to the fermentation broth. The resin and cell mass were filtered and washed with water, and eluted with methanol (2 L). The methanol extracts were concentrated under reduced pressure to afford 8.3 g crude extract.

The procedure for large scale fermentation (5 L) and extraction of the mutant ΔasmI strain is similar to that described in *S. lividans* SBT18/pHG4001 strain, which led to afford 0.9 g crude extract.

Isolation and structure elucidation of metabolites from *S. lividans* SBT18/ pHG4001 and mutants.

The 8.3 g crude extract was loaded on a silica-gel (200 g) column, and eluted with $\text{CH}_2\text{Cl}_2/\text{MeOH}$ (100:0, 100:2, 100:4, 100:8, 100:16, 100:32, 50:50) to give 7 fractions (A1-A7). Fractions A2 and A3 were further separated by a Sephadex LH-20 chromatography and fractionated using $\text{MeOH}/\text{H}_2\text{O}$ (1:1) to give subfractions A2.1–A2.6 and A3.1–A3.7, respectively. Subfractions A2.2 were purified by semipreparative HPLC eluted with 30% MeOH in H_2O at a flow rate of 2 mL/min to afford **1** (20 mg) and **2** (25 mg). Subfractions A2.3 were separated using semipreparative HPLC eluted with 40% MeCN in H_2O to afford **3** (2.1 mg), **6** (1.8 mg), and **7** (0.8 mg). Subfractions A3.3 was purified using semipreparative HPLC eluted with $\text{MeCN}-\text{H}_2\text{O}$ (gradient elution in 25 min from 15% MeCN to 30% MeCN with a flow rate 2.0 mL/min) to afford **4** (1.1 mg), **5** (2.1 mg), and **8** (1.7 mg). Compound **9** (1.6 mg) was purified from subfraction A3.4 using semipreparative HPLC eluted with 60% MeOH at a flow rate of 2 mL/min.

The 0.9 g crude extract obtained from ΔasmI strain was loaded on a silica-gel (30 g), and eluted with $\text{CH}_2\text{Cl}_2/\text{MeOH}$ (100:0, 100:2, 100:4, 100:8, 100:16, 100:32, 50:50) to give 6 fractions (B1-B6). The fraction B2 was further fractionated by a Sephadex LH-20 chromatography and fractionated using MeOH to give subfractions B2.1–B2.5. Subfraction B2.2 were separated using semipreparative HPLC eluted with a gradient MeCN in H_2O (from 15% MeCN to 50% MeCN in 30 min with a flow rate 2.0 mL/min) to afford **17** (5.1 mg), **18** (6.6 mg), and **19** (4.0 mg).

Compound **1**: pale yellow crystal; NMR data see Table S4; HRESIMS m/z 465.1260 $[\text{M}+\text{H}]^+$ (calcd for $\text{C}_{19}\text{H}_{20}\text{N}_4\text{O}_{10}$, 465.1252); UV (MeOH): λ_{max} ($\log \epsilon$) = 253 (3.16), 310 nm (2.81).

Compound 2: yellowish oil; NMR data see Table S5; HRESIMS m/z 483.0919 [M+H]⁺ (calcd for C₁₉H₁₉ClN₄O₉, 483.0913); UV (MeOH): λ_{\max} (log ϵ) =253 (2.97), 310 nm (2.62).

Compound 3: yellowish oil; NMR data see Table S6; HRESIMS m/z 453.0812 [M+H]⁺ (calcd for C₁₈H₁₇ClN₄O₈, 453.0808); UV (MeOH): λ_{\max} (log ϵ) =253 (3.06), 314 nm (2.72).

Compound 4: yellowish oil; NMR data see Table S7; HRESIMS m/z 471.0909 [M+H]⁺ (calcd for C₁₈H₁₉ClN₄O₉, 471.0913); UV (MeOH): λ_{\max} (log ϵ) =253 (3.12), 314 nm (2.89).

Compound 5: yellowish oil; NMR data see Table S8; HRESIMS m/z 501.1024 [M+H]⁺ (calcd for C₁₉H₂₁ClN₄O₁₀, 501.1019); UV (MeOH): λ_{\max} (log ϵ) =253 (3.22), 310 nm (3.20).

Compound 6: yellowish oil; NMR data see Table S9; HRESIMS m/z 350.0948 [M+H]⁺ (calcd for C₁₅H₁₅N₃O₇, 350.0943); UV (MeOH): λ_{\max} (log ϵ) =253 (2.24), 310 nm (3.06).

Compound 7: yellowish oil; NMR data see Table S10; HRESIMS m/z 425.0863 [M+H]⁺ (calcd for C₁₇H₁₇ClN₄O₇, 425.0858); UV (MeOH): λ_{\max} (log ϵ) =253 (2.89), 320 nm (2.98).

Compound 8: yellowish oil; NMR data see Table S11; HRESIMS m/z 240.0507 [M+H]⁺ (calcd for C₁₀H₉NO₆, 240.0503); UV (MeOH): λ_{\max} (log ϵ) =253 (2.71), 310 nm (3.16).

Compound 9: yellowish oil; NMR data see Table S12; HRESIMS m/z 254.0653 [M+H]⁺ (calcd for C₁₁H₁₁NO₆, 254.0659); UV (MeOH): λ_{\max} (log ϵ) =253 (2.91), 310 nm (3.07).

Compound 10: yellowish oil; NMR data see Table S13; HRESIMS m/z 206.0453 [M+H]⁺ (calcd for C₁₀H₇NO₄, 206.0448); UV (MeOH): λ_{\max} (log ϵ) =288 (2.76), 360 nm (3.17).

Compound 17: white powder; NMR data see Table S17; HRESIMS m/z 431.1204 [M+H]⁺ (calcd for C₁₉H₁₈N₄O₈, 431.1197); UV (MeOH): λ_{\max} (log ϵ) =288 (2.88), 360 nm (2.92).

Compound 18: white powder; NMR data see Table S18; HRESIMS m/z 449.0853 [M+H]⁺ (calcd for C₁₉H₁₇ClN₄O₇, 449.0859); UV (MeOH): λ_{\max} (log ϵ) =288 (2.97), 360 nm (3.06).

Compound 19: white powder; NMR data see Table S19; HRESIMS m/z 453.0959 [M+H]⁺ (calcd for C₁₉H₁₉ClN₄O₈, 467.0964); UV (MeOH): λ_{\max} (log ϵ) =288 (2.79), 360 nm (3.05).

Crystal data for ashimide A (1)

C₁₉H₂₀N₄O₁₀ + 2H₂O (M =500.42 g/mol), monoclinic, space group P 21 21 21 (no. 19), a = 6.9557(8) Å, b = 7.4897(8) Å, c = 41.571(5) Å, β = 90°, V = 2165.7(4) Å³, Z = 4, T = 153 K, μ (Cu K α) = 1.120 mm⁻¹, D_{calc} = 1.535 g/cm³, F(000) = 1048; 10157 reflections measured (6° ≤ θ ≤ 68.4°), 3968 unique (R_{int} = 0.0468, R_{sigma} = 0.0412) which were used in all calculations. The final R₁ was 0.0412 (I > 2 σ (I)) and wR₂ was 0.0923 (all data); The crystallographic data have been deposited in the Cambridge Crystallographic Data Centre as CCDC1861590.

Construction of in-frame deletion in cosmid pHG4001.

The gene inactivation was performed by two temperature-sensitive plasmid pKOV-Kan and pDF25 to generate the in-frame deletion mutants as previously described.³ Briefly, the up- and downstream homologous arms were amplified with primers upF/R and downF/R listed in Table S2 using genomic DNA as template. The purified PCR products were ligated to *Bam*HI linearized pKOV-Kan to generate mutation carrying plasmids (pHG4002–pHG4015). The individual plasmid (pHG4002–pHG4015) carrying mutation were transformed into *E. Coli* DH10B competent cells containing pDF25 (chloramphenicol resistant) and grown on the LB agar medium supplemented with Chl, Kan and Apr at 30 °C over night. Several colonies were picked and streaked onto LB agar medium containing all three antibiotic as mentioned above and cultured at 43 °C over night for selection of single cross-over clones. The genotypes of these candidate clones were confirmed by PCR (primers listed in Table S2). The correct single cross over cosmids were isolated, re-transformed into pDF25 competent cells and grown at 30 °C with Chl, Kan, and Apr for double cross-over homologous recombination. The transformants were subjected to liquid LB supplemented with Apr and allowed to resolve at 43 °C for 24 h to eliminate the pDF25 and pKOV-Kan. The cell suspension was diluted at different concentrations and spread on LB agar medium plate supplemented with Apr and sucrose, and incubated at 30 °C for 24 h. Colonies were picked and re-streaked on LB agar medium plate supplemented with Apr and sucrose, and allowed to grow at 30 °C overnight. Colonies that grew on medium with Apr and sucrose were analyzed by PCR (primers listed in Table S2). The genotype of mutated cosmid were confirmed by PCR and DNA sequencing (Table S2 and Figure S3). The afforded mutated cosmid were transformed into *S. lividans* SBT18 through conjugation as mentioned above. The resulting mutant strains were used for further fermentation.

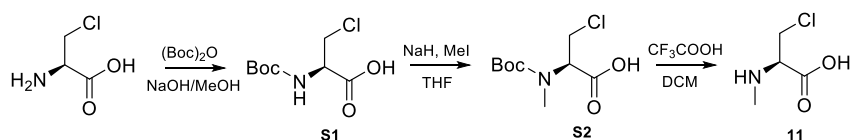
Stable isotope labeling experiment

L-alanine (¹⁵N), glycine-¹⁵N, L-serine-3-¹³C, L-alanine-2,3,3,3-D₄ were purchased from Sigma-aldrich. L-alanine-¹⁵N (400 mg total) was added to 5 × 400 ml cultures, yielding 0.2 mg ashimide B (2) for N-H HMBC analysis. Glycine-¹⁵N (100 mg total), L-serine-3-¹³C (100 mg total) and L-alanine-2,3,3,3-D₄ (100 mg total) were added to 400 ml cultures individually and the cultures were harvested after 10 days' fermentation. The metabolic extracts were used directly for LC-MS analysis.

Adenylation activities of A domain⁴

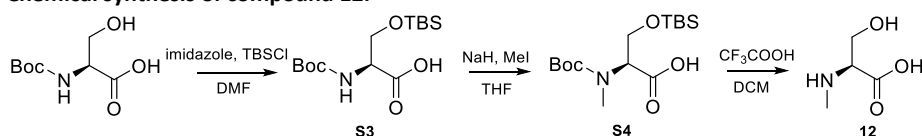
To determine the adenylation activity of A domains against different substrate, we carried out a coupled continuous assay for inorganic pyrophosphate using a unique fluorogenic pyrophosphate sensor in which the presence of pyrophosphate results in the production of a fluorescent product ($\lambda_{\text{ex}}=316$ / $\lambda_{\text{em}}=456$ nm) proportional to the pyrophosphate present (Sigma-Aldrich Pyrophosphate Assay Kit MAK 168). The A domain specificity assays were conducted in a 50 μ L reaction volume containing 50 mM Tris-HCl, pH 7.5, 60 μ M NRPS protein, 12.5 mM MgCl₂, 2.0 mM TCEP, 2 mM amino acid, 4 mM ATP. After reaction at room temperature for 30 min,^{5,6} an equal volume of the Master Reaction Mix were added to each of the sample, and the reaction was incubated for 20 minutes at room temperature. Then, the fluorescence intensity ($\lambda_{\text{ex}}=316$ / $\lambda_{\text{em}}=456$ nm) was measured by a microplate reader (TECAN infinite M200PRO).

Chemical synthesis of compound 11.



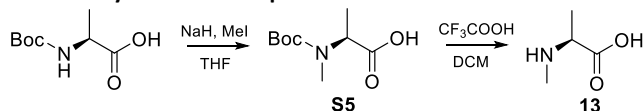
To a stirring solution of L-3-chloroalanine (1g, 8.1 mmol) in 20 mL of 1 M NaOH/MeOH (3:2) solution was added Boc_2O (3.5 g, 16.2 mmol, 2 eq.) at room temperature for 12 h.⁷ The reaction mixture was cooled to 0 °C, acidified to pH 6.0, and extracted with EtOAc (50 mL \times 3). The combined organic solvent was washed with brine, dried over Na_2SO_4 , and evaporated to dryness to afford **S1** (1.2 g), which was directly used for next reaction without purification. Then a suspension of NaH in THF at 0 °C was slowly added the solution of 400 mg **S1** (1.8 mmol) and CH_3I (0.6 g, 4.0 mmol, 2.2 eq.) sequentially. The reaction mixture was warm to room temperature and stirred for 8 h. The reaction mixture was then diluted with diethyl ether (40 mL) and quenched with water (15 mL). The layers were separated, and the aqueous layer was extracted with diethyl ether (2 \times 30 mL), acidified with 10% citric acid solution, and extracted with ethyl acetate (3 \times 60 mL). The combined organic layers were washed by saturated brine, dried over anhydrous Na_2SO_4 , and concentrated in vacuo to yield an colourless oil. The crude material was purified via column chromatography using 30% EtOAc in petroleum ether, to afford **S2** (273 mg, 65%). **S2** (273 mg, 1.2 mmol) was dissolved in a solution of DCM (4 mL) and TFA (3 mL), and stirred at room temperature for 2 h, then concentrated in vacuo to yield almost pure amino acid **11** as a trifluoroacetic acid salt (301 mg, 93%).⁸ ^1H NMR data see Table S14; HRESIMS m/z 138.0312 $[\text{M} + \text{H}]^+$, (calcd for $[\text{C}_4\text{H}_9\text{ClNO}_2]^+$ m/z , 138.0316).

Chemical synthesis of compound 12.



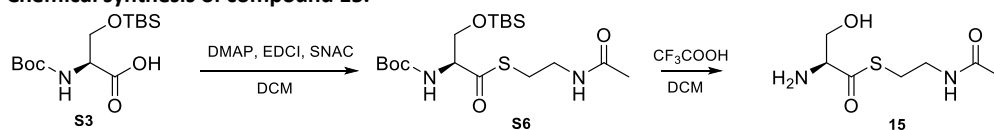
To a solution of N-(tert-butoxycarbonyl)-L-serine (1 g, 4.9 mmol) in anhydrous DMF (24 ml), 15 mmol imidazole (1 g, 14.7 mmol, 3 eq) was added at 0°C, followed by addition of TBSCl (1 g, 6.7 mmol, 1.4 eq). The mixture was warmed to room temperature slowly and stirred for 10 h. Upon total consumption of the substrate, the reaction mixture was poured into a mixture of ice cooled 1N HCl (5 ml) and ether (20 ml) to hydrolyze the silyl ester. The organic layer was separated and the aqueous layer was extracted with ether (20 mL) twice. The combined organic extracts were washed with brine, dried over anhydrous Na_2SO_4 , and concentrated in vacuo to yield the desired product **S3** (1.32g, 85%) without purification.⁹ The almost pure compound **12** (275 mg) was prepared using the method as mentioned in compound **11**. ^1H NMR data see Table S14; HRESIMS m/z 120.0651 $[\text{M} + \text{H}]^+$, (calcd for $[\text{C}_4\text{H}_{10}\text{NO}_3]^+$ m/z , 120.0655).

Chemical synthesis of compound 13.



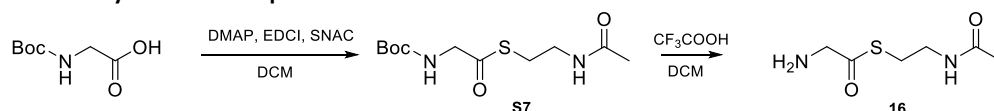
Compound **13** (245 mg) was prepared using the method as mentioned in compound **11**. ^1H NMR data see Table S14; HRESIMS m/z 104.0709 $[\text{M} + \text{H}]^+$, (calcd for $[\text{C}_4\text{H}_{10}\text{NO}_2]^+$ m/z , 104.0706).

Chemical synthesis of compound 15.¹⁰



To a solution of **S3** (50 mg, 0.16 mmol) in DCM (5 ml), EDCl (N-(3-Dimethylaminopropyl)-N'-ethylcarbodiimide hydrochloride, 33 mg; 1.1 eq), DMAP (4-Dimethylaminopyridine, 3.8 mg, 0.03 mmol, 0.2 eq) and SNAC (N-Acetylcysteamine, 21 mg, 0.18 mmol, 1.1 eq) were added at room temperature. The reaction was stirred for 12 h, and concentrated under reduced pressure. The product **S6** (51.3 mg) was purified by semi-preparative HPLC using 30 % MeCN in H_2O at a flow rate 2 mL/min to afford **S6** (56 mg). Deprotection of the Boc and TBS groups using 30% TFA in DCM at room temperature for 30 min from **S6** directly obtain compound **15** (21 mg) as an almost pure product. ^1H and ^{13}C NMR data see Table S15; HRESIMS m/z 207.2671 $[\text{M} + \text{H}]^+$, (calcd for $[\text{C}_7\text{H}_{15}\text{N}_2\text{O}_3\text{S}]^+$ m/z , 207.0798).

Chemical synthesis of compound 16.



Compound **16** (89 mg) was prepared using the same method as mentioned in **15**. ^1H and ^{13}C NMR data see Table S16; HRESIMS m/z 177.0690 $[\text{M} + \text{H}]^+$, (calcd for $[\text{C}_6\text{H}_{13}\text{N}_2\text{O}_2\text{S}]^+$ m/z , 177.0692).

Chemical complementation of compound 10 into ΔasmH mutant, ΔasmJ mutant and ΔasmR mutant.

ΔasmH mutant, ΔasmJ mutant and ΔasmR mutant were cultured in a 20 ml scale at 28°C in fermentation medium individually. After 24 hours cultivation, compound **10** (1.3 mg, 2 μmol) dissolved in DMSO was supplemented into fermentation broth and cultured for another 12 hours. After extraction by XAD-16 resin, the eluted methanol solution was then analyzed by LC-MS.

Chemical complementation of compounds 11-14 into $\Delta asmO$ mutant and $\Delta asmP$ mutant.

$\Delta asmO$ mutant and $\Delta asmP$ mutant strains were cultured in a 20 ml scale at 28°C in fermentation medium, respectively. After 24 hours cultivation, compounds **11–14** (each 5 mg) dissolved in H₂O was individually supplemented into the fermentation broth and cultivated for another 12 hours. After extraction by XAD-16 resin, the eluted methanol solution was then analyzed by LC-MS.

Chemical complementation of compounds 17–18 into $\Delta asmS$ mutant.

$\Delta asmS$ mutant strain was cultured in a 20 mL scale at 28°C in fermentation medium. After 24 hours cultivation, compounds **11–13** (each 1.5 mg) dissolved in DMSO were supplemented into fermentation broth individually and cultured for another 12 hours. The metabolic extract was then analyzed by LC-MS.

Protein Expression and Purification.

DNA fragments containing target genes including *asmD*, *asmI*, ferredoxin gene (ctg1_441) and ferredoxin reductase gene (ctg1_4885) were amplified from genomic DNA of *S. sp.* NA03103 with primers listed in Table S2. The purified PCR products were ligated with linearized pET28a (linearized by NdeI and HindIII) to afford pHG4016-pHG4019, respectively. And DNA fragments containing target genes including *asmC*, *asmM*, *asmN* and *asmS* were ligated with linearized pET22b (treated with NdeI and HindIII) to afford pHG4020-pHG4023, respectively. The obtained pHG4016-pHG4023 were further introduced into *E. coli* BL21(DE3), respectively. The transformants were cultivated in 400 mL LB medium supplemented with 50 µg/mL kanamycin (pHG4016-pHG4019) or 50 µg/mL Ampicillin (pHG4020-pHG4023) at 37 °C (220 rpm) until OD₆₀₀ value reached around 0.6. The culture was cooled to 4 °C and induced with 0.1 mM IPTG, and continued to cultivate at 16 °C (220 rpm) for 18 h. After centrifugation at 4000 rpm for 10 min, cells were resuspended in lysis buffer (100 mM Tris, pH 8.0, 15 mM imidazole, 300 mM NaCl, 10 % glycerol) and lysed on ice by sonication. After centrifugation at 15000 rpm for 30 min, the supernatant was filtered and purified by ÄKTA FPLC system equipped with a 5 mL Histrap HP column (GE lifesciences). The proteins were pooled and desalted by a PD10 column (GE Healthcare) with 100 mM phosphate buffer (pH 7.0) and 10% glycerol and stored at -80°C.

In vitro assay of AsmD.

The AsmD reaction solution (100 µL) contained 5 µM AsmD, 1mM compound **20**, 1 mM THF, 10 µM PLP, and 100 mM phosphate buffer (pH 7.5). Reaction was incubated at 30 °C for 1 h, and terminated by adding 100 µL acetonitrile. Then the mixture was centrifuged at 15,000 g for 30 min and the supernatant was analyzed by HPLC. The HPLC analysis was performed using a 18 min solvent gradient from 5% (0–10 min) and 5% to 100% (10–18 min) methanol in water supplied with 0.1 TFA at a flow rate of 0.5 mL/min.

In vitro assay of AsmI.

The AsmI-catalyzed reaction was carried out in a 100 µL reaction system containing 100 mM phosphate buffer (pH 7.0), 100 µM substrate, 5 mM NADPH, 2µM FDR, 2µM FDX and 30 µM AsmI. After incubation at 30°C for 1 h, 1.5 h, 2 h, and 3 h, the reaction was quenched by adding 100 µL methanol. The reaction mixture was then centrifuged at 15, 000 g for 10 min and the supernatant was analyzed by HPLC or LC-MS. The HPLC analysis was performed using a 18 min solvent gradient from 10% to 90% (0–15 min) and 100% (15–18min) methanol in water supplied with 0.1 TFA at a flow rate of 0.5 mL/min with a UV detection at 310 nm. The LC-MS analysis was performed using a 18 min solvent gradient from 10% to 90% (0–13 min) and 100% (13–15 min) methanol in water supplied with 0.1 TFA at a flow rate of 0.5 mL/min.

Cytotoxicity assay.

The in vitro cytotoxicity against the tested cell lines was determined using the MTT method. MCF-7 cells was seeded in 96-well plates at density of 1.5×10⁴ cells per well and different concentrations compound **2** was added into the medium after 8 h. 4 mg/mL of MTT (20 µl per well) was added to the medium at the end of culture and incubated at 37°C for 4 h. After 4 h incubation, the formazan production was dissolved by DMSO and readied absorbance at 570 nm.

Apoptosis analysis.

The apoptosis induction of compound **2** in MCF-7 was measured by FITC-labeled annexin-V/PI apoptosis detection kit according to manufacturer's instruction. Briefly, various concentrations of compound **2** was added to the medium of MCF-7 cells (1×10⁵ cells per wells in 6-well plates) and cultured for 48 h. After harvested washed with PBS, MCF-7 cells were stained with FITC-labeled annexin-V and PI diluted in binding buffer. 15 minutes later, the cells were analyzed using flow cytometry (FACScalibur, USA)

Table S1. Bacterial plasmids and strains.

Plasmid/Strain	Relevant characteristics	Source
Plasmid		
pJTU2554	Cosmid vector	Ref 11
pKOV - Kan	plasmid used for gene disruption, temperature sensitive	Ref 12
pDF25	plasmid used for gene disruption, temperature sensitive	Ref 13
pET28a(+)	Protein expression vector used in <i>E.coli</i> , encoding N-terminal His-tag, kanamycin resistance	Novagen
pET22b(+)	Protein expression vector used in <i>E.coli</i> , encoding N-terminal His-tag, Ampicillin resistance	Novagen
pHG4001	pJTU2554 harboring the intact <i>asm</i> gene cluster	This study
pHG4002	pKOV derived plasmid for disruption of <i>asmA</i>	This study
pHG4003	pKOV derived plasmid for disruption of <i>asmB</i>	This study
pHG4004	pKOV derived plasmid for disruption of <i>asmC</i>	This study
pHG4005	pKOV derived plasmid for disruption of <i>asmD</i>	This study
pHG4006	pKOV derived plasmid for disruption of <i>asmH</i>	This study
pHG4007	pKOV derived plasmid for disruption of <i>asmI</i>	This study
pHG4008	pKOV derived plasmid for disruption of <i>asmJ</i>	This study
pHG4009	pKOV derived plasmid for disruption of <i>asmK</i>	This study
pHG4010	pKOV derived plasmid for disruption of <i>asmM</i>	
pHG4011	pKOV derived plasmid for disruption of <i>asmN</i>	
pHG4012	pKOV derived plasmid for disruption of <i>asmO</i>	This study
pHG4013	pKOV derived plasmid for disruption of <i>asmP</i>	This study
pHG4014	pKOV derived plasmid for disruption of <i>asmR</i>	This study
pHG4015	pKOV derived plasmid for disruption of <i>asmS</i>	This study
pHG4016	pET28a(+) derived plasmid for expressing N-terminal His-tag AsmD	This study
pHG4017	pET28a(+) derived plasmid for expressing N-terminal His-tag AsmI	This study
pHG4018	pET28a(+) derived plasmid for expressing N-terminal His-tag Ctg1_4885	This study
pHG4019	pET28a(+) derived plasmid for expressing N-terminal His-tag Ctg1_441	This study
pHG4020	pET22b(+) derived plasmid for expressing N-terminal His-tag AsmC	This study
pHG4021	pET22b(+) derived plasmid for expressing N-terminal His-tag AsmM	This study
pHG4022	pET22b(+) derived plasmid for expressing N-terminal His-tag AsmN	This study
pHG4023	pET22b(+) derived plasmid for expressing N-terminal His-tag AsmS	This study
<i>E. coli</i> strains		
DH5 α	General cloning host	Ref 14
DH10B	General cloning host	
BL21 (DE3)	Heterologous host for protein expression	NEB
ET12567 (pUZ8002)	Methylation-deficient host used for <i>E. coli-Streptomyces</i> intergeneric conjugation	Ref 15
<i>Streptomyces</i> strains		
<i>S. lividans</i> SBT18		
NA03103	Model actinomycete used for gene heterologous expression.	Ref 16
HG04001	Wild type strain for ashimides production	This study
HG04002	Heterologous expression of cosmid 31E5 in <i>S. lividans</i> SBT18	This study
HG04003	Δ <i>asmA</i> , in-frame deletion mutant strain	This study
HG04004	Δ <i>asmB</i> , in-frame deletion mutant strain	This study
HG04005	Δ <i>asmC</i> , in-frame deletion mutant strain	This study
HG04006	Δ <i>asmD</i> , in-frame deletion mutant strain	This study
HG04007	Δ <i>asmH</i> , in-frame deletion mutant strain	This study
HG04008	Δ <i>asmI</i> , in-frame deletion mutant strain	This study
HG04009	Δ <i>asmI</i> , in-frame deletion mutant strain	This study
HG04010	Δ <i>asmJ</i> , in-frame deletion mutant strain	This study
HG04011	Δ <i>asmK</i> , in-frame deletion mutant strain	This study
HG04012	Δ <i>asmO</i> , in-frame deletion mutant strain	This study
HG04013	Δ <i>asmM</i> , in-frame deletion mutant strain	This study
HG04014	Δ <i>asmN</i> , in-frame deletion mutant strain	This study
HG04015	Δ <i>asmP</i> , in-frame deletion mutant strain	This study
HG04016	Δ <i>asmR</i> , in-frame deletion mutant strain	This study
HG04016	Δ <i>asmS</i> , in-frame deletion mutant strain	This study

Table S2. Primers used in this study.

Name	Sequence
screen-up-F	GGACAACCTGCTCACAA
screen-up-R	GGCGTTCTCGATGTGCT
screen-down-F	TGTCCTTCGGGTCGTAGAA
screen-down-R	GAGCTGGGCAAGGAGATG
asmA-up-F	CTGGCGGCCGTTACTAGTGGATCCTGGTGAGGACGGAGTTGA
asmA-up-R	ATGTACGCCGTCAGCACGCCGCTCATACTGCGCCAC
asmA-down-F	TTACACCCGAAACCCTTTACGTGATCCGGCAGGCG
asmA-down-R	TCTCCGGTCGACTCTAGAGGATCCGAGGCAAACGCCTGGTC
asmB-up-F	CTGGCGGCCGTTACTAGTGGATCCGCTCGGGATGTGAAGAAG
asmB-up-R	CGTTCTCGATGTGCTCGGGGTACCAGCCGTAGTACGG
asmB-down-F	GGGTTGCGTTACGTGATCCCTTCTACCGCGTCGACAAG
asmB-down-R	TCTCCGGTCGACTCTAGAGGATCCATGGGAGGAGGAGCGGTT
asmC-up-F	CTGGCGGCCGTTACTAGTGGATCCTGAGCCGCTGATCCAGA
asmC-up-R	TGGGAGGTCACGGTCAAGAGGCGAGCTTCTTCCAC
asmC-down-F	GTGGAAGAAGCTCGCCTTTGACCGTGACCTCCA
asmC-down-R	TCTCCGGTCGACTCTAGAGGATCCGCGTCGAGGAAGATGATGAA
asmD-up-F	CTGGCGGCCGTTACTAGTGGATCCCGGAGGTCAGGATGACGTA
asmD-up-R	GATGACGTGGACTGGGAAACGATCGGGACCAACACACTC
asmD-down-F	GAGTGTGTTGGTCCCGATCGTTTCCAGTCCACGTCATC
asmD-down-R	TCTCCGGTCGACTCTAGAGGATCCGCCGATTCCAGGGTCTTG
asmH-up-F	CTGGCGGCCGTTACTAGTGGATCCCTCATCGGTAAGGTCTCACATC
asmH-up-R	CTGGACGAGAGGAAGCCGGACCCCTTCTGAGCCTT
asmH-down-F	AAGGCTCATGAAGGGTCCGGCTTCTCTCGTCCAG
asmH-down-R	TCTCCGGTCGACTCTAGAGGATCCCTGAACAACGTCCTGCTCAAC
asmI-up-F	CTGGCGGCCGTTACTAGTGGATCCAGGCGGAGAAGGTGTTGTAGA
asmI-up-R	TCGGAACCCCTCCGACCACCCCGGACTCAGTCTCTG
asmI-down-F	CAGGACGTAGTCCGGCGGTGGTGCAGGAGGTTCCGA
asmI-down-R	TCTCCGGTCGACTCTAGAGGATCCCGGTTCCAGCCGTGTTATG
asmJ-up-F	CTGGCGGCCGTTACTAGTGGATCCAGGTTCTCGGGCATGAAGA
asmJ-up-R	ACGTACACCACGCAGCCGAGAGCACCCGGAACTCA
asmJ-down-F	TGAGTTCGCGGTGCTCTCGGGTGCCTGGTGTACGT
asmJ-down-R	TCTCCGGTCGACTCTAGAGGATCCAGCATGAACTGGCGGTTCTC
asmK-up-F	CTGGCGGCCGTTACTAGTGGATCCGATGACGGTGTCTCTCTTG
asmK-up-R	TGGAAGCAAGGTCCGCACTCCACCCACTTCTGTCT
asmK-down-F	AGACAGAAGTGGGTGGAGTGCCGACCTTGCTTTCCA
asmK-down-R	TCTCCGGTCGACTCTAGAGGATCCACCCGACGACAGGTCAA
asmM-up-F	AACGACGGCCAGTGCCAAGCTTTCATCCGGCCCGCGTCC
asmM-up-R	CCCCTGAGCCGCTGCGTGTGGTCCCGCATGACGGG
asmM-down-F	CCCGTCATGCGGGACACACGCAGCGGCTCACGGG
asmM-down-R	AGCTATGACATGATTACGAATTCGCGGAGCGTGGACC
asmN-up-F	AACGACGGCCAGTGCCAAGCTTTCGACGGTCCGGTAGTCGAG
asmN-up-R	TTCCAGGCCGGGTGGCCAGCCCGCCTGGAAG
asmN-down-F	GTGTCGGCGAGTGCTGCCAGCCCGCCTGGAAG
asmN-down-R	AGCTATGACATGATTACGAATTCGCGGGTGTGGTACGGC
asmO-up-F	CTGGCGGCCGTTACTAGTGGATCCCGACATGACCGGCAACT
asmO-up-R	TCTGCGGTGCGGTGTGGCATGGCTCCACCTCGCAC
asmO-down-F	GTGCGAGGTGGAGCCATGCCACCCGACACAGGA
asmO-down-R	TCTCCGGTCGACTCTAGAGGATCCACCCGACACAGGA
asmP-up-F	CTGGCGGCCGTTACTAGTGGATCCGTCTCGCGCCAGTAGGCCA
asmP-up-R	TTTTCGCGGAAGGGGCCCGCTCCTCTGTGGTCG
asmP-down-F	CGACCACAGGAGGAGCGCGGCCCTTCCCGCAAAA
asmP-down-R	TCTCCGGTCGACTCTAGAGGATCCGGATCAGCGGCTTACGCC
asmR-up-F	CTGGCGGCCGTTACTAGTGGATCCGACGATGCTGTCTTCTACAAC
asmR-up-R	GGCCTTCCAGCTGATCAGGCAAGGAACGTAAGGCC
asmR-down-F	GGGCCTTACGTTCTTGCCTGATCAGCTGGAAGGCC
asmR-down-R	TCTCCGGTCGACTCTAGAGGATCCGACGTTGAGCACCTGGAA
asmS-up-F	CTGGCGGCCGTTACTAGTGGATCCCGCAGTCTGAGCCTAAAT
asmS-up-R	AGCGGTAATGCATCAACTCGTGTCTCCGGGTTCCAC
asmS-down-F	GTGAACCCGGAGAGCACGAGTTGATGCAGTACCGCT
asmS-down-R	TCTCCGGTCGACTCTAGAGGATCCCACTACGTGGAGGAGTTCTT
asmA-PO-F	GGCTCGACCATTCTGTTGAT
asmA-PO-R	GCTCCAGCATCGTGTGA

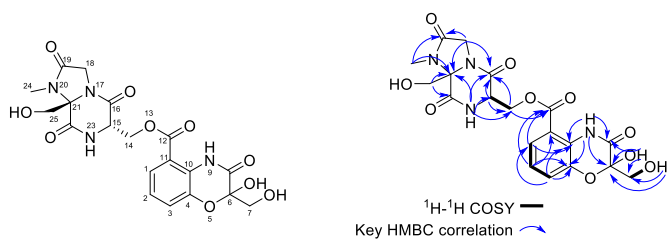
asmA-NE-F	TATGAGCGGGTGGAGAAAGTA
asmA-NE-R	GGATCACGTAACCGAACCC
asmB-PO-F	GTATGAGCGGGTGGAGAAAG
asmB-PO-R	CAGCGTGACCGTGAACA
asmB-NE-F	TCGGACGAGGACCTCAC
asmB-NE-R	TTGTCGACGCGGTAGAAAC
asmC-PO-F	CCCGAGCACATCGAGAAC
asmC-PO-R	TCAACCGGAACGTCGTG
asmC-NE-F	GGACTCCACGCACATCTC
asmC-NE-R	ACGTTCCGGCCACATGAA
asmD-PO-F	TTGACCGTGACCTCCCA
asmD-PO-R	GCAGATAGCCGTTCAACCAC
asmD-NE-F	GAGGACCATGTGGGTGTC
asmD-NE-R	ACTGGGAAACCGATGCC
asmH-PO-F	CCAGTTCACCGGTACAG
asmH-PO-R	CCACCTGTACAAGCCCTTC
asmH-NE-F	TCGTCGAGTCCATCGTCA
asmH-NE-R	CGGGTCGAACTTCGTATC
asmI-PO-F	GCGGAACAGGGTCAACTC
asmI-PO-R	ACAACCACCTGCTGAACAA
asmI-NE-F	GTGCCGAAGGGCTTGTA
asmI-NE-R	CTACAACGACGAGGAACTG
asmJ-PO-F	CACGTTTCGTTCCCTTTCT
asmJ-PO-R	ACTCCACCCACTTCTGTCT
asmJ-NE-F	CCTTCTCGTTGCCGAACA
asmJ-NE-R	CCTGAACGCTCCGAAC
asmK-PO-F	CCTTCTCGTTGCCGAACA
asmK-PO-R	GATCAGACTGCCGTAGATGC
asmK-NE-F	ACAGAAGTGGGTGGAGTG
asmK-NE-R	TGGGAAACGCCGAGATG
asmM-PO-F	CCGGAACCTCGTCGCCTTC
asmM-PO-R	CTCCTCGGCCACATCCGG
asmN-PO-F	GCCGCCACCGGTCA
asmN-PO-R	CCACGGTGGGAGGCCCC
asmO-PO-F	CGGTTCATCGACTCCAACAG
asmO-PO-R	GGCACTTGTGAGGAAGAA
asmO-NE-F	TATGCCGTGCATCCGAAG
asmO-NE-R	GCGGTAGAACGGCATCAT
asmP-PO-F	TCACCGGACTCACCTACC
asmP-PO-R	GTAAGTGTGTCGGTTCATGAAG
asmP-NE-F	CAAACCGGTGCTGATGATCTA
asmP-NE-R	ACCGAGTACCGGGTGAA
asmR-PO-F	CCAGCAGCCTGACTTGTAAAT
asmR-PO-R	GGACGGCTTCTCGTGTTT
asmR-NE-F	GACGCGCAGGTCTACTAC
asmR-NE-R	GATGCACATCGCTCCT
asmS-PO-F	GCCCTGATCAGCTGGAAG
asmS-PO-R	AAGACCGAGGGCCTCA
asmS-NE-F	CCAGGTGCTCAACGTCTAC
asmS-NE-R	CATGTACGCGGGCAGAA
asmI-pET28a-F	GGTGCCGCGCGGCAGCCATATGAACGAGTCGGAACCC
asmI-pET 28a-R	GCTCGAGTGCGGCCCAAGCTTTCAGGTCCGCCGCCGGAC
4885-pET 28a-F	GGTGCCGCGCGGCAGCCATATGGTGGTTCGACGCGGATCAG
4885-pET 28a-R	GCTCGAGTGCGGCCCAAGCTTCTATGCGACGAGGCTTTC
441-pET 28a-F	GGTGCCGCGCGGCAGCCATATGCGGATCGGCATCGAC
441-pET 28a-R	GCTCGAGTGCGGCCCAAGCTTTCAGCCCACCGGCTCCGA
asmD-pET28a-F	GGTGCCGCGCGGCAGCCATATGGTGGACTGGGAAACCGAT
asmD-pET28a-R	GCTCGAGTGCGGCCCAAGCTTTCACGGCTGCATCACCTC
asmC-pET22b-F	AAGAAGGAGATATACATATGGTTCAGCAGTCCCGCG
asmC-pET22b-R	CTCGAGTGCGGCCCAAGCTTTCGACGCGGAGTTCGTCGCG
asmM-pET22b-F	AAGAAGGAGATATACATATG AGCCTGGACCGGTGGGG
asmM-pET22b-R	CTCGAGTGCGGCCCAAGCTT GCGTTCGCGGGGCACCCG
asmN-pET22b-F	AAGAAGGAGATATACATATG GTGACACACGTCGACGAT
asmN-pET22b-R	CTCGAGTGCGGCCCAAGCTTTCGGGCCCGTCTTCCCG
asmS-pET22b-F	AAGAAGGAGATATACATATG GTGAACCCGGAGAGCAGC
asmS-pET22b-R	CTCGAGTGCGGCCCAAGCTT ACTCGATCTCCTTGAGGC

Table S3. Deduced functions of ORFs in the *asm* gene cluster^a

ORF	Amino acids ^b	Blastp homologue	Identity/coverage [%]	Protein ID ^c
AsmA	291	response regulator	95/100	EHN75269.1
AsmB	482	sensor histidine kinase	93/98	KPC71983.1
AsmC	1076	non-ribosomal peptide synthetase		
AsmD	450	FmoH alanine/alpha-methylserine hydroxymethyltransferase	53/87	BAP16692.1
AsmE	488	transmembrane transporter	44/96	AAM77999.1
AsmF	180	hypothetical protein		
AsmG	398	putative 3-deoxy-D-arabinose-heptulosonic-7-phosphate synthase	49/97	ACN39016.1
AsmH	648	phenazine biosynthesis protein phzE	52/94	SDS26303.1
AsmI	476	BM3 cytochrome P450	39/91	3PSX_A
AsmJ	239	SgcG oxidoreductase	48/87	AAL06666.1
AsmK	413	LtmK cytochrome P450	41/88	ABB88538.1
AsmL	273	hypothetical protein		
AsmM	1089	non-ribosomal peptide synthetase		
AsmN	1331	non-ribosomal peptide synthetase		
AsmO	394	CmdE halogenase	25/77	Q0VZ69.1
AsmP	222	CtvB O-methyl transferase	32/92	Q0C9L6.1
AsmQ	258	transcriptional regulator	34/95	BAL56037.1
AsmR	461	SgcD5 amide bond formation	48/92	ANY94435.1
AsmS	806	non-ribosomal peptide synthase		

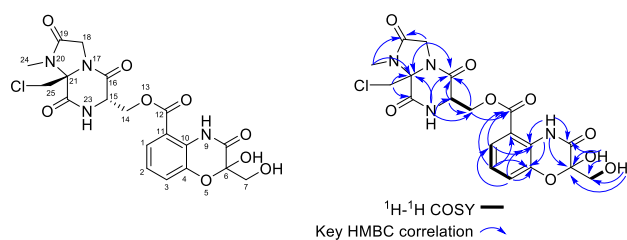
^a The sequence has been deposited in GenBank with the accession number MH752201. ^b Numbers are in amino acids. ^c Given in numbers are NCBI accession numbers.

Table S4. ^1H NMR (600 MHz) and ^{13}C NMR (150 MHz) data of **1** in $\text{DMSO-}d_6$.



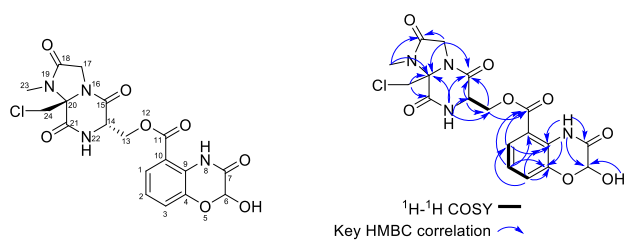
No.	δ_{C}	δ_{H} (mult, J, Hz)
1	124.5, CH	7.58 (d, 8.4, 1.8)
2	122.8, CH	7.08 (td, 8.4, 1.8)
3	122.9, CH	7.30 (d, 8.4)
4	142.4, C	
6	97.2, C	
6-OH		7.67 (d, 14.1)
7	63.5, CH_2	3.96 (dd, 11.5, 4.8) 3.58 (m)
7-OH		5.22 (t, 4.8)
8	163.4, C	
9		NH 10.04 (d, 3.4)
10	128.7, C	
11	113.9, C	
12	166.4, C	
13		
14	63.3, CH_2	4.65 (m) 4.61 (m)
15	53.1, CH	4.77 (q, 3.0)
16	162.8, C	
17		
18	47.4, CH_2	4.14 (t, 14.4) 3.82 (m)
19	168.7, C	
20		
21	79.9, C	
22	166.9, C	
23		NH 9.00 (d, 11.7)
24	27.7, CH_3	3.04 (s)
25	61.4, CH_2	3.91 (m) 3.78 (m)
25-OH		5.75 (t, 5.4)

Table S5. ^1H NMR (600 MHz) and ^{13}C NMR (150 MHz) data of **2** in $\text{DMSO-}d_6$.



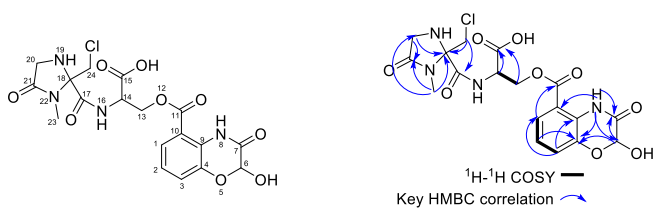
No.	δ_{C}	δ_{H} (mult, J, Hz)
1	124.6, CH	7.62 (dd, 8.0, 3.2)
2	122.9, CH	7.08 (t, 8.0)
3	122.9, CH	7.31 (d, 8.0)
4	142.4, C	
6	97.2, C	
7	63.5, CH_2	3.96 (dd, 11.5, 3.9) 3.59 (m)
8	163.4, C	
9		NH 10.06 (d, 3.4)
10	128.7, C	
11	113.8, C	
12	166.4, C	
13		
14	63.0, CH_2	4.64 (m) 4.62 (m)
15	52.8, CH	4.97 (m)
16	163.4, C	
17		
18	48.0, CH_2	3.89 (d, 15.9) 4.20 (dd, 15.9, 11.5)
19	168.5, C	
20		
21	78.8, C	
22	165.5, C	
23		NH 9.22 (d, 11.7)
24	27.5, CH_3	3.06 (s)
25	47.3, CH_3	4.48 (d, 12.6) 4.42 (dd, 12.6, 2.6)

Table S6. ^1H NMR (600 MHz) and ^{13}C NMR (150 MHz) data of **3** in $\text{DMSO-}d_6$.



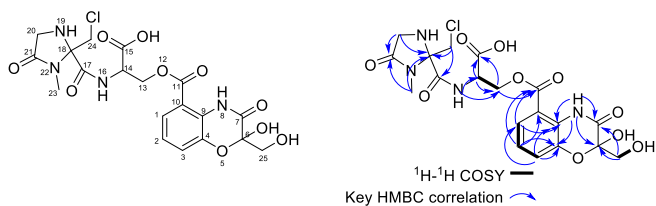
No.	δ_{C}	δ_{H} (mult, J, Hz)
1	125.5, CH	7.79 (d, 7.8, 1.8)
2	122.8, CH	7.11 (t, 7.8)
3	123.5, CH	7.37 (d, 7.8)
4	141.5, C	
6	90.2, C	
6-OH		5.63 (s)
7	162.5, CH_2	
8		NH 10.15 (d, 12.8)
9	128.7, C	
10	114.0, C	
11	166.1, C	
12		
13	61.9, CH_2	4.72 (m) 4.56 (m)
14	51.1, CH	4.76 (m)
15	164.7, C	
16		
17	48.7, CH_2	4.54 (m) 4.49 (m)
18	167.1, C	
19		
20	79.9, C	
21	167.2, C	
22		
23	25.1, CH_3	2.75 (s)
24	43.8, CH_2	4.60 (m) 4.40(m)

Table S7. ^1H NMR (600 MHz) and ^{13}C NMR (150 MHz) data of **4** in $\text{DMSO-}d_6$.



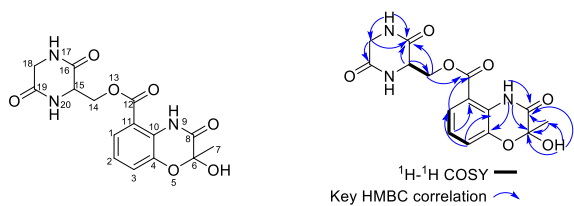
No.	δ_{C}	δ_{H} (mult, J, Hz)
1	125.0, CH	7.78 (dd, 7.8, 1.2)
2	122.5, CH	7.11 (t, 7.8)
3	123.0, CH	7.37 (d, 7.8)
4	141.0, C	
6	89.8, C	5.63 (s)
7	162.0, CH_2	
8		NH 10.12 (d, 7.2)
9	128.4, C	
10	113.6, C	
11	165.7, C	
12		
13	61.4, CH_2	4.72 (m) 4.50 (m)
14	50.6, CH	4.68 (m)
15	166.8, C	
16		NH 8.70 (brs)
17	164.3, C	4.49 (m)
18	81.5, C	
19		
20	48.2, CH_2	
21	166.7, C	
22		
23	24.6, CH_3	2.75 (s)
24	43.4, CH_2	4.60 (m) 4.41(m)

Table S8. ^1H NMR (600 MHz) and ^{13}C NMR (150 MHz) data of **5** in $\text{DMSO-}d_6$.



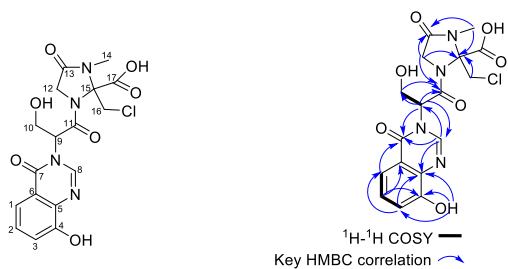
No.	δ_{C}	δ_{H} (mult, J, Hz)
1	124.5, CH	7.76 (dd, 7.8, 1.2)
2	122.3, CH	7.09 (t, 7.8)
3	122.6, CH	7.33 (d, 7.8)
4	141.8, C	
6	96.8, C	
7	162.9, CH_2	
8		NH 10.13 (d, 7.2)
9	128.6, C	
10	112.8, C	
11	165.9, C	
12		
13	61.4, CH_2	4.73 (m) 4.60 (m)
14	50.6, CH	4.77 (brs)
15	166.8, C	
16		NH 8.73 (brs)
17	164.2, C	
18	81.5, C	
19		NH 8.73 (brs)
20	48.1, CH_2	4.41 (m) 4.62 (m)
21	166.9, C	
22		
23	24.6, CH_3	2.75 (s)
24	43.3, CH_2	4.49 (m)
25	63.0, CH_2	3.97 (dd, 11.5, 3.4) 3.61 (dd, 11.5, 2.0)

Table S9. ^1H NMR (600 MHz) and ^{13}C NMR (150 MHz) data of **6** in $\text{DMSO-}d_6$.



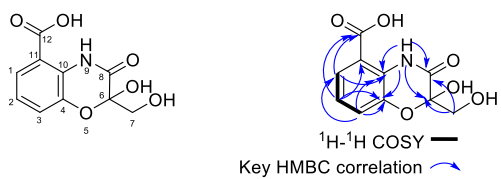
No.	δ_{C}	δ_{H} (mult, J, Hz)
1	124.7, CH	7.96 (dd, 7.8, 1.2)
2	122.3, CH	7.09 (t, 7.8)
3	122.8, CH	7.32 (d, 7.8)
4	141.8, C	
6	95.2, C	
7	22.7, CH_3	1.68 (s)
8	163.5, C	
9		NH 10.01 (d, 7.2)
10	129.3, C	
11	113.2, C	
12	165.8, C	
13		
14	63.3, CH_2	4.68 (m) 4.64 (m)
15	51.4, CH	4.36 (m)
16	166.1, C	
17		NH 8.95 (brs)
18	40.9, CH_2	3.91 (m) 3.90 (m)
19	170.6, C	
20		NH 8.46 (brs)

Table S10. ^1H NMR (600 MHz) and ^{13}C NMR (150 MHz) data of **7** in $\text{DMSO-}d_6$.



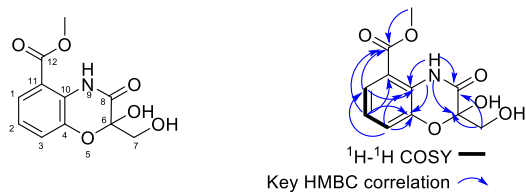
No.	δ_{C}	δ_{H} (mult, J, Hz)
1	116.0, CH	7.56 (dd, 7.8, 1.2)
2	128.0, CH	7.37 (t, 7.8)
3	119.1, CH	7.23 (d, 7.8)
4	153.0, C	4-OH 9.94 (s)
5	136.2, C	
6	121.9, C	
7	160.0, C	
8	144.3, C	8.28 (s)
9	57.6, C	5.52 (dd, 8.4, 5.4)
10	58.3, C	
11	166.0, C	
12	48.5, CH_2	3.90 (m) 4.61 (m)
13	166.7, C	4.77 (brs)
14	24.5, CH_3	2.69 (s)
15	81.2, C	
16	43.2, CH_2	4.33 (m)
17	167.1, C	

Table S11. ^1H NMR (600 MHz) and ^{13}C NMR (150 MHz) data of **8** in $\text{DMSO-}d_6$.



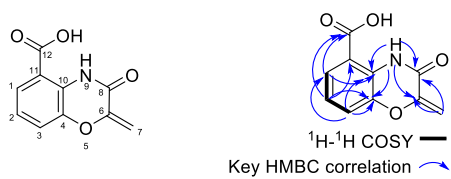
No.	δ_{C}	δ_{H} (mult, J, Hz)
1	124.5, CH	7.61 (d, 7.8)
2	122.9, CH	7.06 (t, 7.8)
3	122.3, CH	7.26 (d, 7.8)
4	142.3, C	
6	97.2, C	
7	63.5, CH_2	3.58 (d, 11.4) 3.96 (d, 11.4)
8	163.3, C	
9		NH 10.55(s)
10	129.1, C	
11	114.6, C	
12	169.3, C	

Table S12. ^1H NMR (600 MHz) and ^{13}C NMR (150 MHz) data of **9** in $\text{DMSO-}d_6$.

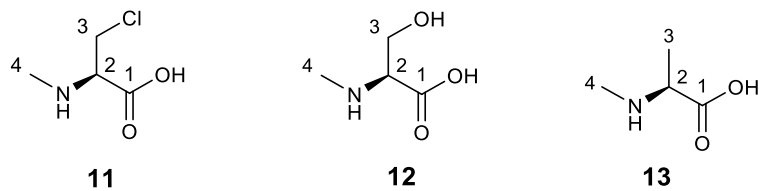


No.	δ_{C}	δ_{H} (mult, J, Hz)
1	123.6, CH	7.60 (d, 7.8)
2	122.5, CH	7.08 (t, 7.8)
3	122.2, CH	7.30 (d, 7.8)
4	142.5, C	
6	96.8, C	
7	63.0, CH_2	3.58 (d, 11.4) 3.96 (d, 11.4)
8	162.9, C	
9		NH 10.25(s)
10	128.3, C	
11	113.7, C	
12	166.9, C	
12-O CH_3	52.6, CH_3	3.89 (s)

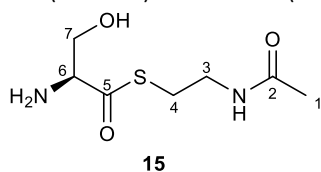
Table S13. ^1H NMR (600 MHz) and ^{13}C NMR (150 MHz) data of **10** in $\text{DMSO-}d_6$.



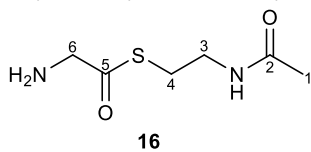
No.	δ_{C}	δ_{H} (mult, J, Hz)
1	125.3, CH	7.63 (d, 7.8)
2	122.5, CH	7.08 (t, 7.8)
3	122.0, CH	7.31 (d, 7.8)
4	141.5, C	
6	148.0, C	
7	98.9, CH_2	5.47 (brs) 5.14 (brs)
8	155.6, C	
9		NH 10.97 (s)
10	127.8, C	
11	115.5, C	
12	169.2, C	

Table S14. ^1H NMR (400 MHz) data of **11–13** in D_2O .

No.	11	12	13
	δ_{H} (mult, J, Hz)	δ_{H} (mult, J, Hz)	δ_{H} (mult, J, Hz)
2	3.68 (dd, 7.2, 6.8)	3.80 (m)	3.47 (q, 4.8)
3	4.48 (brs)	3.83 (dd, 5.2, 4.0);	1.46 (d, 4.8)
	3.80 (brs)	3.73 (dd, 5.2, 4.0)	
4	2.75 (s)	3.23 (s)	2.65 (s)

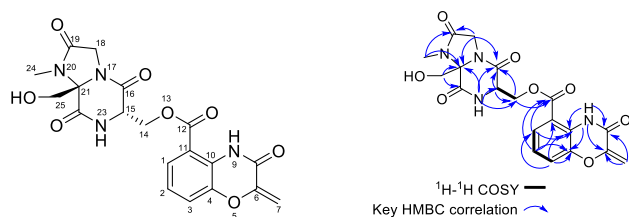
Table S15. ^1H NMR (600 MHz) and ^{13}C NMR (150 MHz) data of **15** in D_2O .

No.	δ_{C}	δ_{H} (mult, J, Hz)
1	23.0, CH_3	1.91 (s)
2	174.1, C	
3	42.2, CH_2	3.26 (t, 4.4)
4	38.1, CH_2	2.56 (t, 4.4)
5	195.6, C	
6	48.8, CH	3.24 (m)
7	60.6, CH_2	4.37 (m) 3.90 (m)

Table S16. ^1H NMR (400 MHz) and ^{13}C NMR (100 MHz) data of **16** in D_2O .

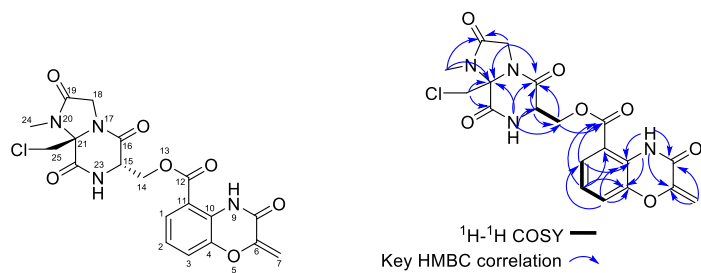
No.	δ_{C}	δ_{H} (mult, J, Hz)
1	21.4, CH_3	1.73 (s)
2	174.3, C	
3	38.2, CH_2	3.16 (t, 6.4)
4	27.9, CH_2	2.92 (t, 6.4)
5	194.3, C	
6	46.4, CH_2	3.24 (s)

Table S17. ^1H NMR (600 MHz) and ^{13}C NMR (150 MHz) data of **17** in $\text{DMSO-}d_6$.



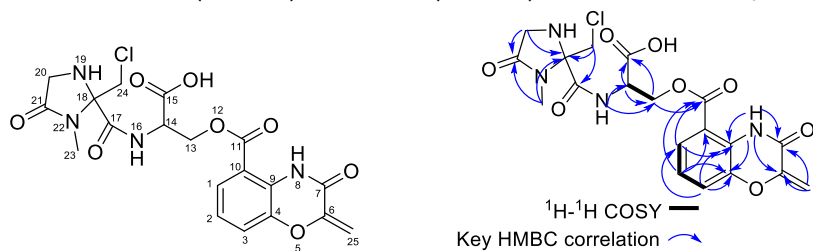
No.	δ_{C}	δ_{H} (mult, J, Hz)
1	125.8, CH	7.79 (dd, 8.0, 3.2)
2	122.8, CH	7.13 (t, 8.0)
3	120.9, CH	7.40 (d, 8.0)
4	141.5, C	
6	147.8, C	
7	99.4, CH_2	5.50 (d, 1.8) 5.18 (d, 1.8)
8	155.5, C	
9		NH 10.31 (s)
10	127.8, C	
11	113.6, C	
12	163.9, C	
13		
14	61.8, CH_2	4.67 (m) 4.60 (m)
15	51.1, CH	4.65 (m)
16	167.4, C	
17		
18	48.2, CH_2	4.49 (d, 15.9) 4.26 (d, 15.9)
19	167.3, C	
20		
21	83.0, C	
22	166.1, C	
23		
24	25.2, CH_3	2.71 (s)
25	70.2, CH_2	3.48 (m) 3.54(m)

Table S18. ^1H NMR (600 MHz) and ^{13}C NMR (150 MHz) data of **18** in $\text{DMSO-}d_6$.



No.	δ_{C}	δ_{H} (mult, J, Hz)
1	123.3, CH	7.49 (dd, 8.0, 3.2)
2	123.4, CH	7.13 (t, 8.0)
3	119.4, CH	7.31 (d, 8.0)
4	141.5, C	
6	147.9, C	
7	99.1, CH_2	5.45 (d, 1.8) 5.15 (d, 1.8)
8	155.3, C	
9		NH 11.36 (s)
10	126.4, C	
11	110.9, C	
12	164.3, C	
13		
14	67.9, CH_2	4.69 (m) 4.62 (m)
15	67.4, CH	5.42 (m)
16	167.8, C	
17		
18	49.1, CH_2	4.43 (d, 15.9) 4.69 (d, 15.9)
19	167.6, C	
20		
21	81.6, C	
22	167.3, C	
23		
24	24.9, CH_3	2.76 (s)
25	43.4, CH_2	4.37 (m)

Table S19. ^1H NMR (600 MHz) and ^{13}C NMR (150 MHz) data of **19** in $\text{DMSO-}d_6$.



No.	δ_{C}	δ_{H} (mult, J , Hz)
1	123.4, CH	7.48 (dd, 7.8, 1.2)
2	123.2, CH	7.12 (t, 7.8)
3	119.5, CH	7.31 (d, 7.8)
4	141.5, C	
6	147.9, C	
7	155.3, CH	
8		NH 11.36 (d, 7.2)
9	128.8, C	
10	111.0, C	
11	164.3, C	
12		
13	67.84, CH_2	4.69 (m) 4.61 (m)
14	67.2, CH	5.41 (brs)
15	167.6, C	
16		
17	167.3, C	
18	81.5, C	
19		
20	48.9, CH_2	4.443 (m) 4.69 (m)
21	167.8, C	
22		
23	24.9, CH_3	2.76 (s)
24	43.4, CH_2	4.37 (m)
25	99.1, CH_2	5.45 (d, 1.8) 5.15 (d, 1.8)

Measured in $\text{DMSO-}d_6$.

Table S20. Substrate specificity predictions for the adenylation domains of the NRPSs encoded in the *asm* Gene Cluster.¹⁷

A domain	Signature residues	Predicted substrate
AsmC	D L Y N V A S V F R	cysteine
AsmM	D I Y H L G L I T-	glycine
AsmN	D M F N V G L I P R	cysteine
AsmS	G M V L R A V V P D	glycine/alanine/valine

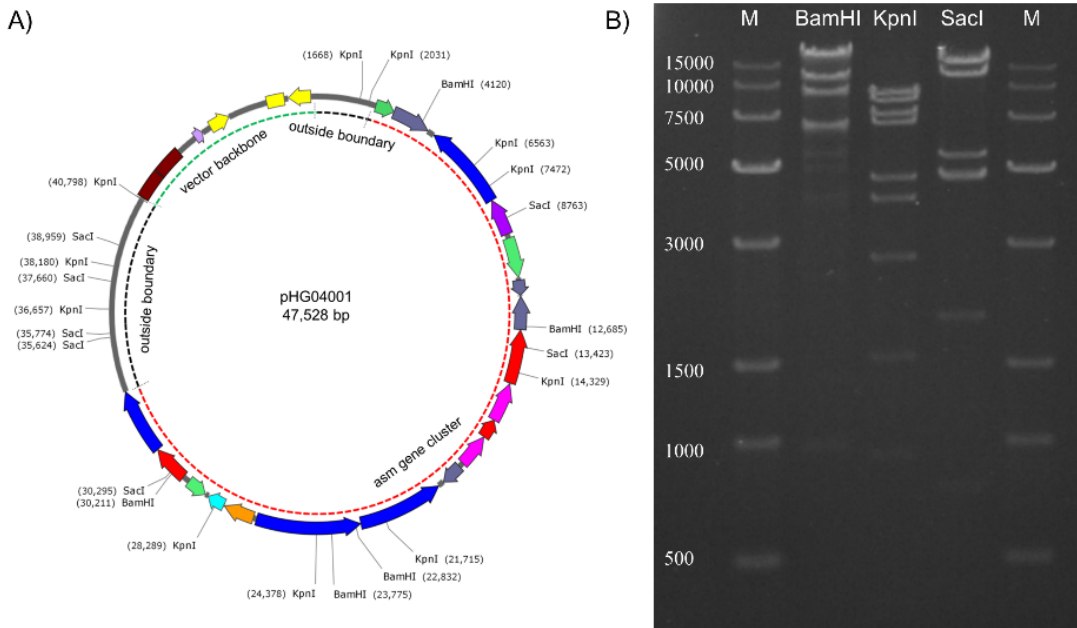


Figure S1. Verification of cosmid pHG4001. A) Physical map of pJTU2554 harboring the intact *asm* gene cluster. B) agarose gel electrophoresis of pHG4001 cosmid. M: 15K marker.

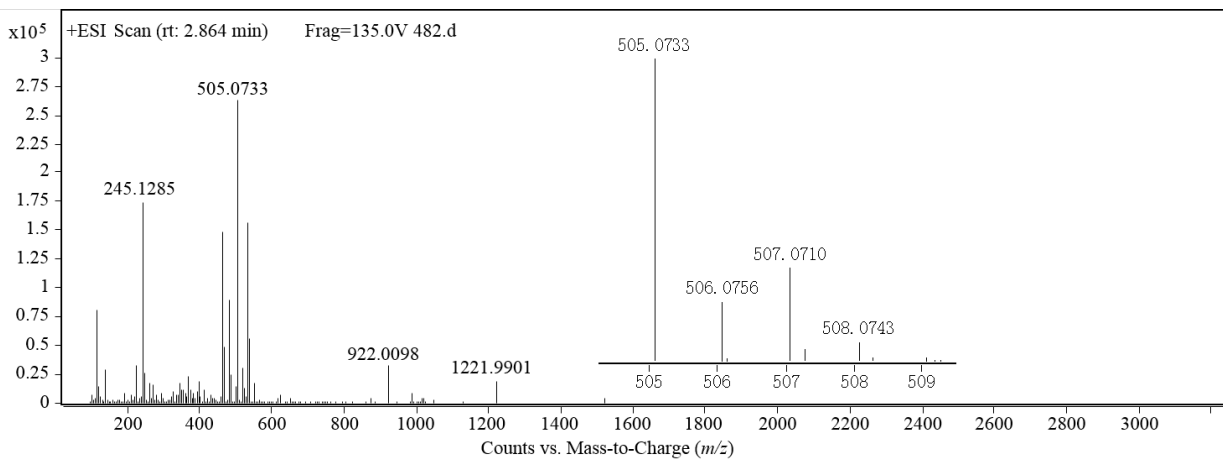


Figure S2. HR-ESIMS spectrum of **2**.

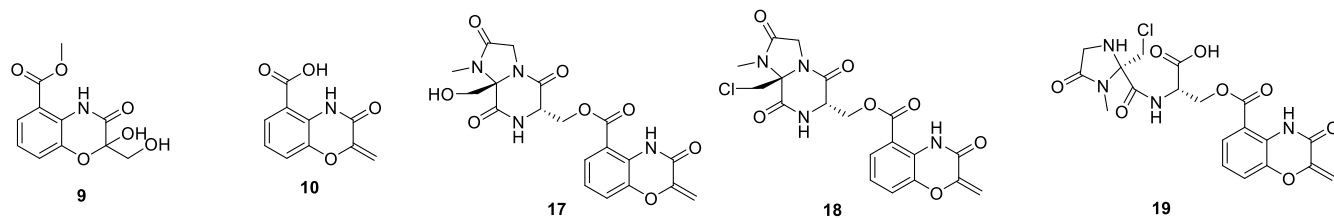
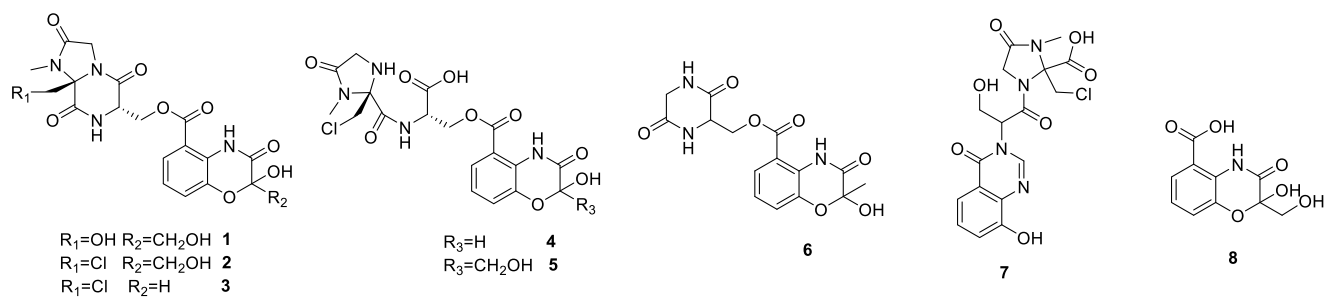


Figure S3. Structures of compounds **1–10** and **17–19**.

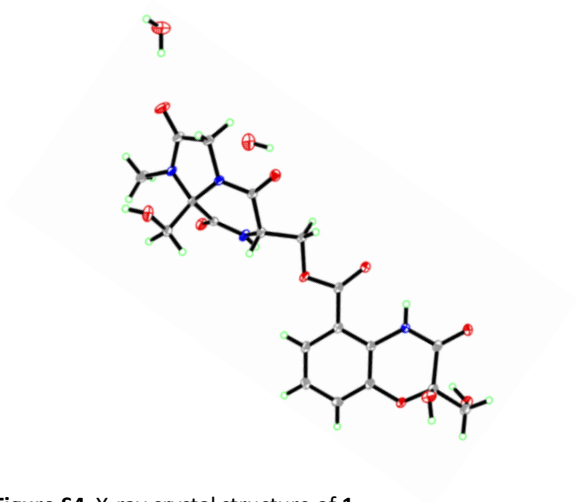


Figure S4. X-ray crystal structure of **1**.

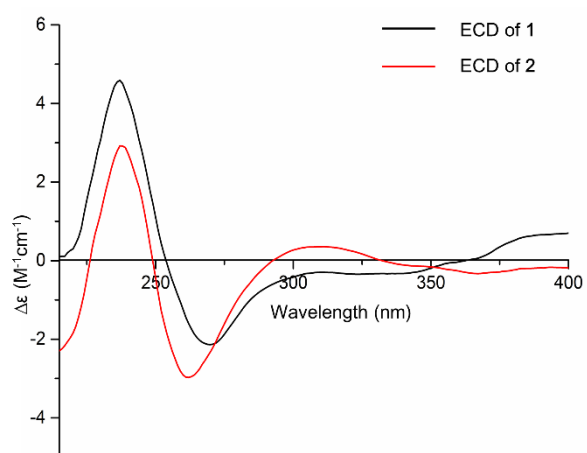


Figure S5. Comparison of CD spectra for **1** and **2**.

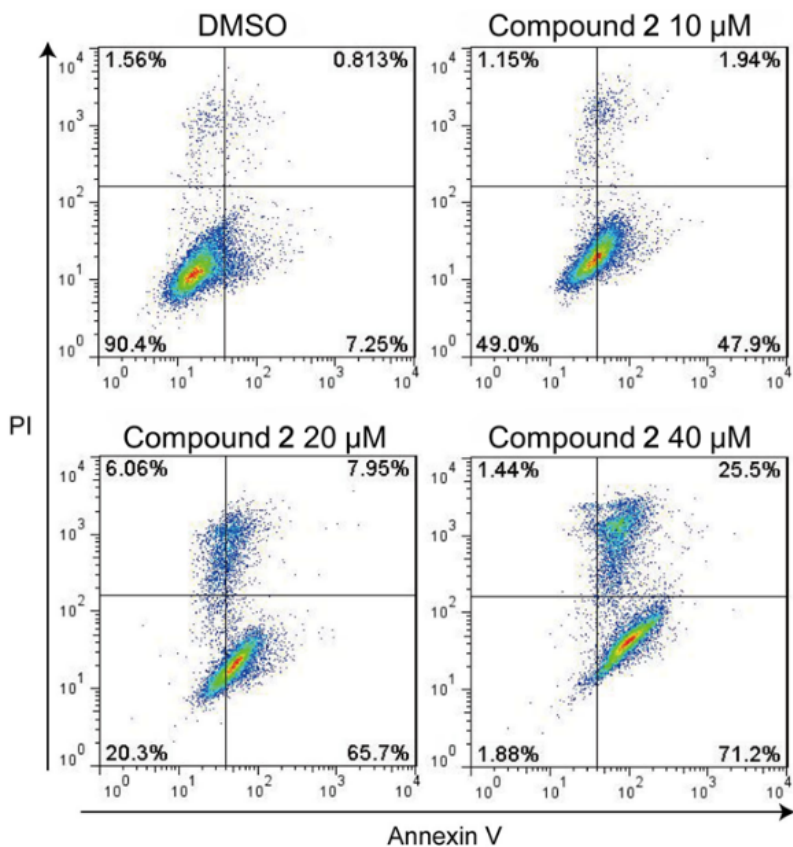


Figure S6. Apoptosis of MCF-7 cell was detected through flow cytometry after treated with different concentration of compound 2 contrasted with DMSO. The percente of apoptotic cells including Annexin-V⁺ PI⁻ early apoptotic cells in lower-right quadrant and Annexin-V⁺ PI⁺ late apoptotic cells in upper-right quadrant was increased along with compound concentration.

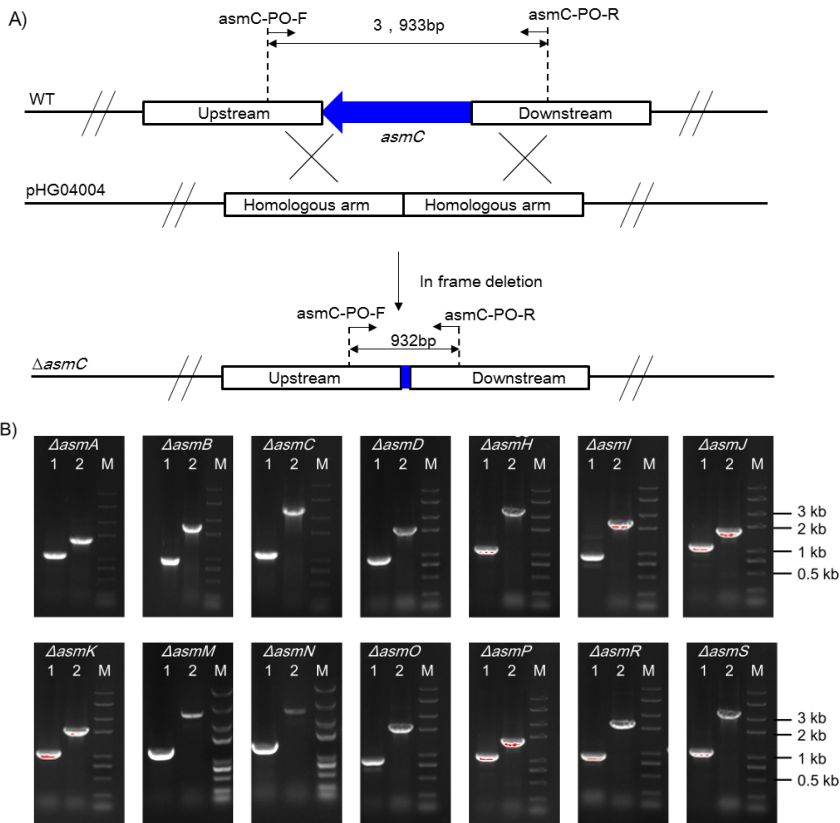


Figure S7. Construction of in-frame deletion in cosmid pHG4001. A) Gene disruption with homologous recombination strategies. B) PCR verification of *asm* mutants: Lane 1, amplified with PO-F/R and mutants; Lane 2, amplified with PO-F/R and pHG4001.

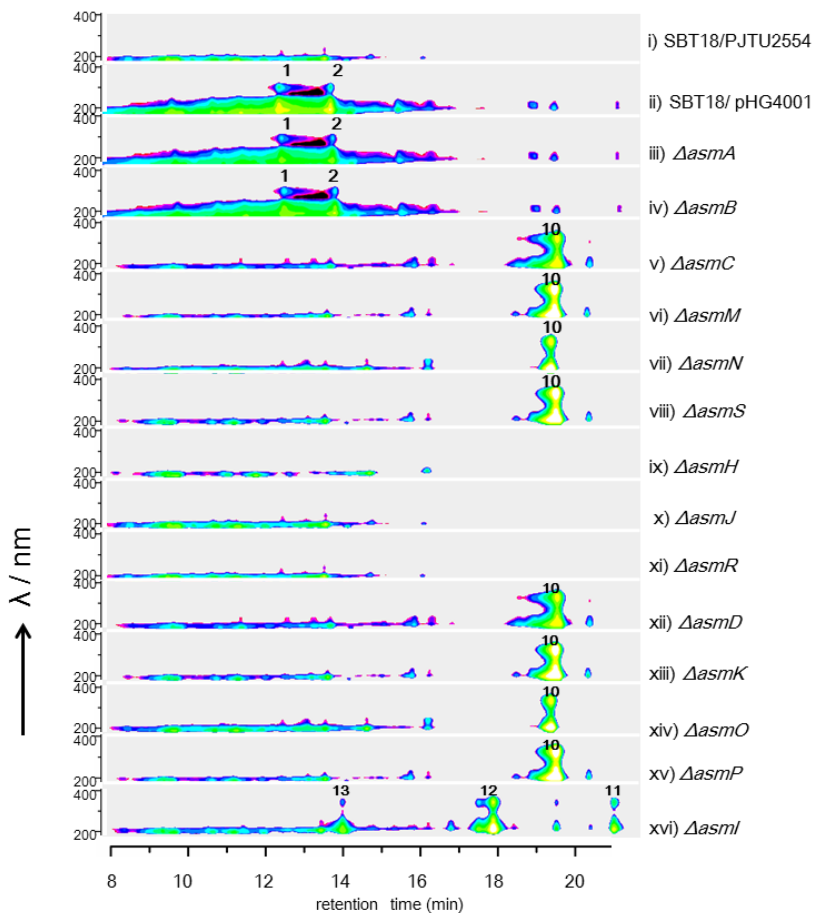
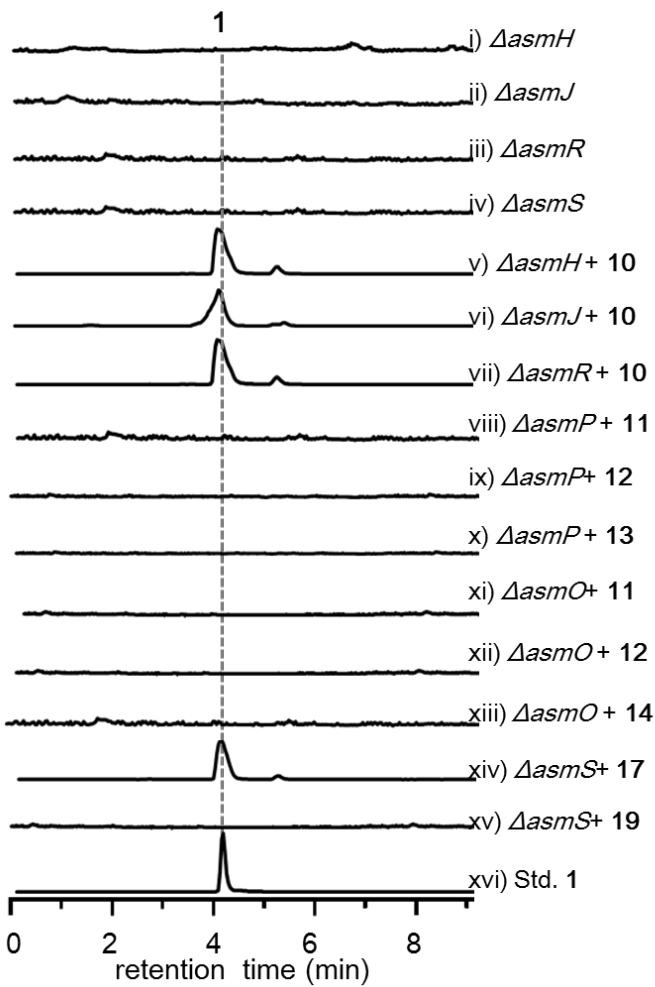


Figure S8. HPLC contour plot of metabolic extracts. The metabolic extracts from mutant strains were analyzed through HPLC equipped with DAD (Diode Array Detector), which can cover the UV absorbance from 200 nm to 400 nm.

A) +EIC (465.0)



B) +EIC (483.0)

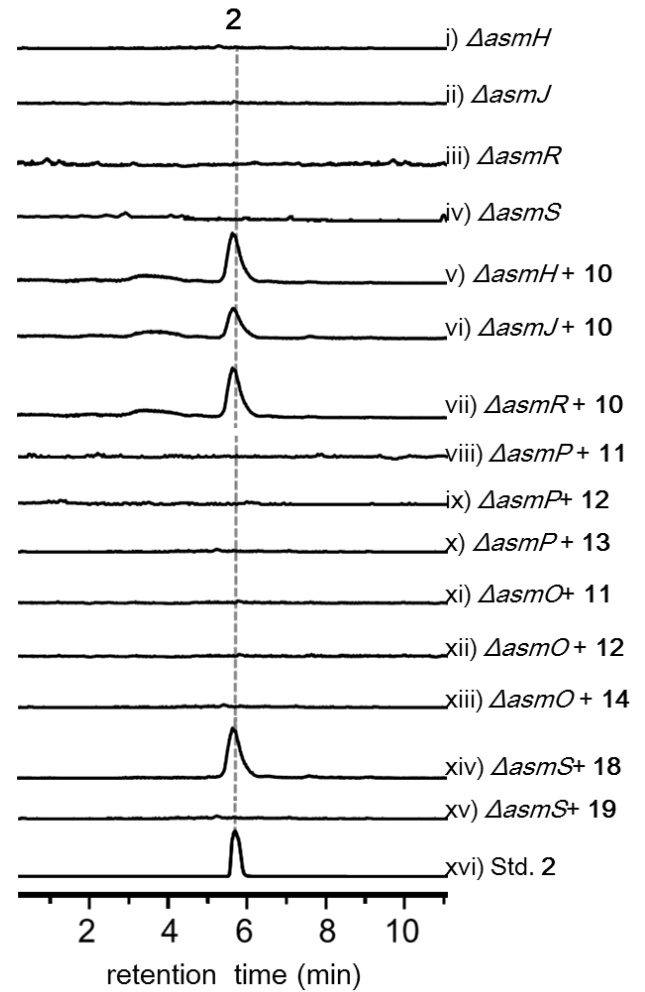


Figure S9. Chemical complementation of compounds into mutants. LC-MS analyses of A) compound 1 and B) compound 2 for different mutant strains. i) $\Delta asmH$ mutant; ii) $\Delta asmJ$ mutant; iii) $\Delta asmR$ mutant; iv) $\Delta asmS$ mutant; v) $\Delta asmH$ mutant fed with 10; vi) $\Delta asmJ$ mutant fed with 10; vii) $\Delta asmR$ mutant fed with 10; viii) $\Delta asmS$ mutant fed with 17; ix) $\Delta asmS$ mutant fed with 19; x) $\Delta asmO$ mutant fed with 11; xi) $\Delta asmP$ mutant fed with 11; xii) $\Delta asmO$ mutant fed with 12; xiii) $\Delta asmP$ mutant fed with 13; xiv) $\Delta asmO$ mutant fed with 13; xv) $\Delta asmP$ mutant fed with 14; A, xvi) standard of 1. B, xvi) standard of 2.

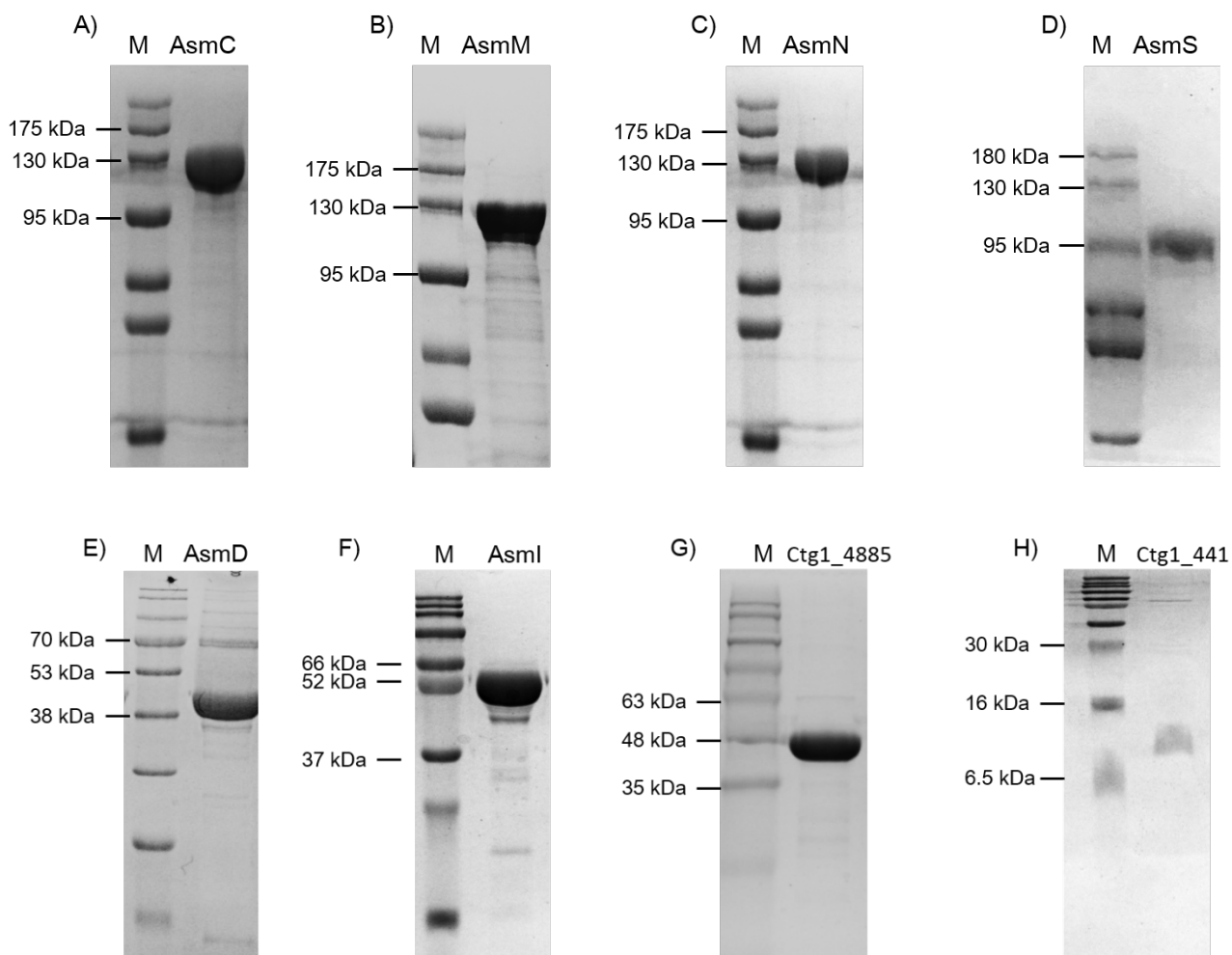


Figure S10. SDS-PAGE analysis of proteins. A) AsmC (calculated molecule weight: 118.6 kDa); B) AsmM (calculated molecule weight: 115.8 kDa); C) AsmN (calculated molecule weight: 144.4 kDa); D) AsmS (calculated molecule weight: 87.2 kDa); E) AsmD (calculated molecule weight: 49.2 kDa); F) AsmI (calculated molecule weight: 55.2 kDa); G) Ctg1_4885 (ferredoxin reductase from *S. sp.* NA03103, calculated molecule weight: 47.3 kDa); H) Ctg1_441 (ferredoxin from *S. sp.* NA03103, calculated molecule weight: 8.9 kDa).

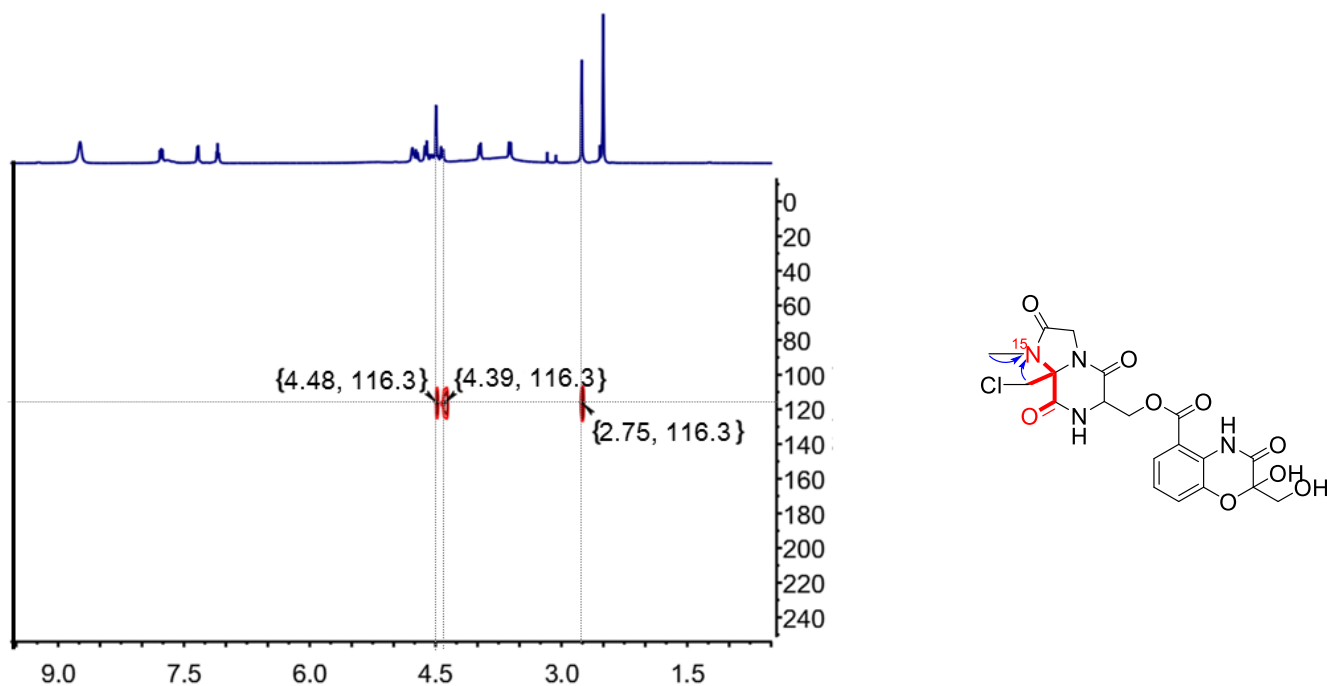


Figure S11. ^1H - ^{15}N HMBC correlations of **2** feeding with ^{15}N -alanine in $\text{DMSO-}d_6$.

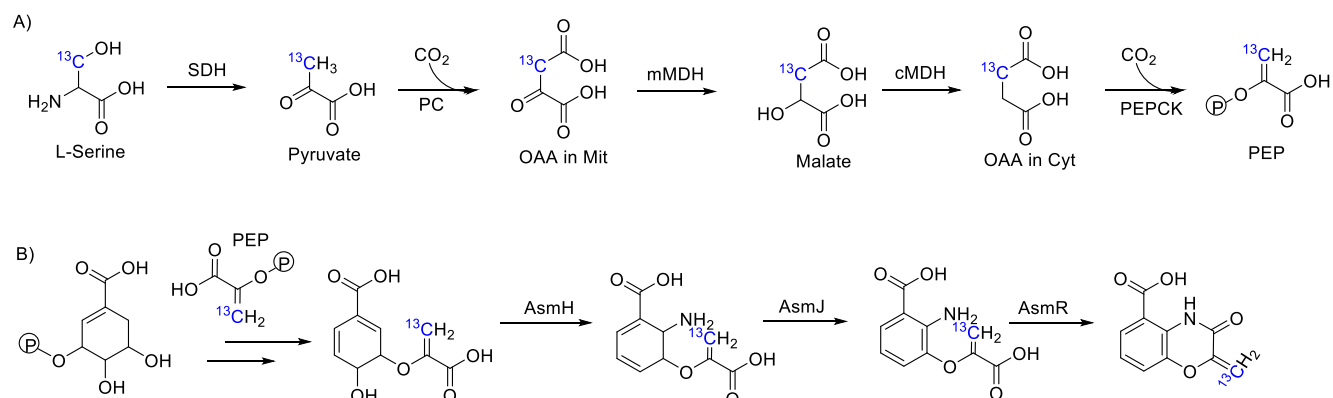


Figure S12. A) Pathway of L-serine to phosphoenolpyruvic acid (PEP);¹⁸ B) Pathway of chorismic acid to compound **10**.¹⁹ SDH: serine dehydratase, mMDH and cMDH: mitochondrial and cytosolic malate dehydrogenase, respectively, PEP: phosphoenolpyruvate, PEPCK: phosphoenolpyruvate carboxykinase, OAA: oxaloacetate, Mit: mitochondria.²⁰

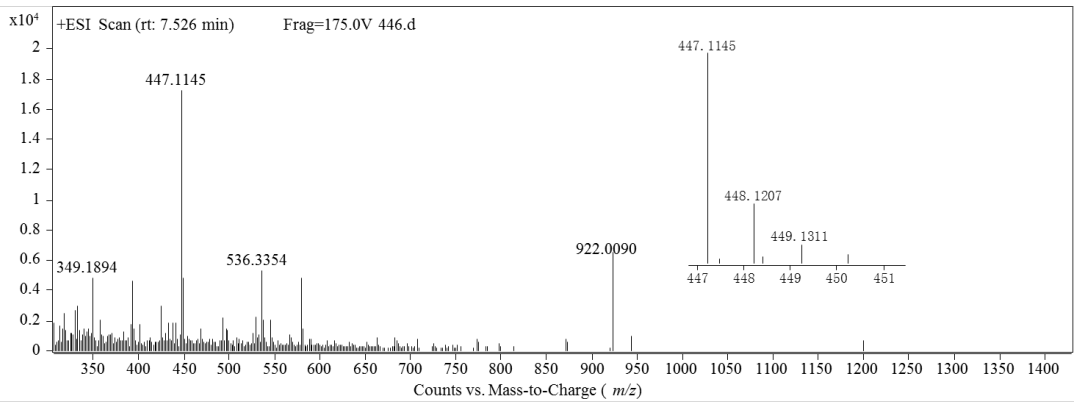


Figure S13. HRESIMS spectrum of **20**.

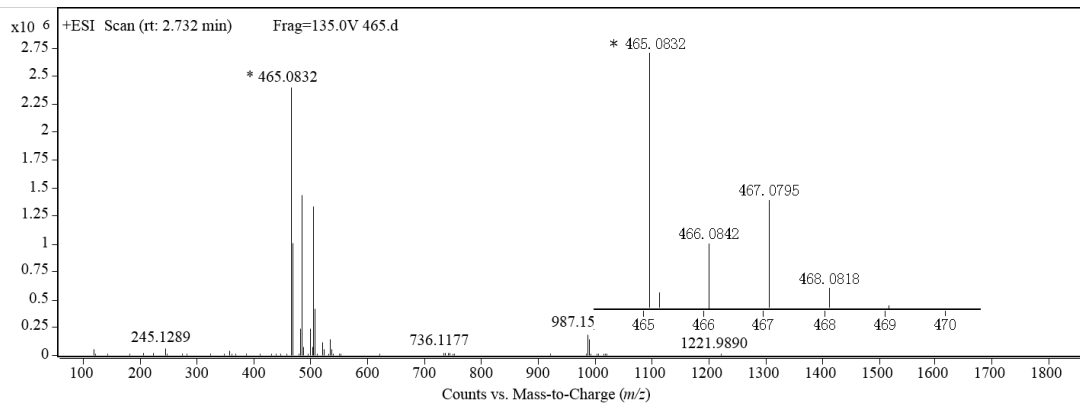


Figure S14. HRESIMS spectrum of **21**.

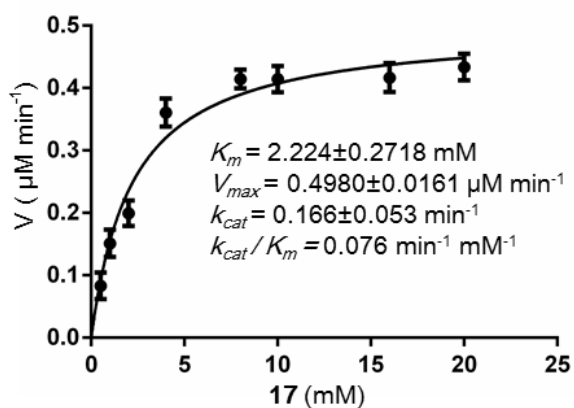


Figure S15. Pseudo-first order kinetic studies of Asml toward the formation of **1** from **17**. Under steady-state conditions, plots of initial velocity of formation of **1** versus the concentration of **17** (0.5mM, 1 mM, 2 mM, 4 mM, 8mM, 10mM, 16 mM and 20mM) displayed Michaelis-Menten kinetics.

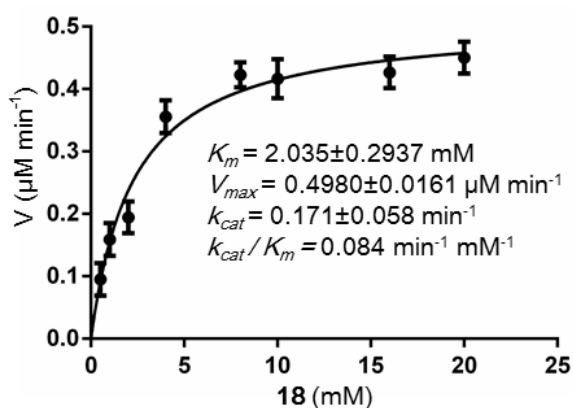


Figure S16. Pseudo-first order kinetic studies of Asml toward the formation of **2** from **18**. Under steady-state conditions, plots of initial velocity of formation of **2** versus the concentration of **18** (0.5mM, 1 mM, 2 mM, 4 mM, 8mM, 10mM, 16 mM and 20mM) displayed Michaelis-Menten kinetics.

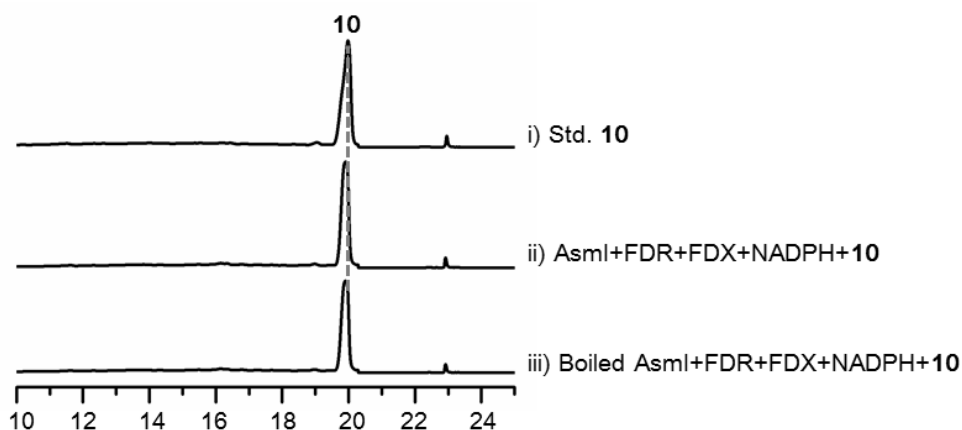


Figure S17. *In vitro* assays of Asml using **10** as substrate.

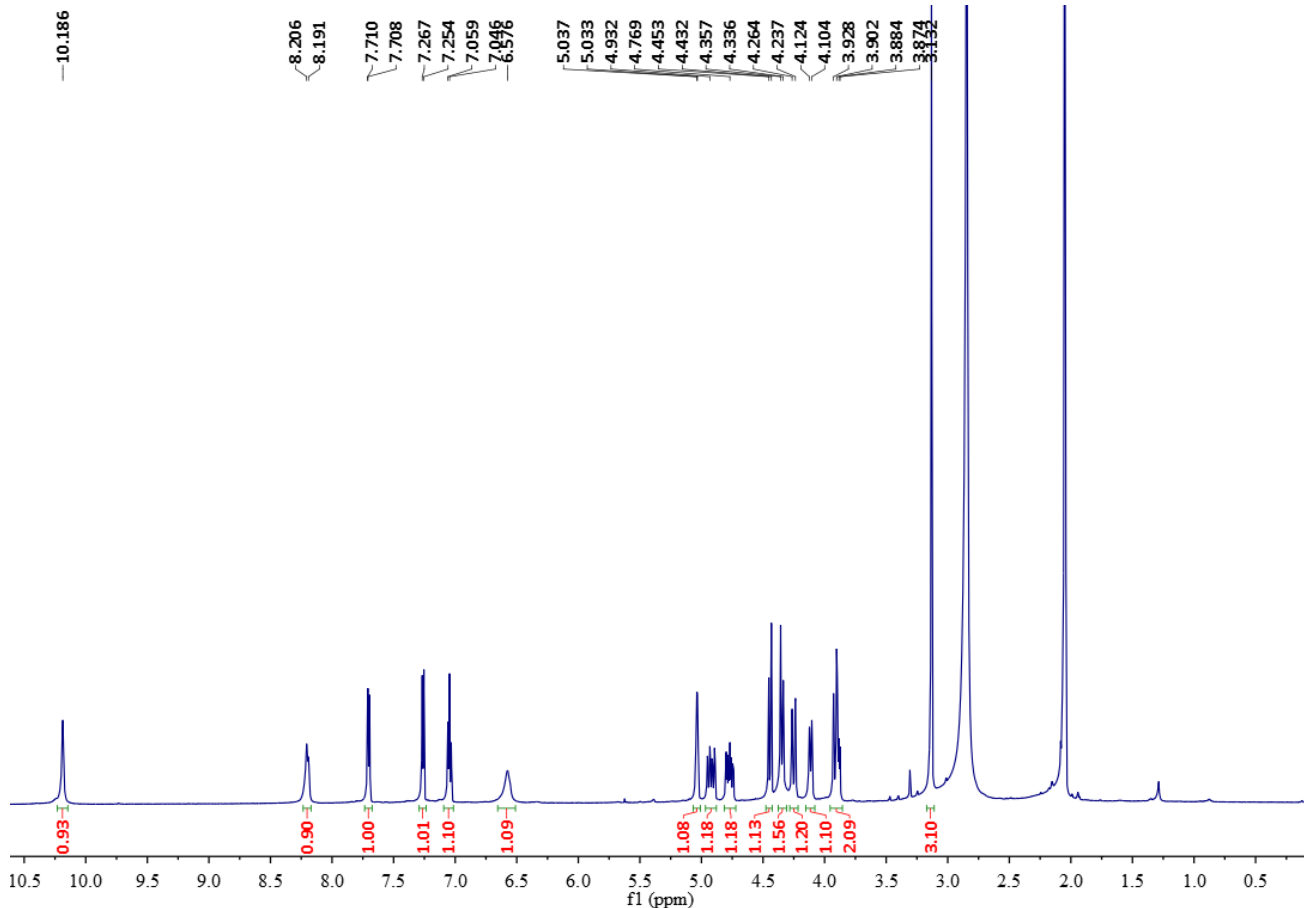


Figure S18. ¹H NMR spectrum of ashimide A (**1**) in DMSO-*d*₆ at 600 MHz.

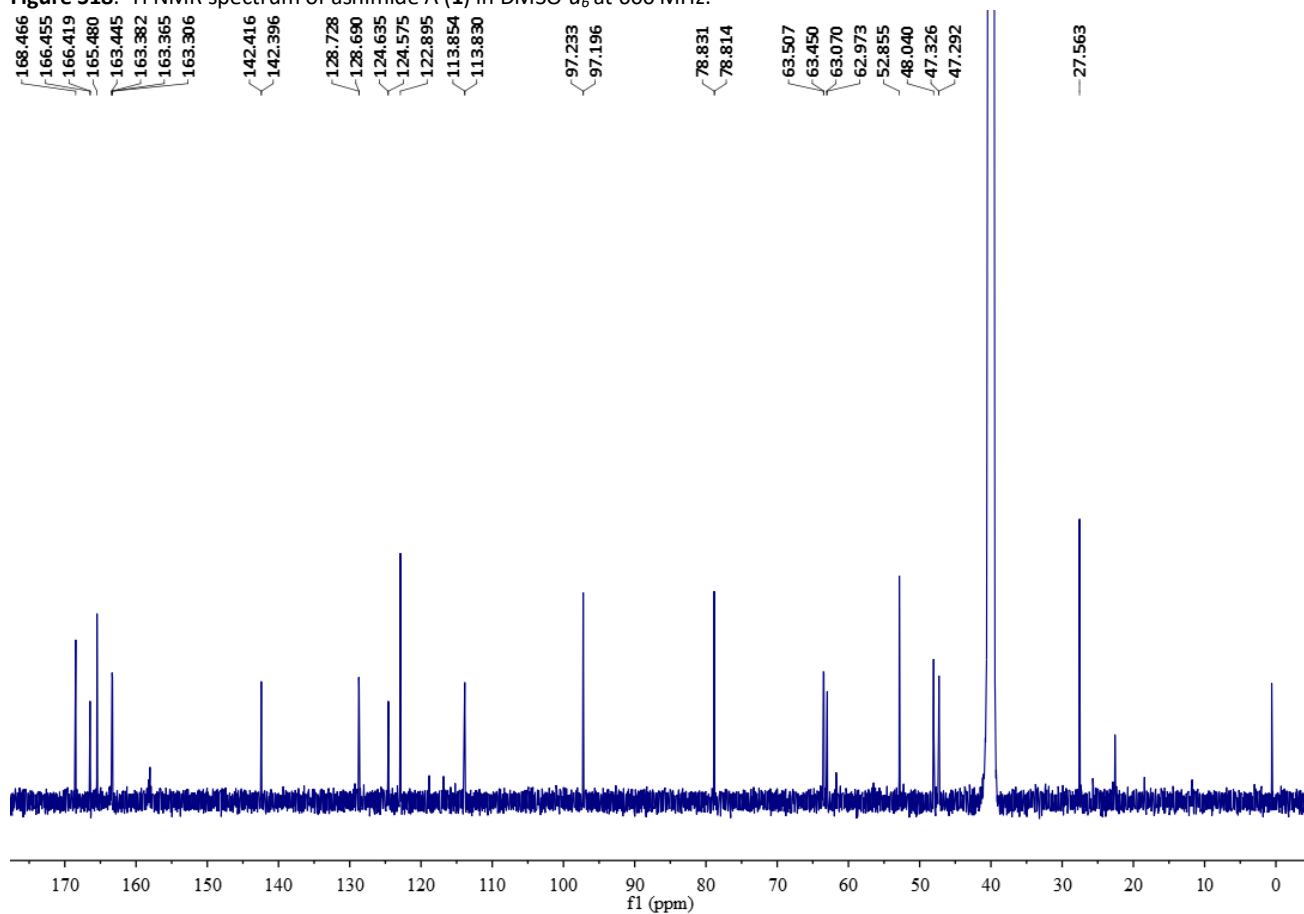


Figure S19. ¹³C NMR spectrum of ashimide A (**1**) in DMSO-*d*₆ at 150 MHz.

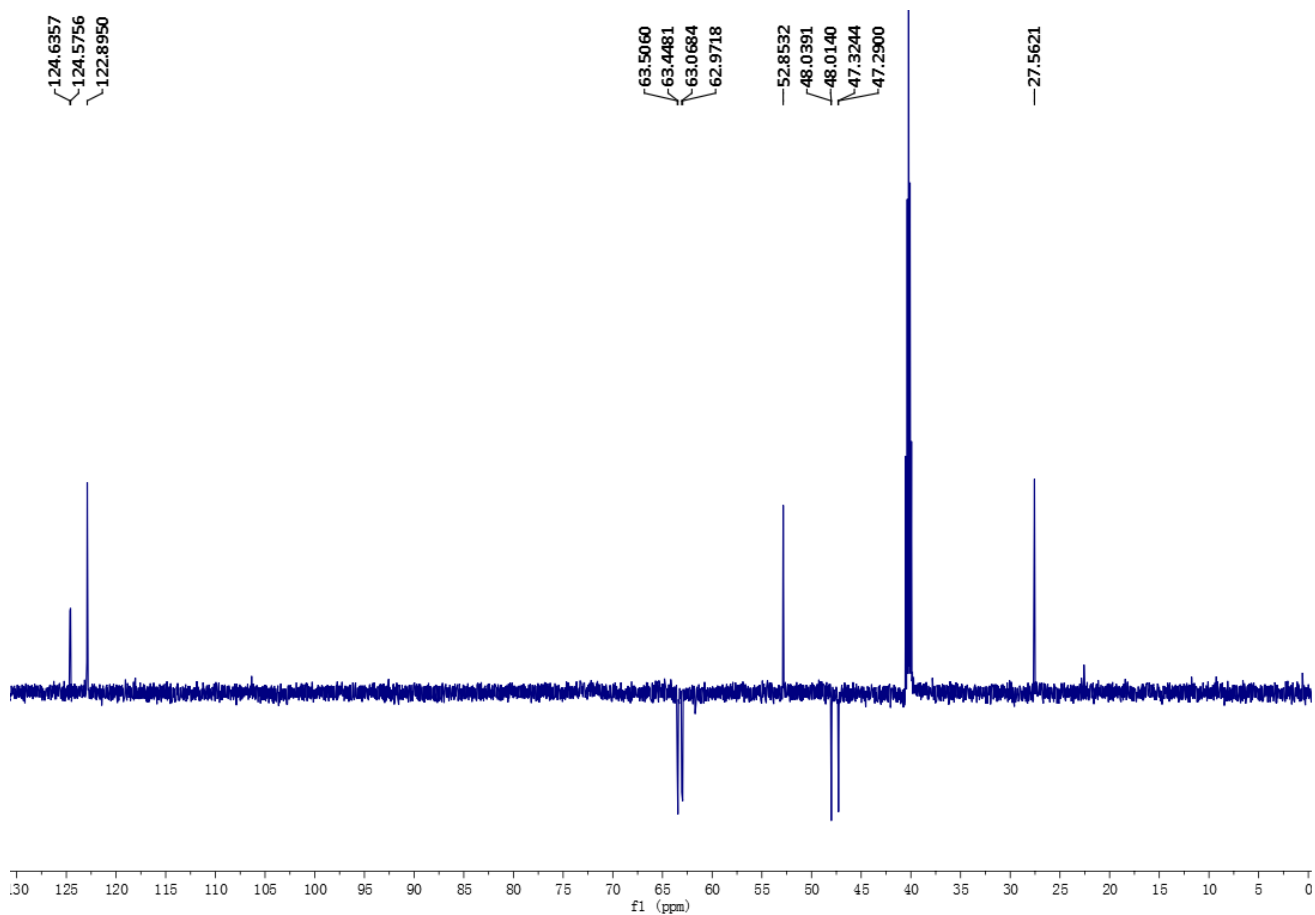


Figure S20. DEPT 135 spectrum of ashimide A(1) in DMSO- d_6 .

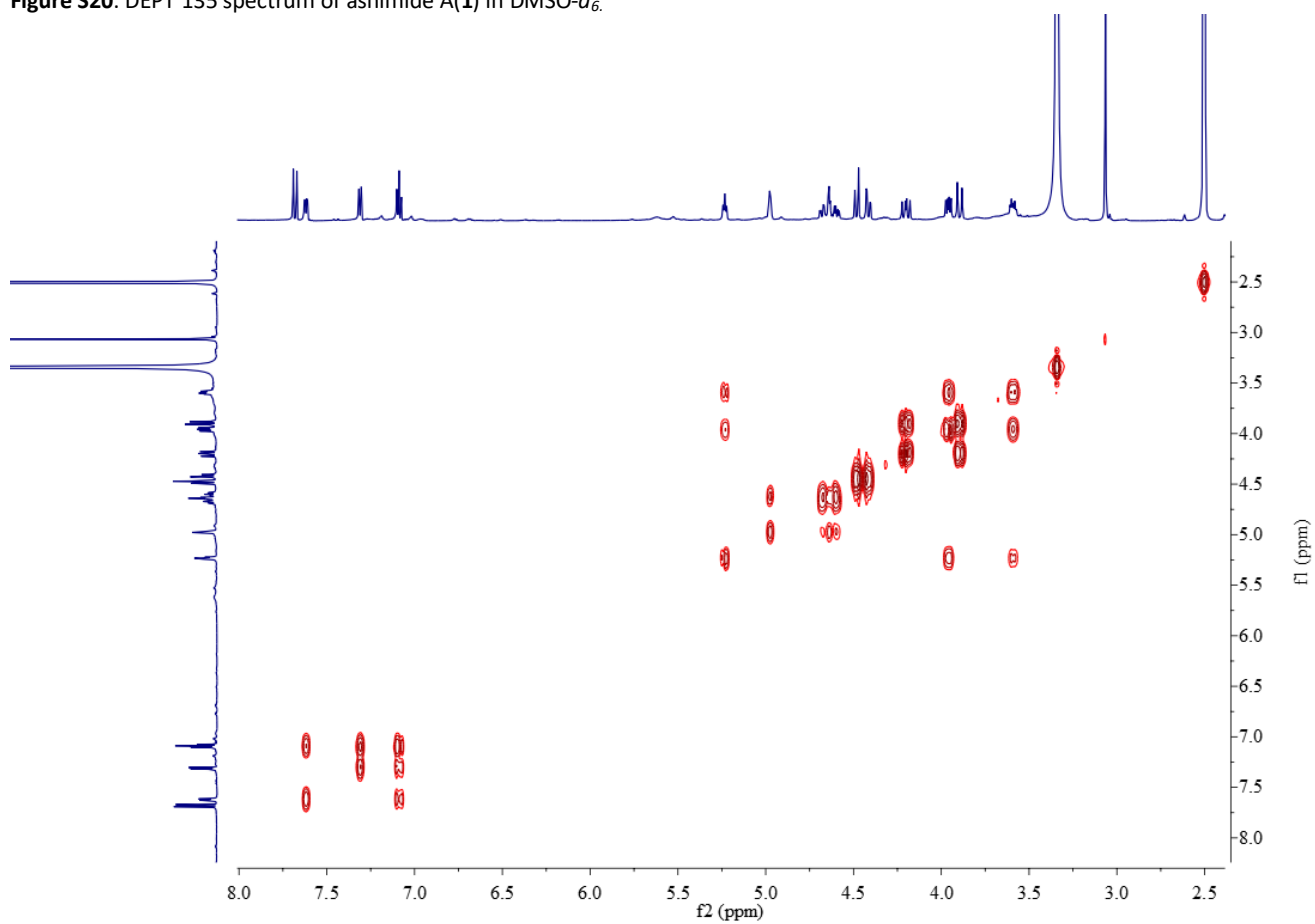


Figure S21. ^1H - ^1H COSY NMR spectrum of ashimide A(1) in DMSO- d_6 .

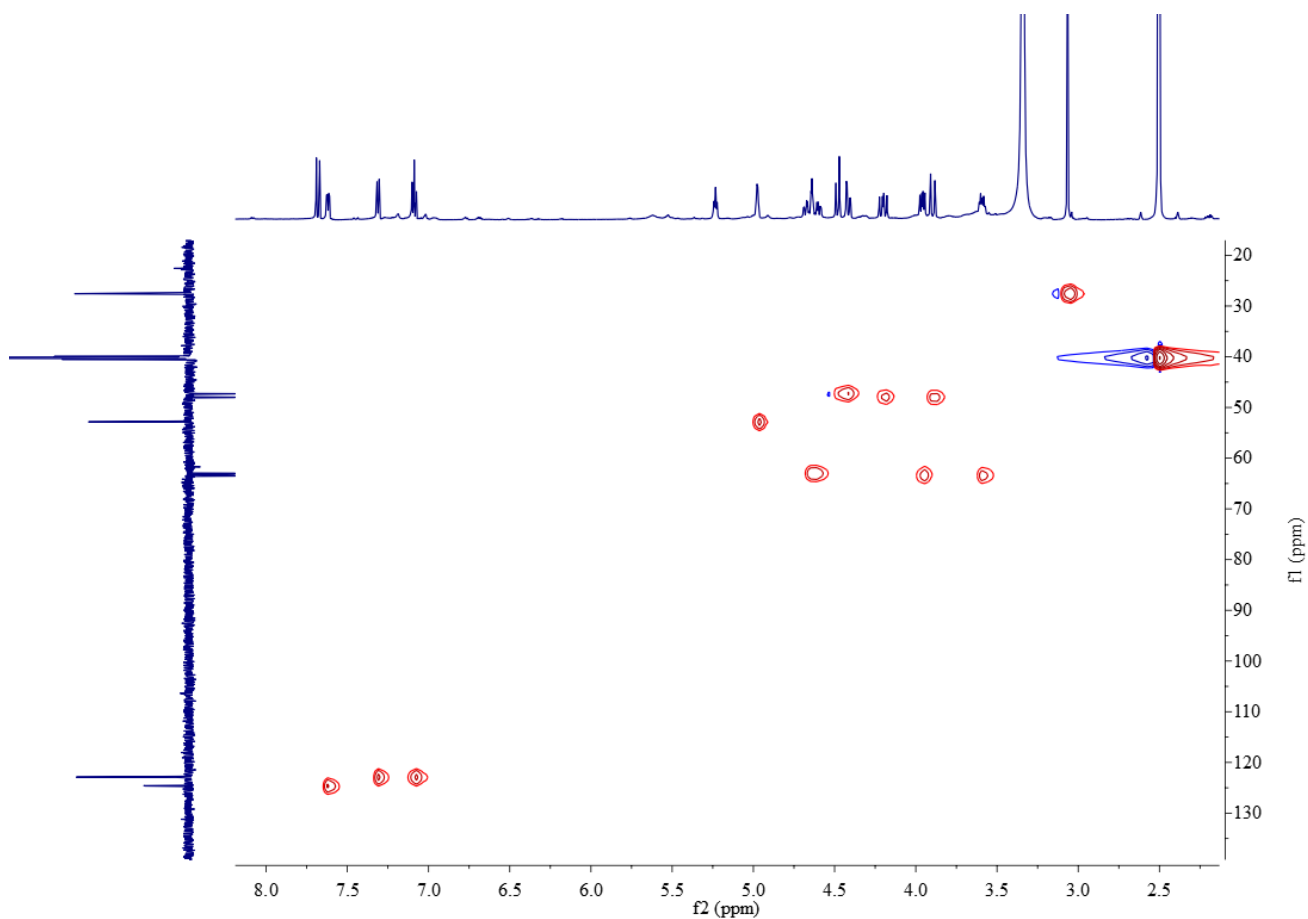


Figure S22. HSQC NMR spectrum of ashimide A(1) in DMSO- d_6 .

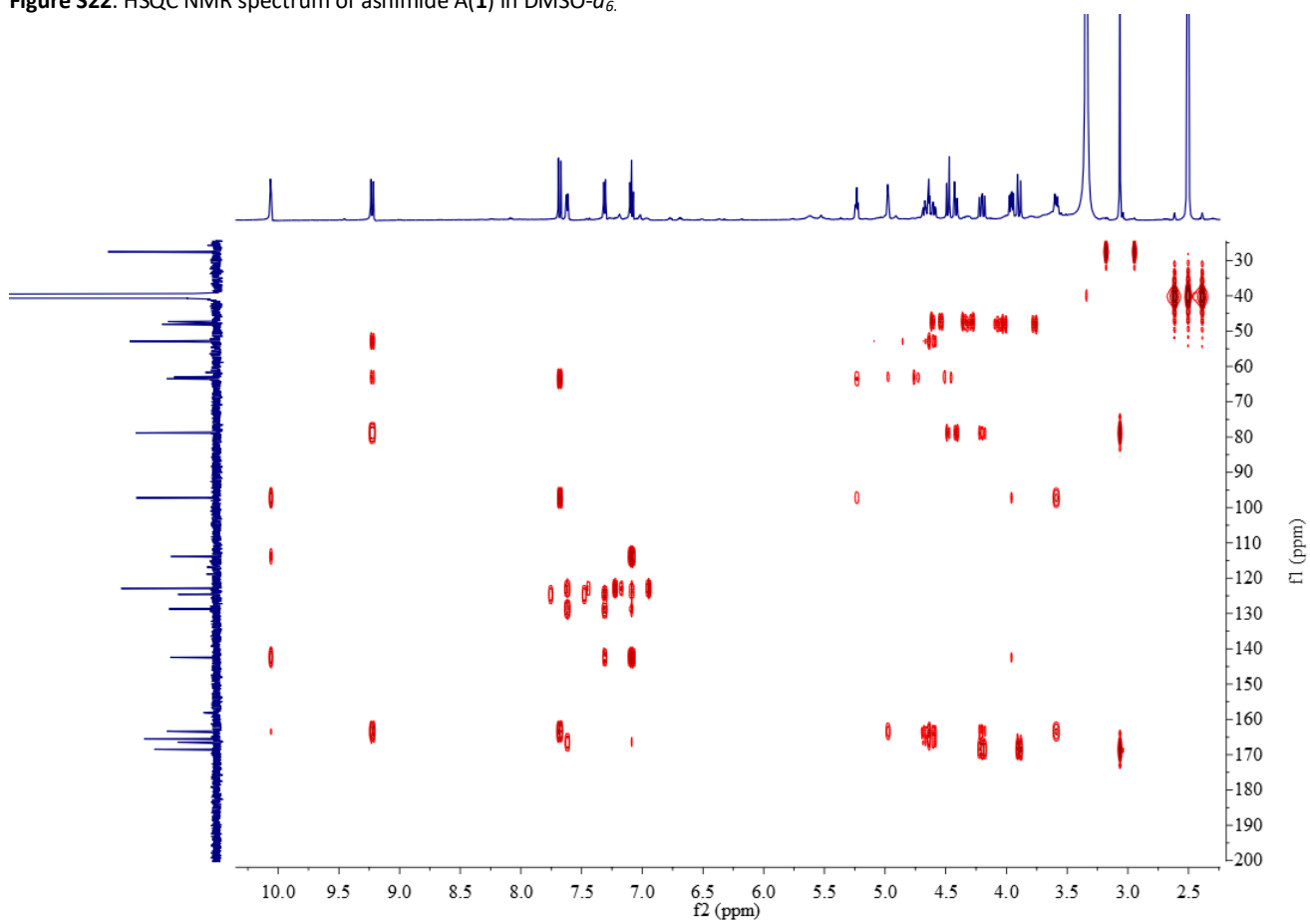


Figure S23. HMBC NMR spectrum of ashimide A(1) in DMSO- d_6 .

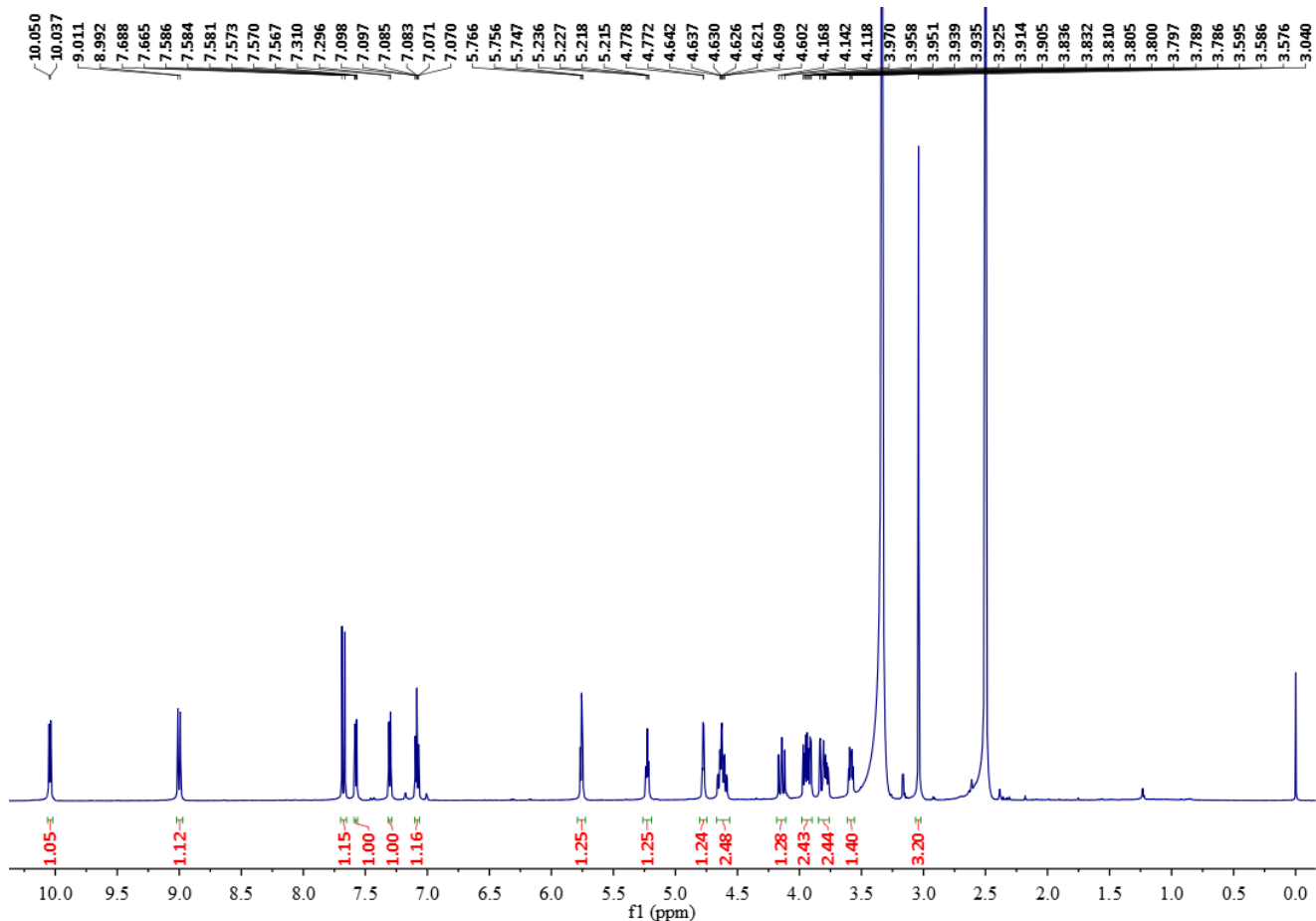


Figure S24. ^1H NMR spectrum of ashimide B (**2**) in $\text{DMSO-}d_6$ at 600 MHz.

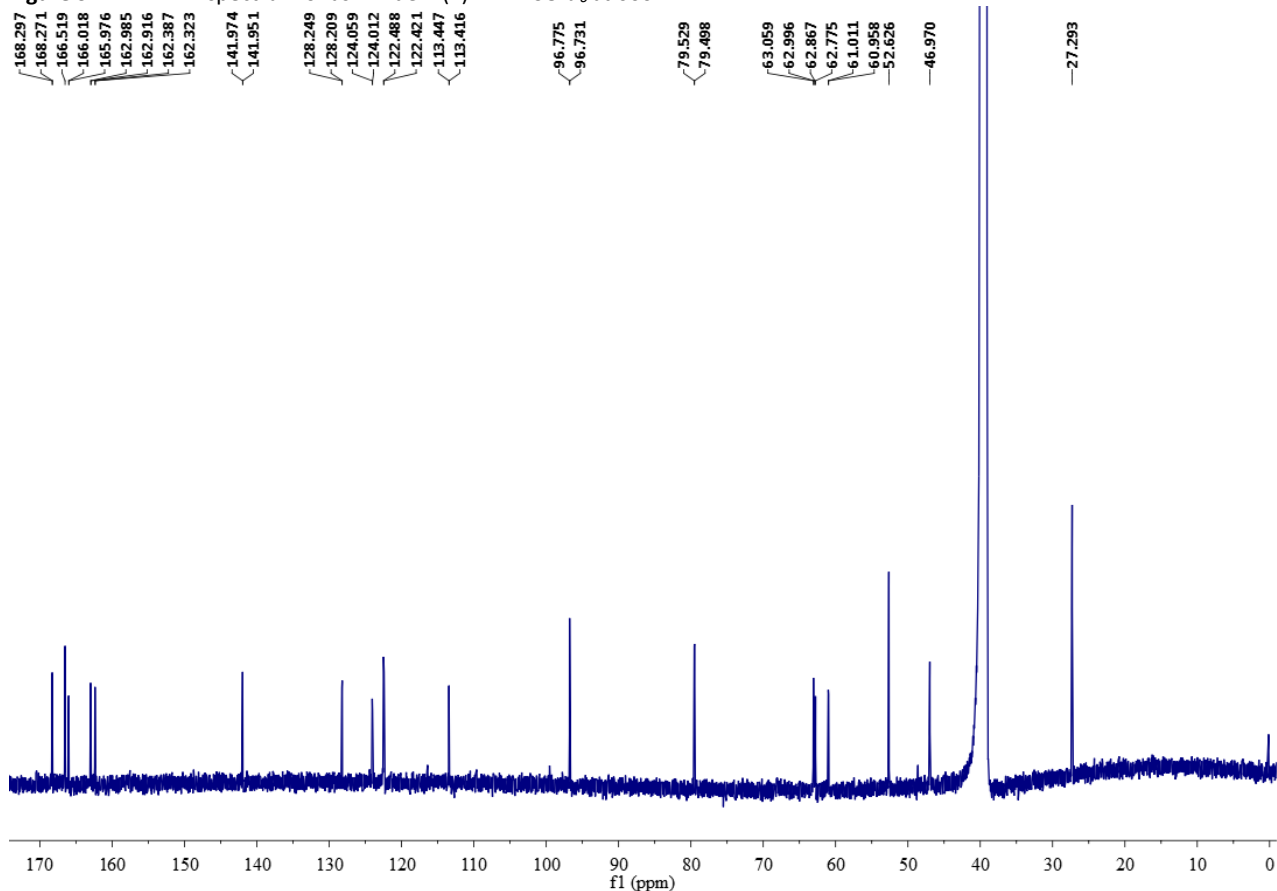


Figure S25. ^{13}C NMR spectrum of ashimide B (**2**) in $\text{DMSO-}d_6$ at 150 MHz.

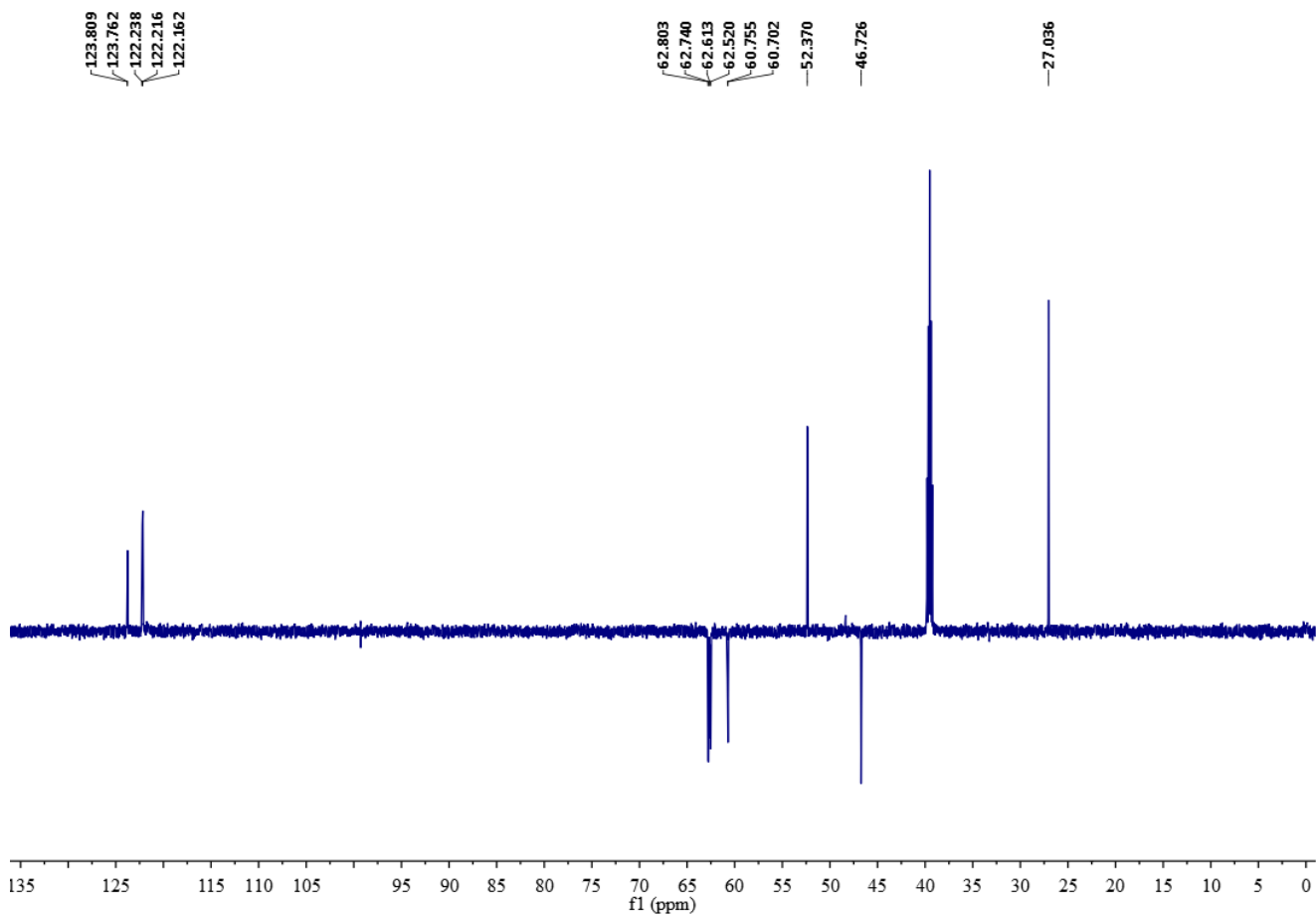


Figure S26. DEPT 135 spectrum of ashimide B (**2**) in DMSO- d_6 .

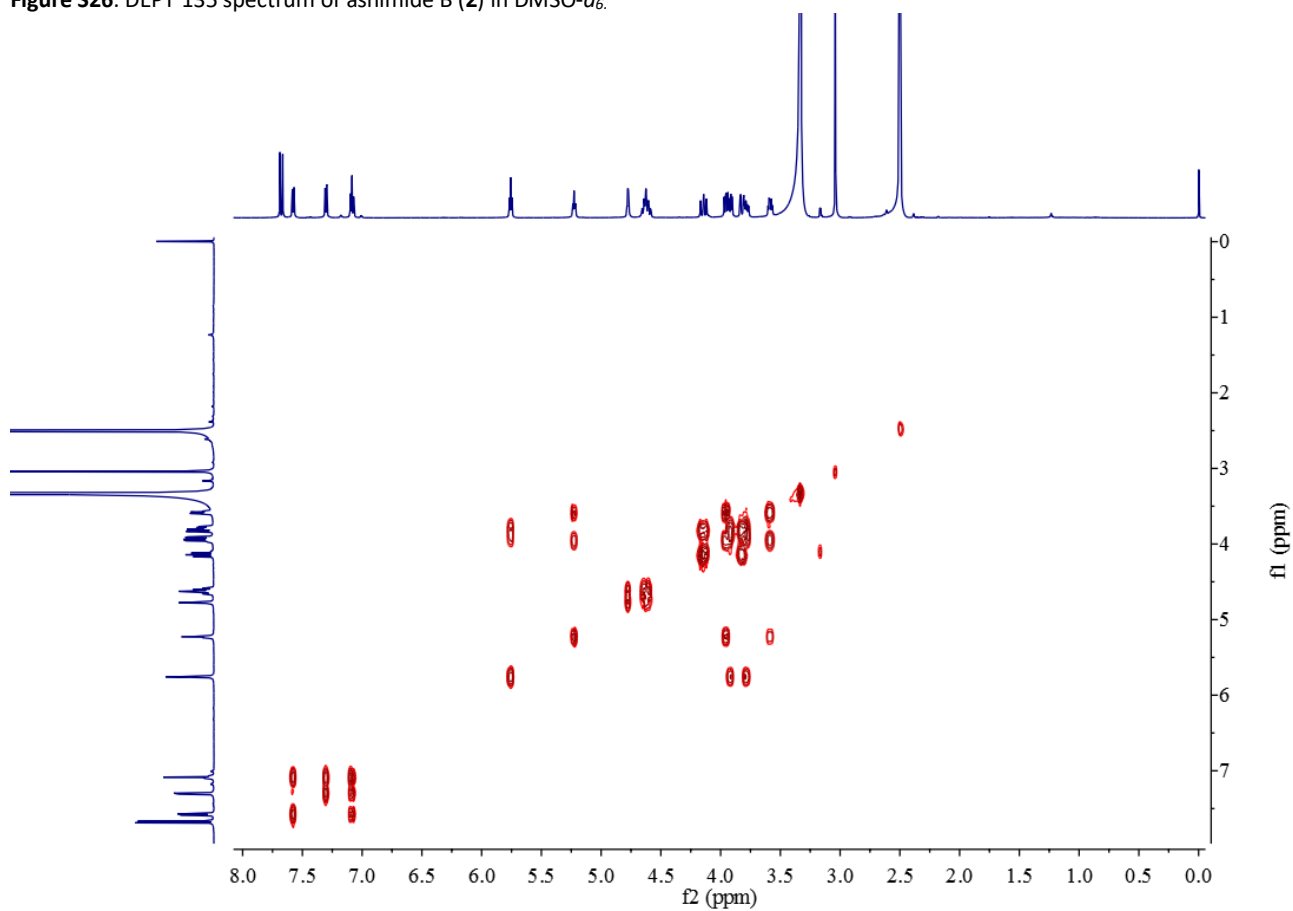


Figure S27. ^1H - ^1H COSY NMR spectrum of ashimide B (**2**) in DMSO- d_6 .

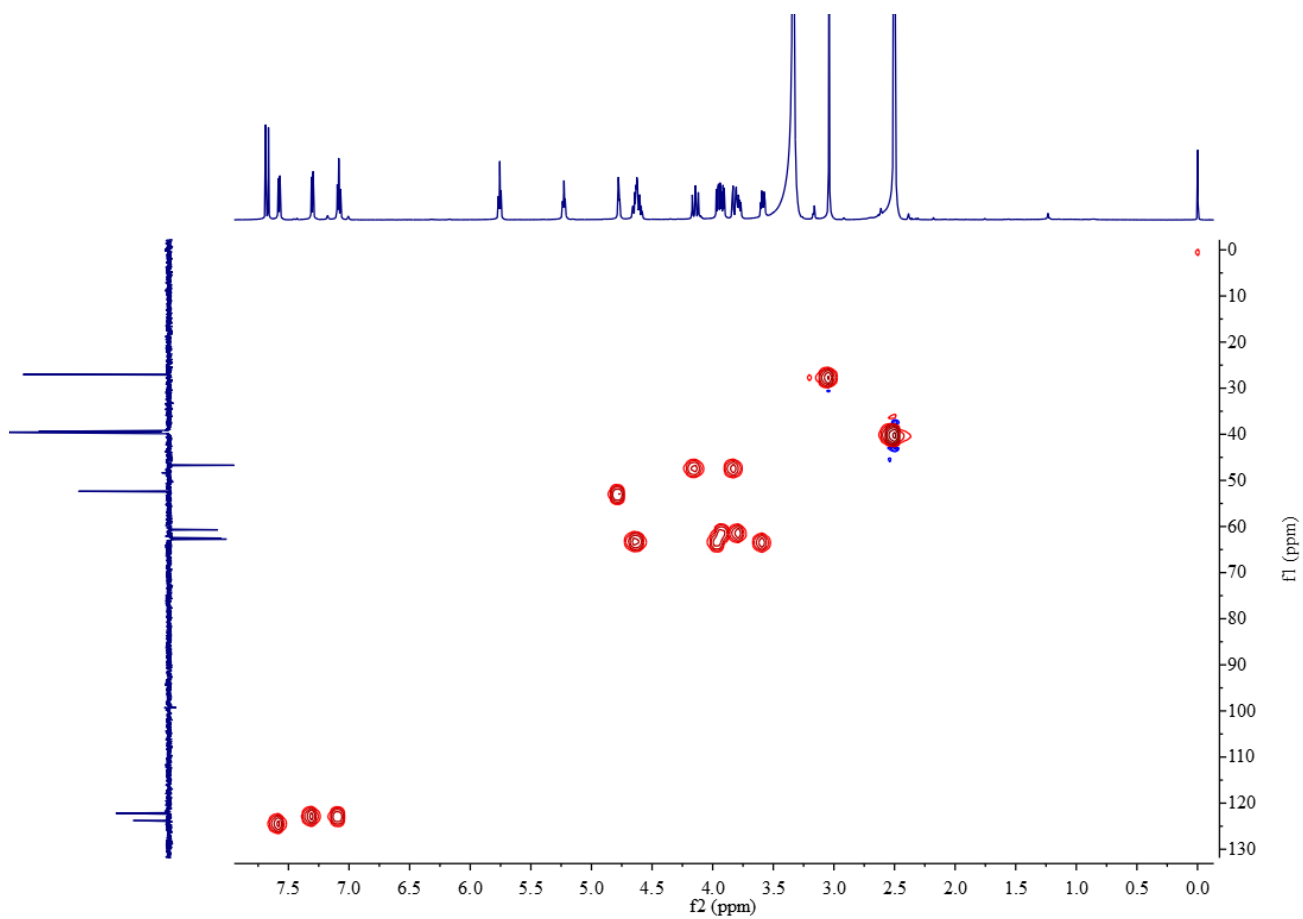


Figure S28. HSQC NMR spectrum of ashimide B (**2**) in DMSO- d_6 .

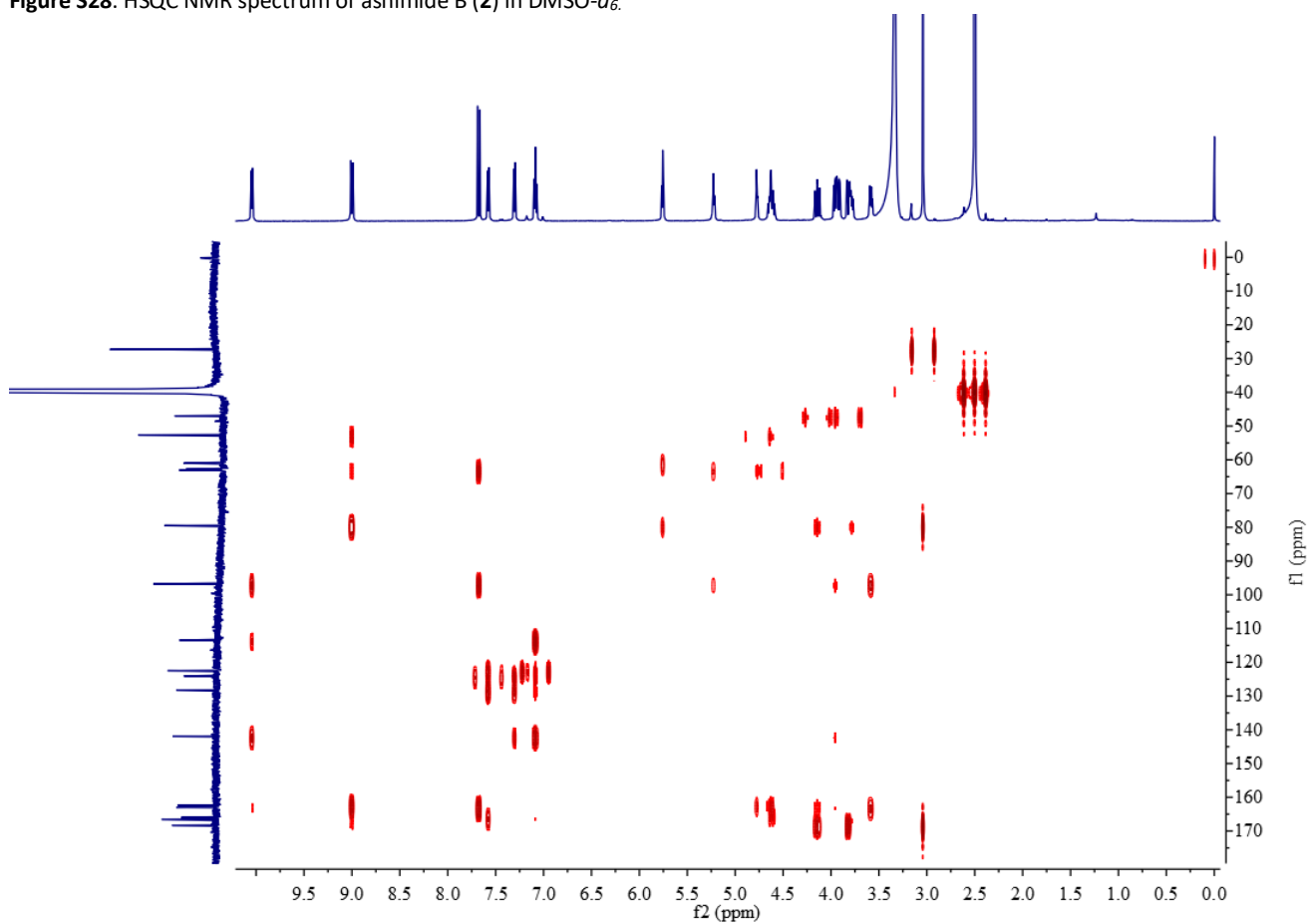


Figure S29. HMBC NMR spectrum of ashimide B (**2**) in DMSO- d_6 .

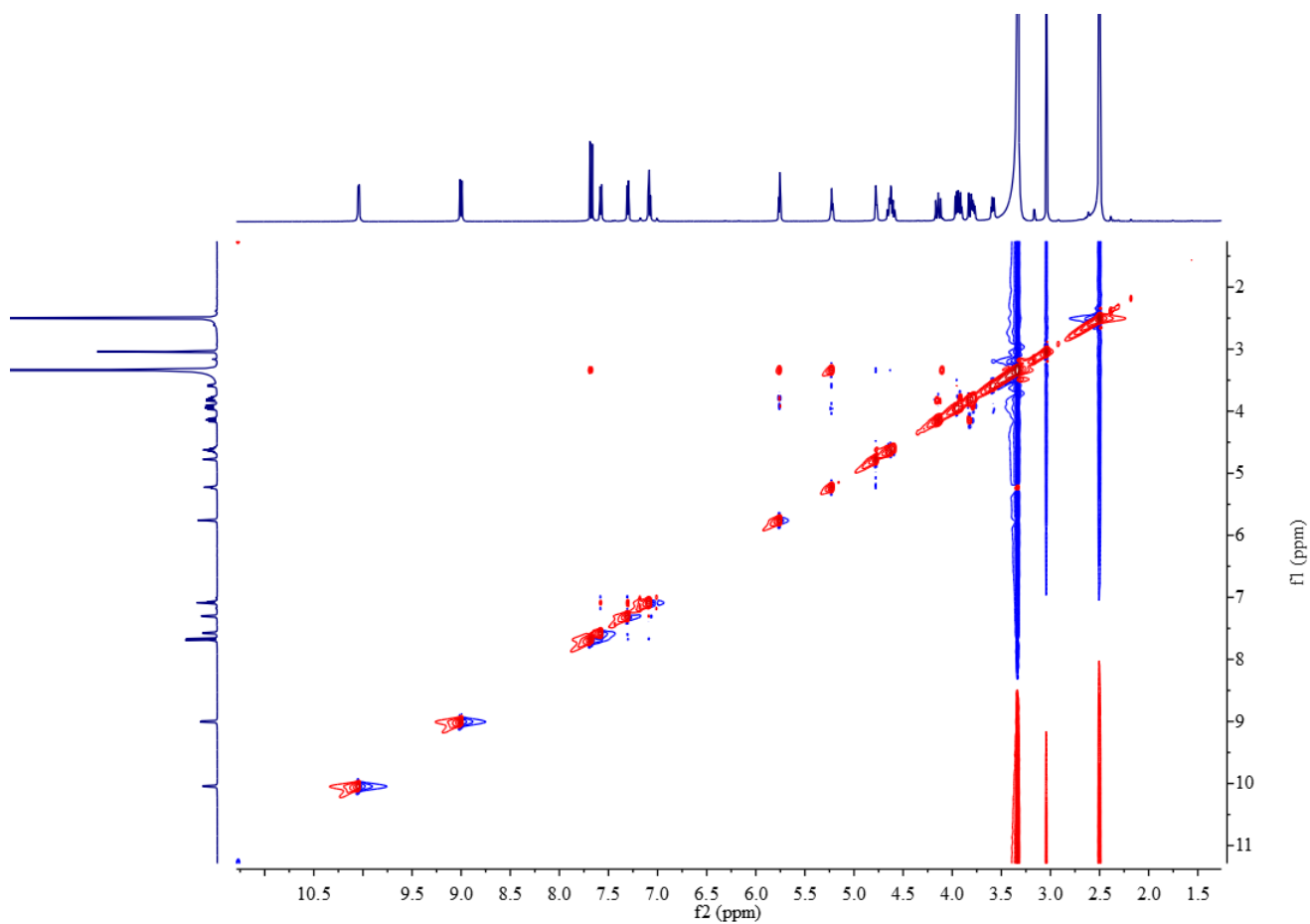


Figure S30. NOESY spectrum of ashimide B (**2**) in DMSO- d_6 .

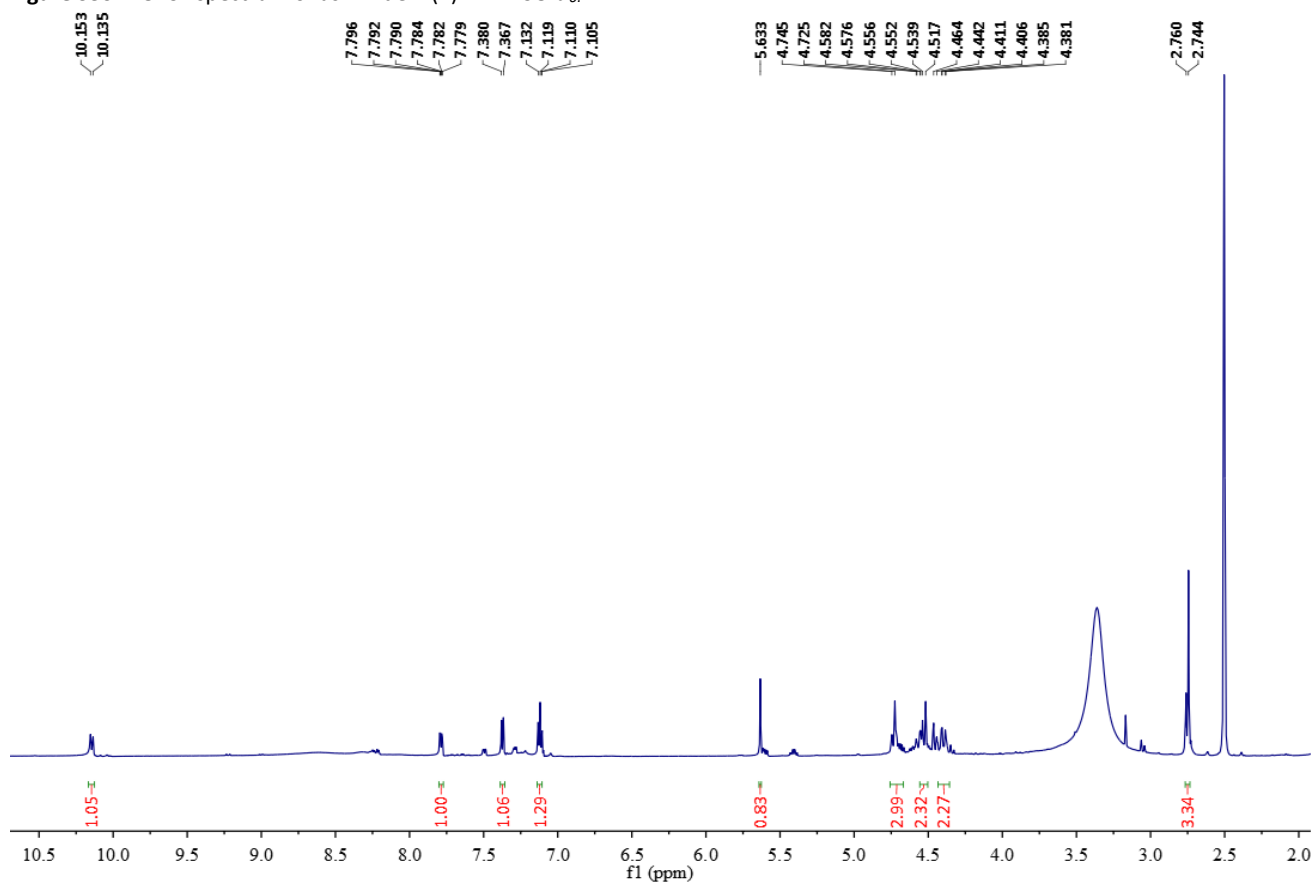


Figure S31. ^1H NMR spectrum of **3** in DMSO- d_6 at 600 MHz.

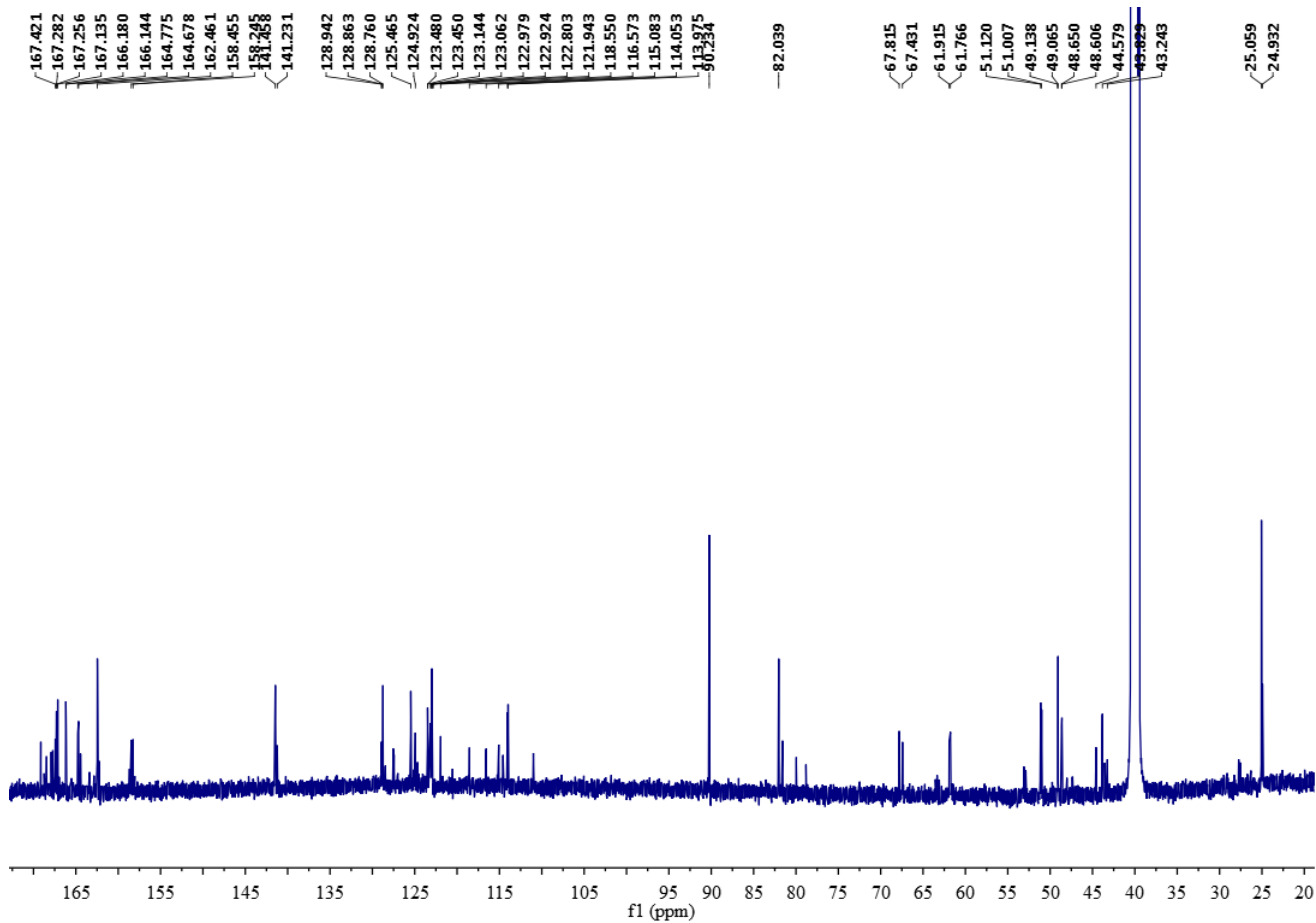


Figure S32. ^{13}C NMR spectrum of **3** in $\text{DMSO-}d_6$ at 150MHz.

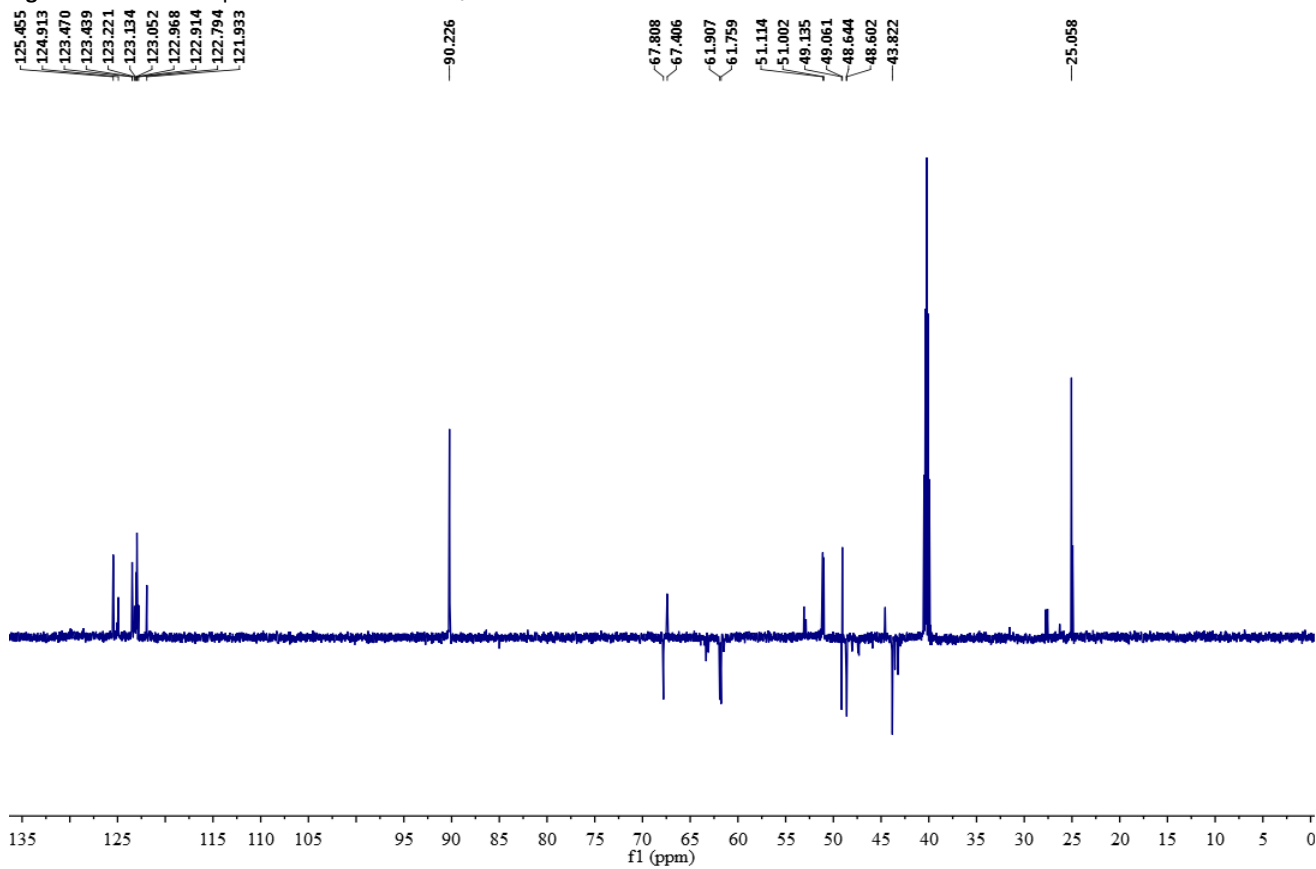


Figure S33. DEPT 135 spectrum of **3** in $\text{DMSO-}d_6$.

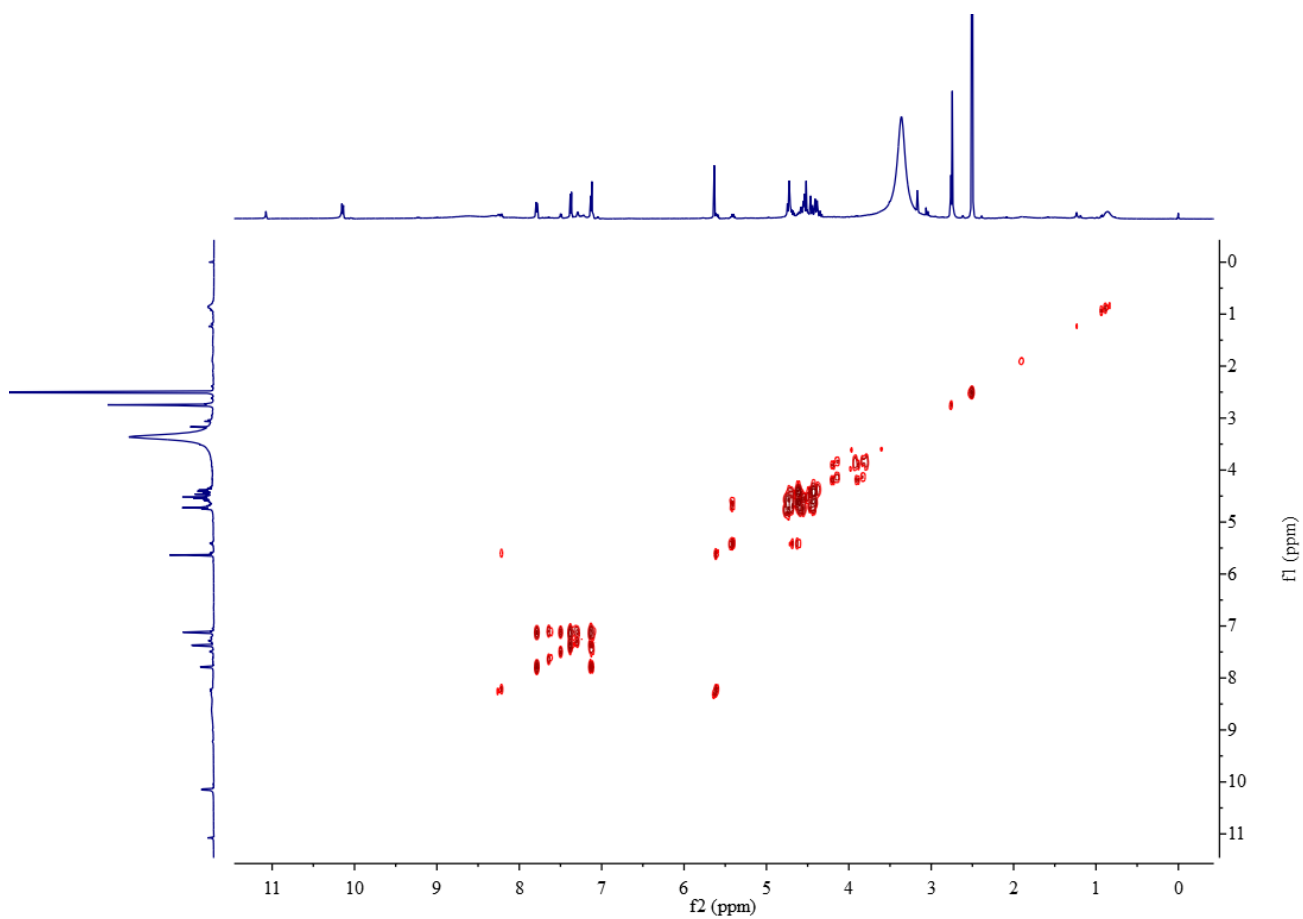


Figure S34. ^1H - ^1H COSY NMR spectrum of **3** in $\text{DMSO-}d_6$.

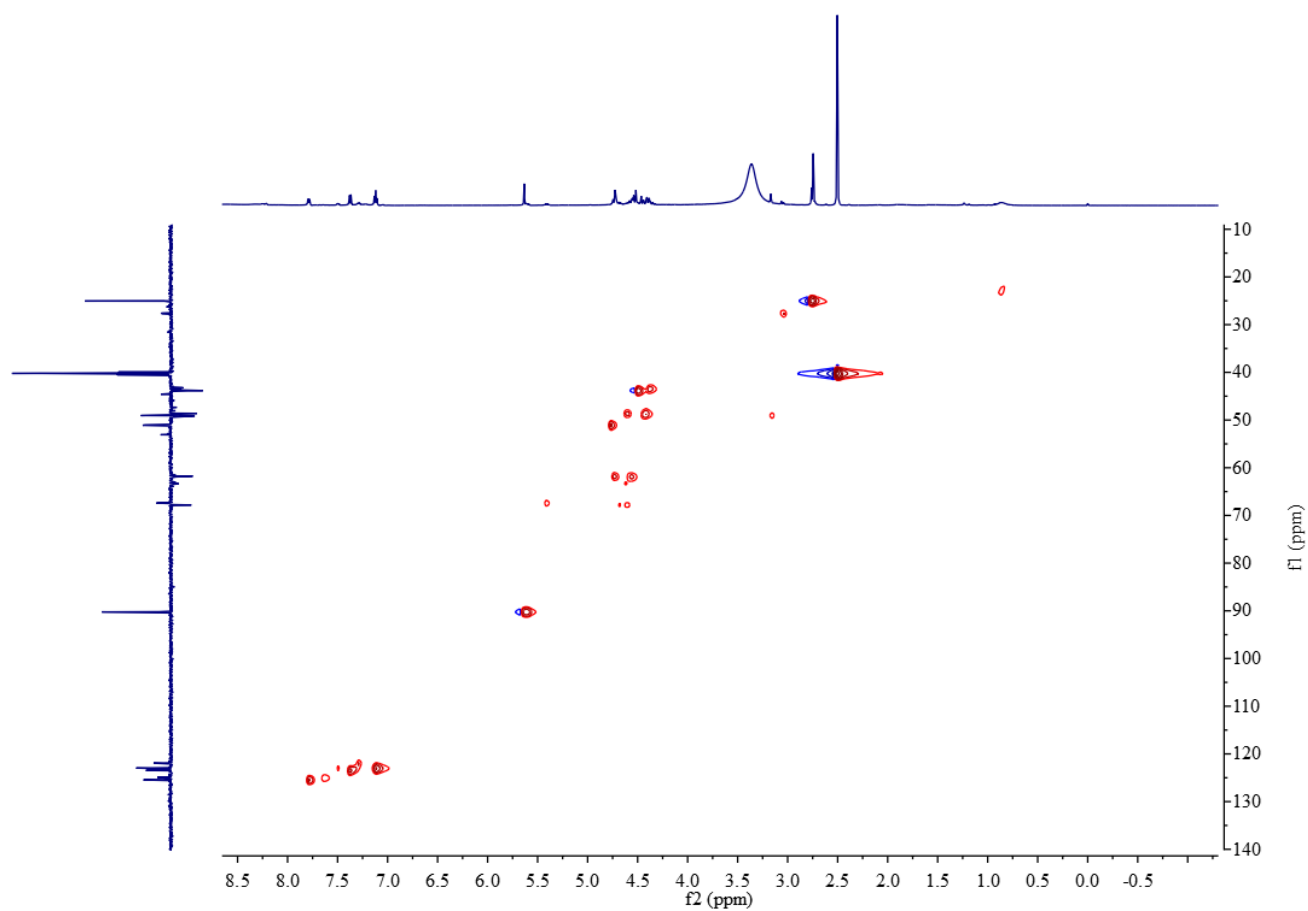


Figure S35. HSQC NMR spectrum of **3** in $\text{DMSO-}d_6$.

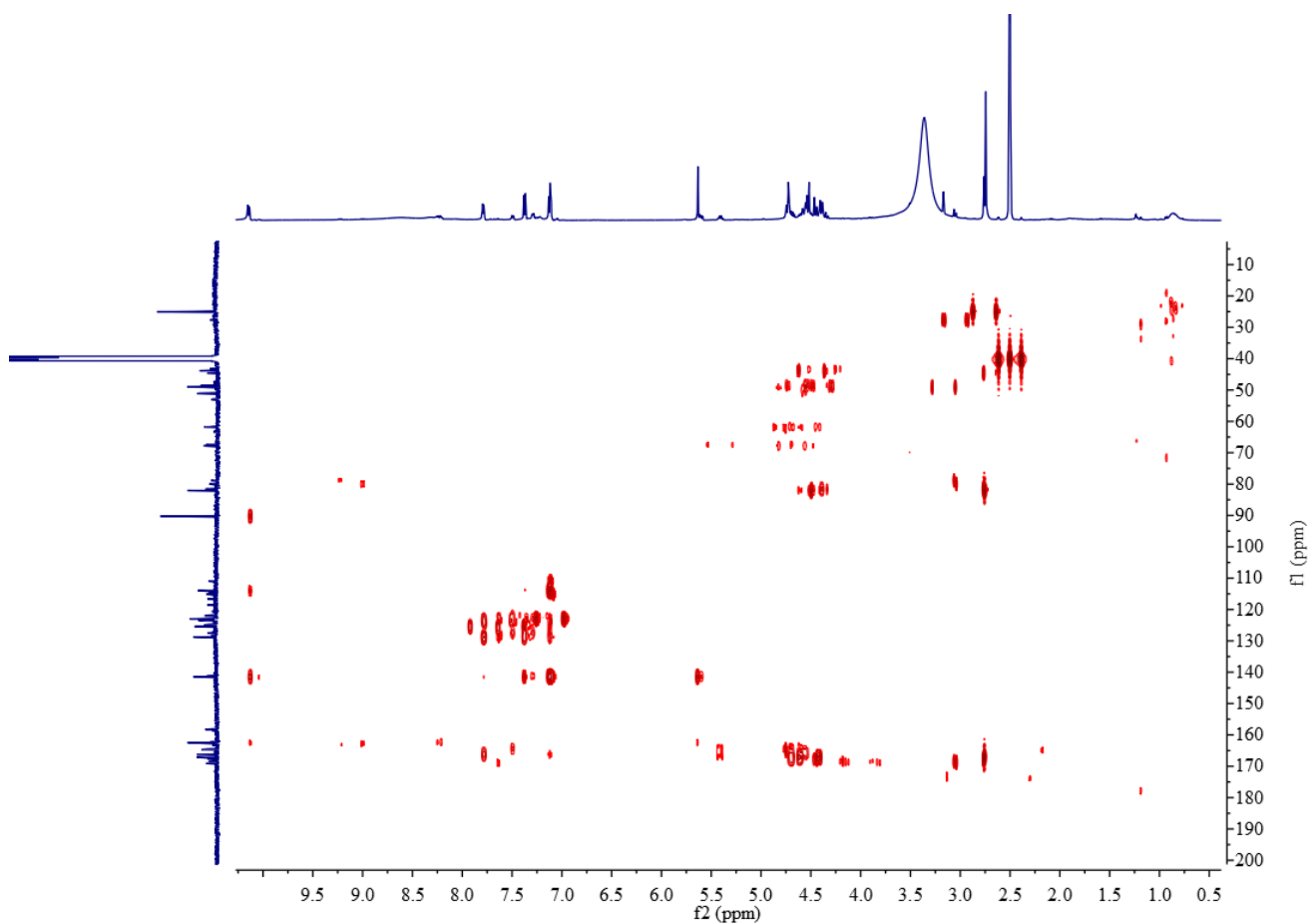


Figure S36. HMBC NMR spectrum of **3** in DMSO- d_6 .

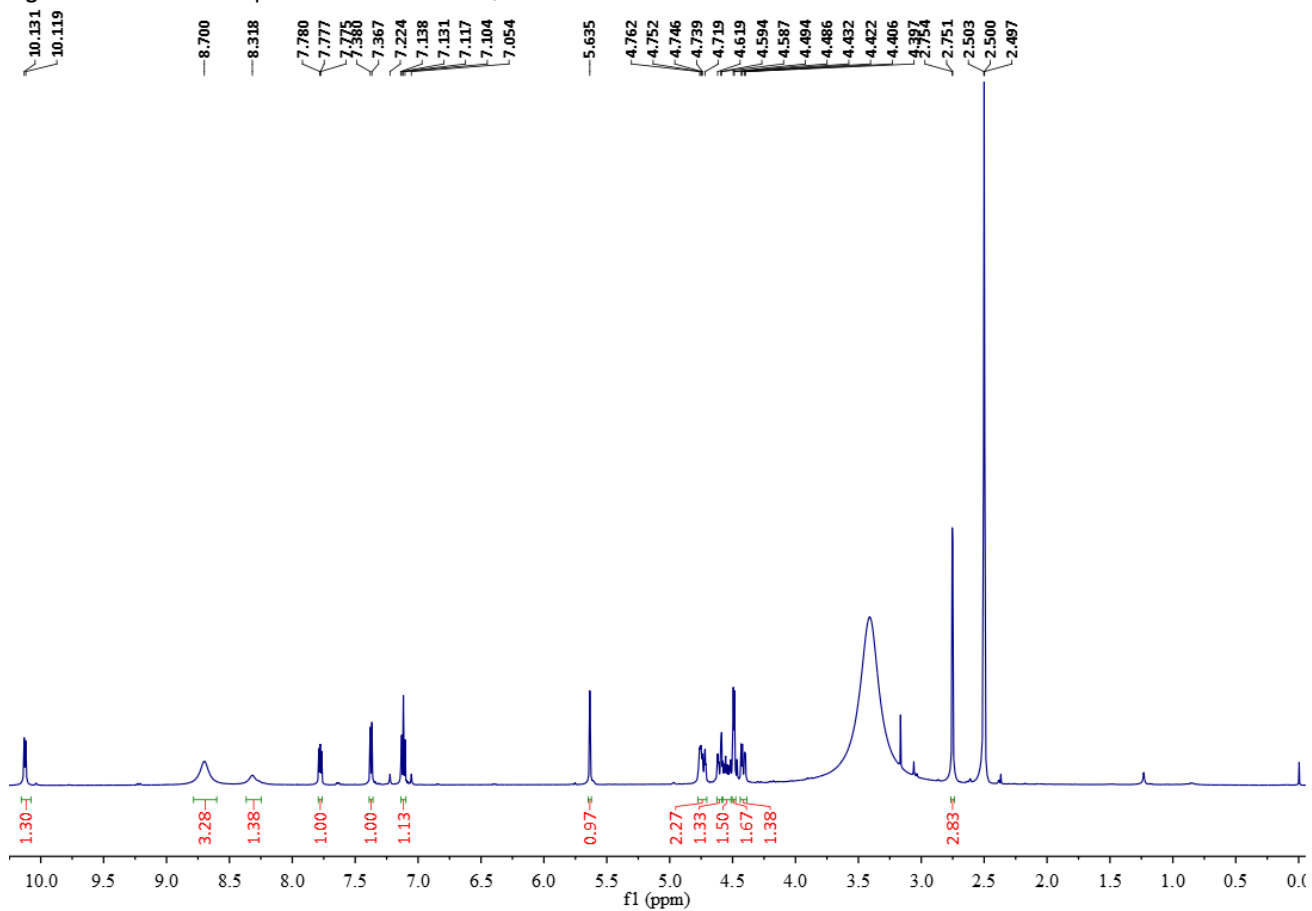


Figure S37. ^1H NMR spectrum of **4** in DMSO- d_6 at 600 MHz.

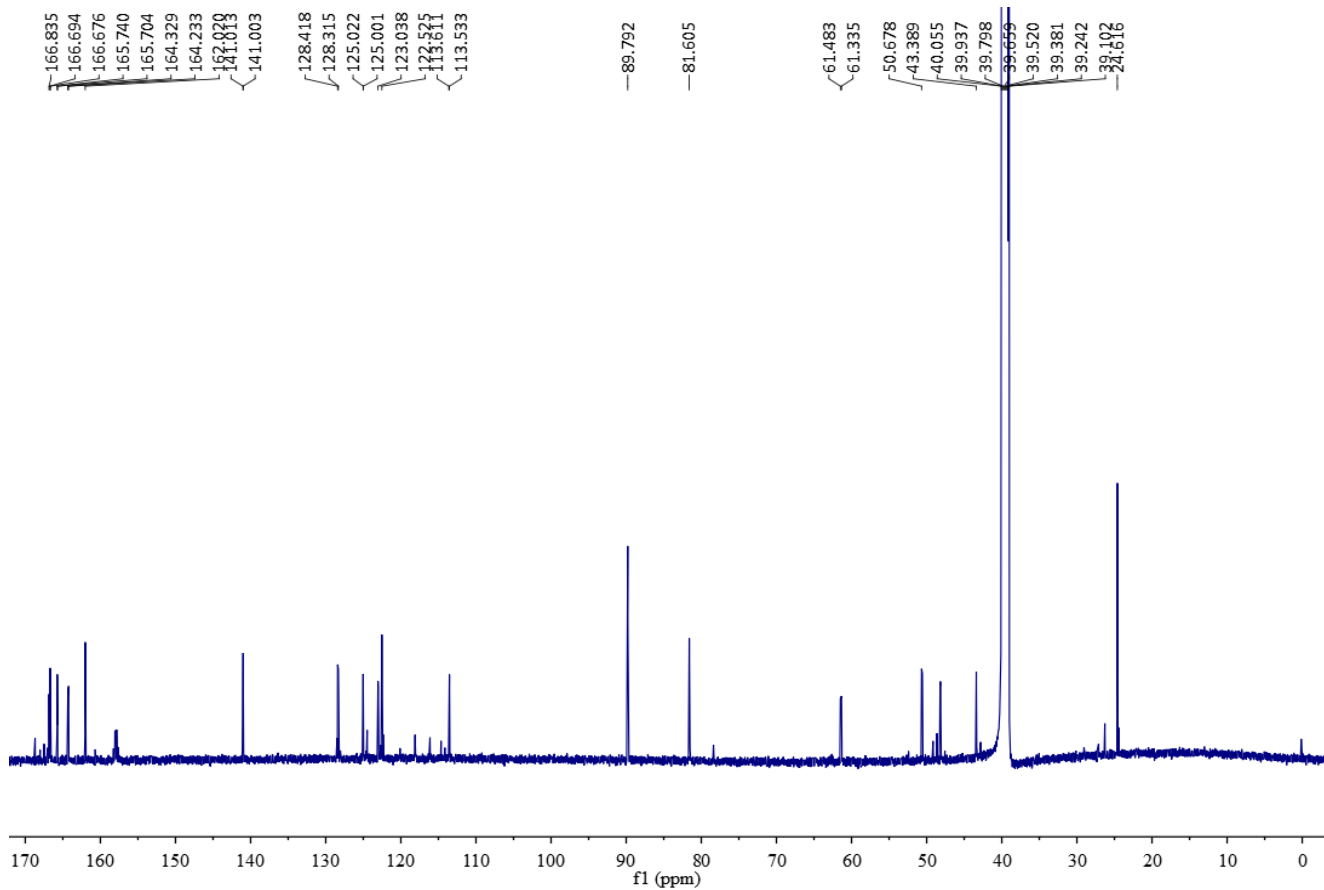


Figure S38. ^{13}C NMR spectrum of **4** in $\text{DMSO-}d_6$ at 150MHz.

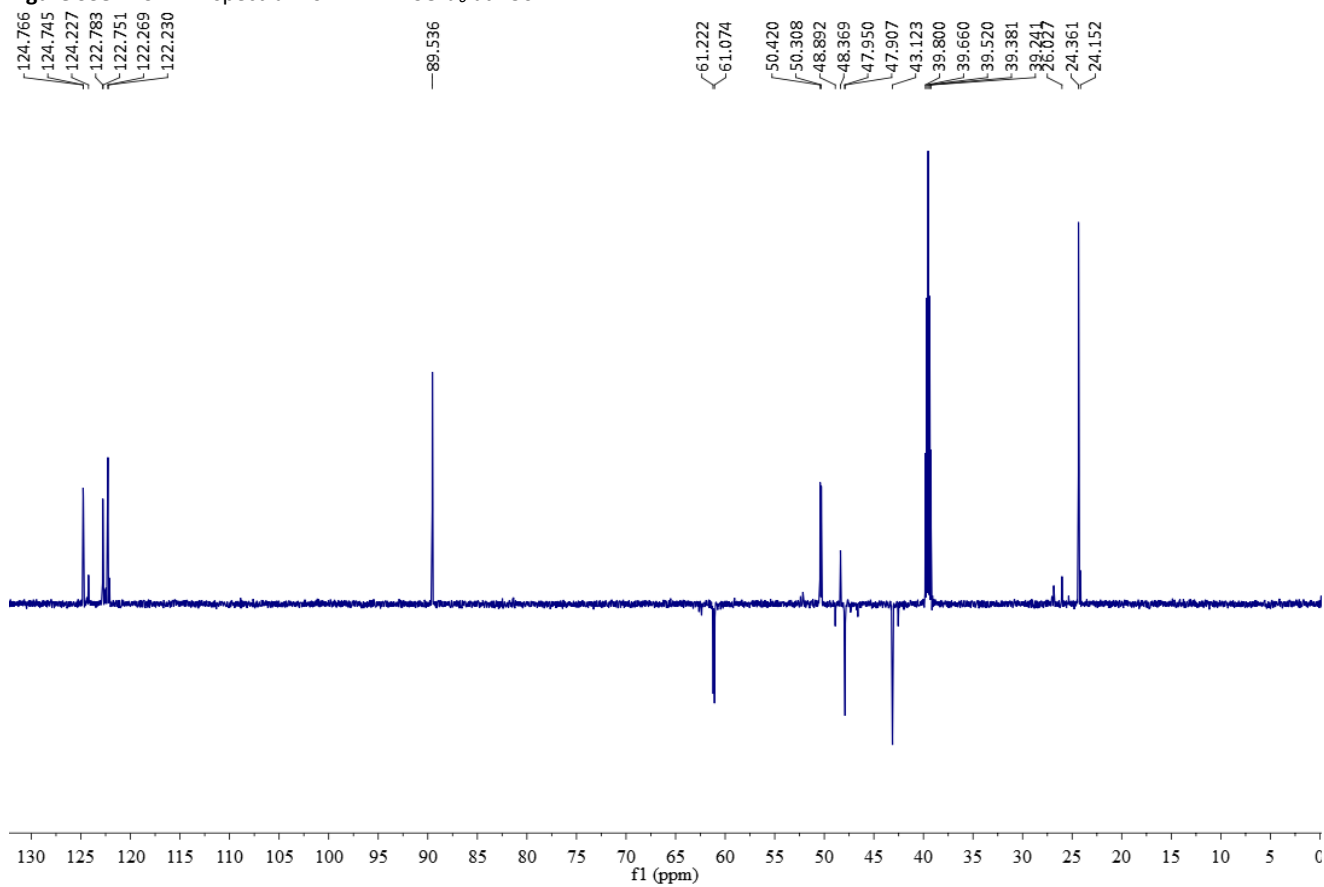


Figure S39. DEPT 135 spectrum of **4** in $\text{DMSO-}d_6$.

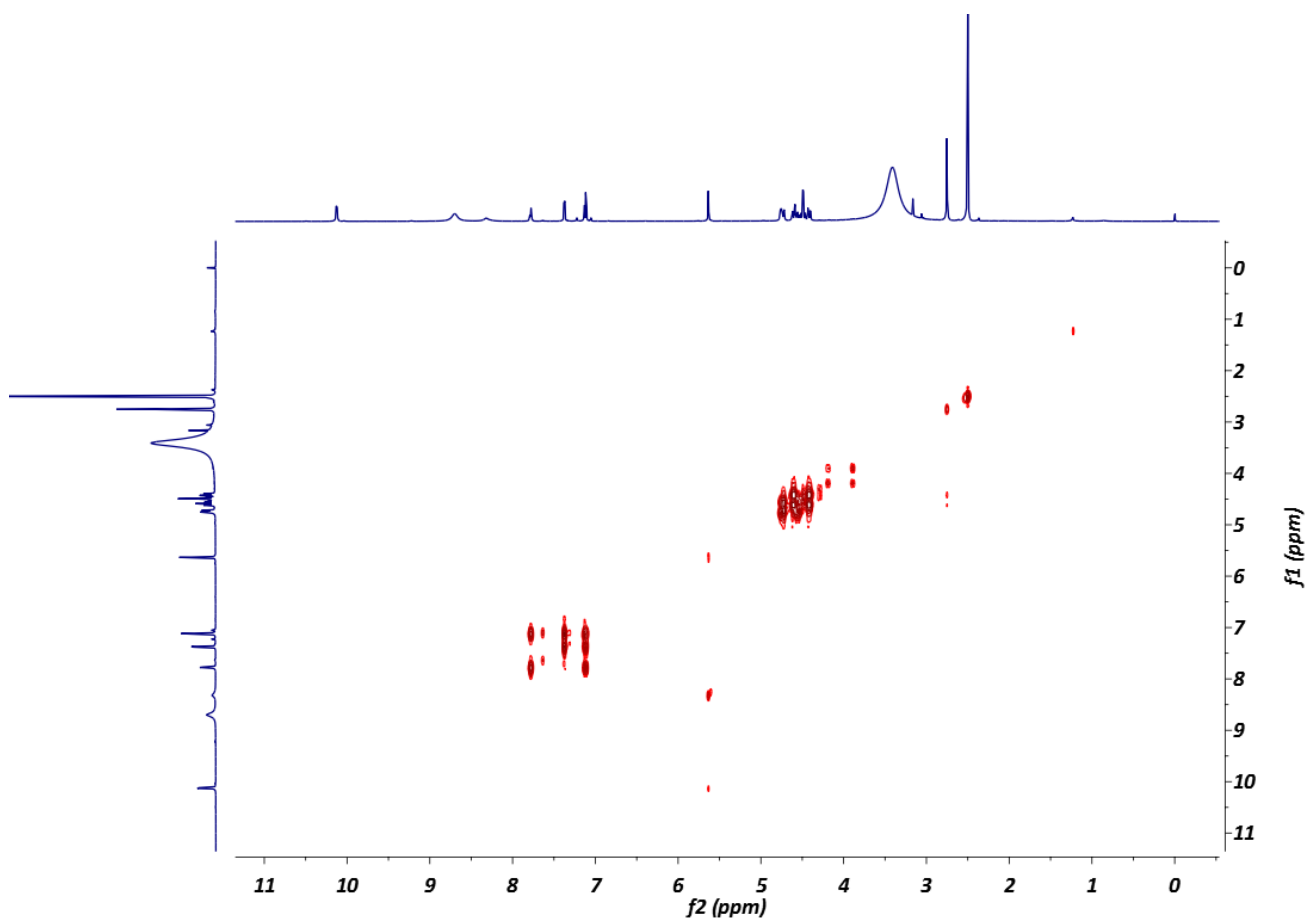


Figure S40. ^1H - ^1H COSY NMR spectrum of **4** in $\text{DMSO-}d_6$.

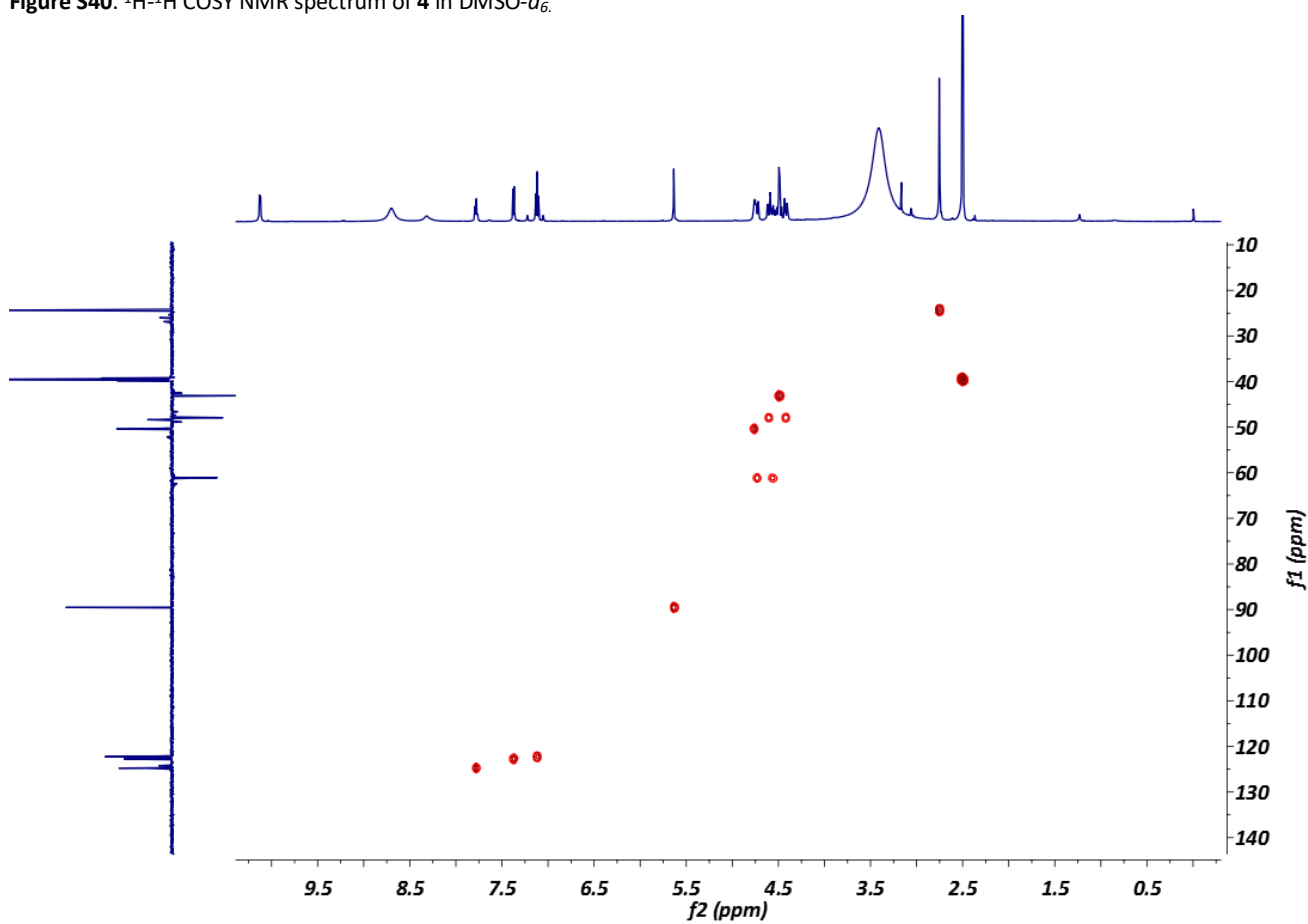


Figure S41. HSQC NMR spectrum of **4** in $\text{DMSO-}d_6$.

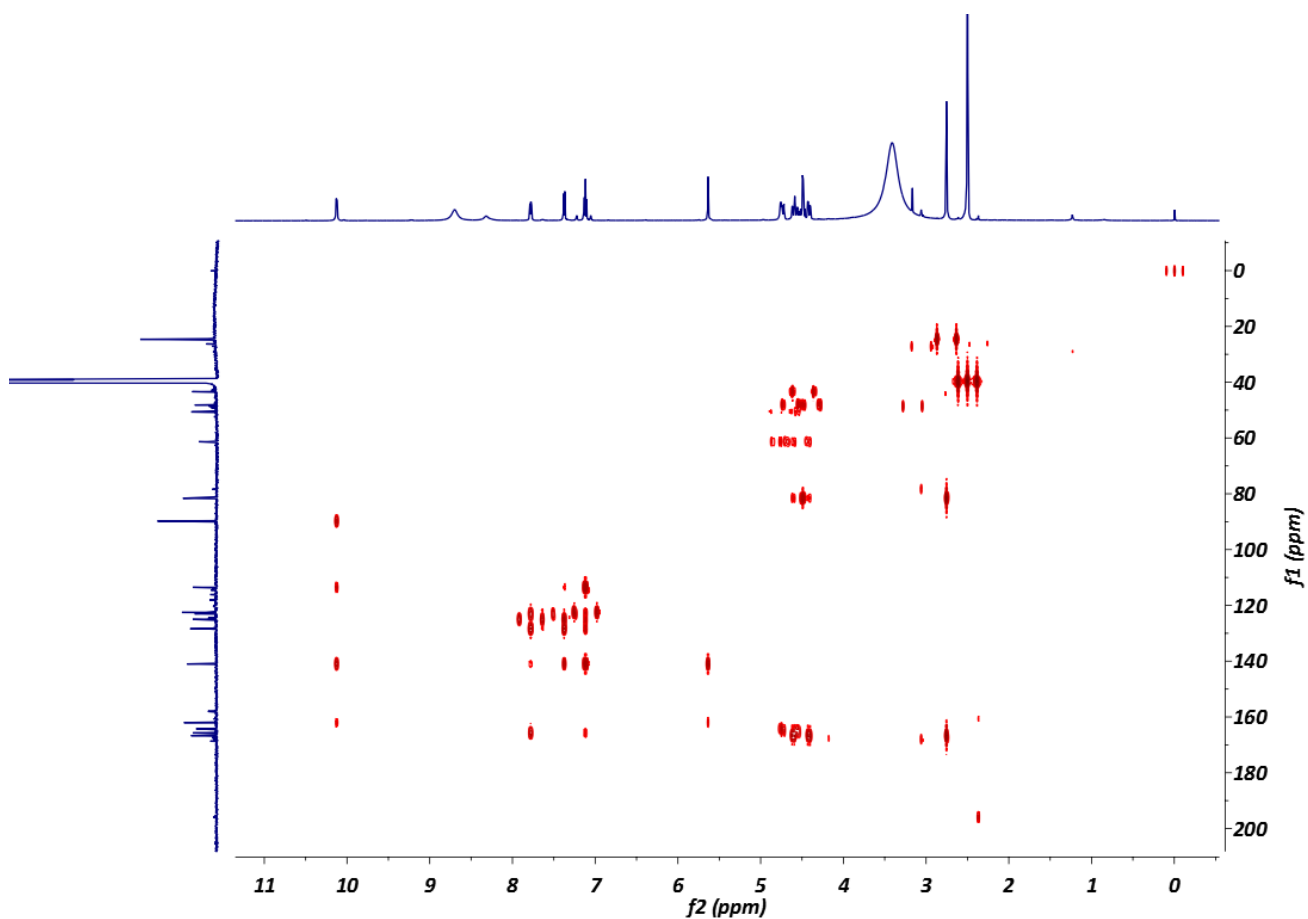


Figure S42. HMBC NMR spectrum of **4** in DMSO- d_6 .

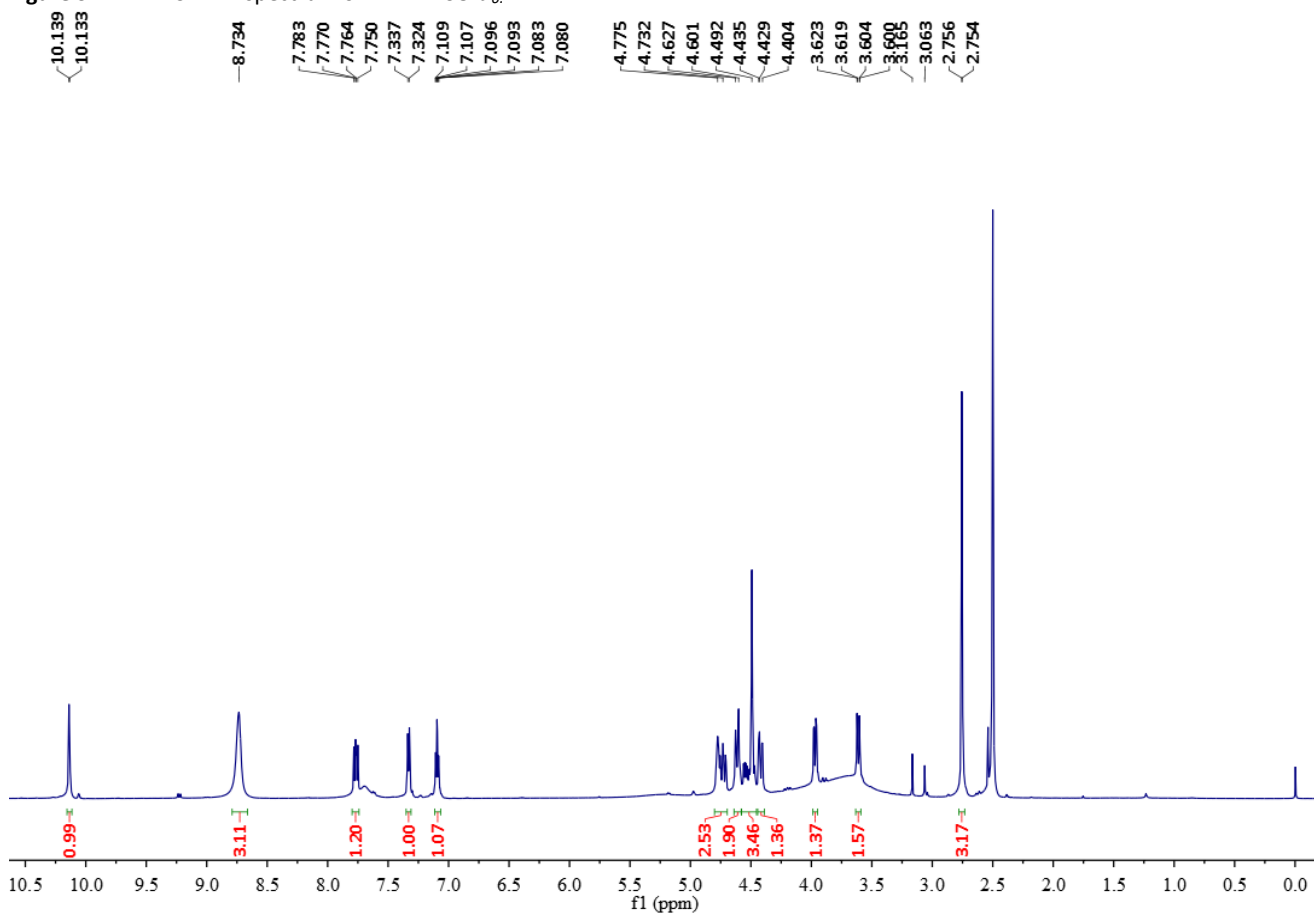


Figure S43. ^1H NMR spectrum of **5** in DMSO- d_6 at 600 MHz.

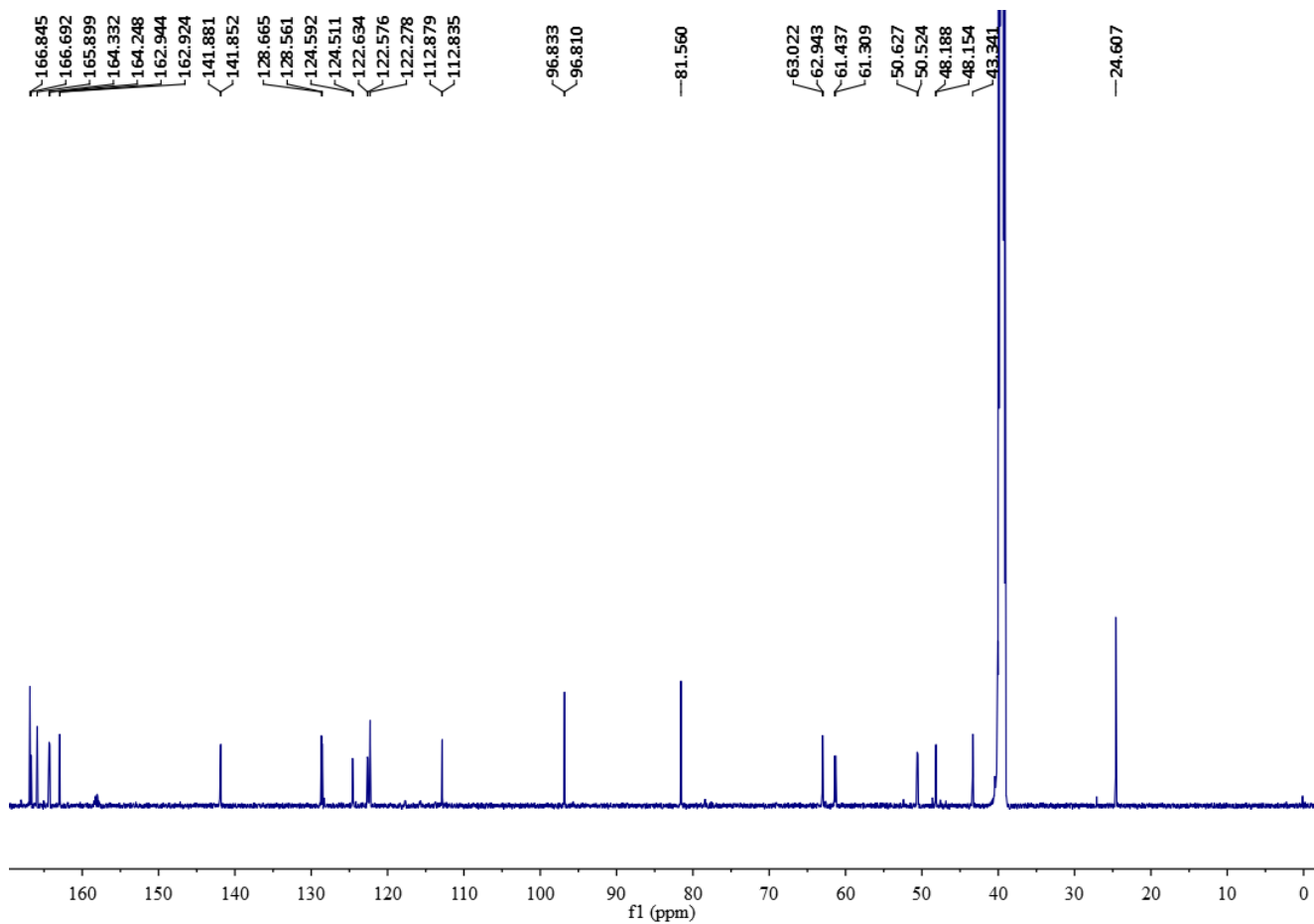


Figure S44. ^{13}C NMR spectrum of **5** in $\text{DMSO-}d_6$ at 150 MHz.

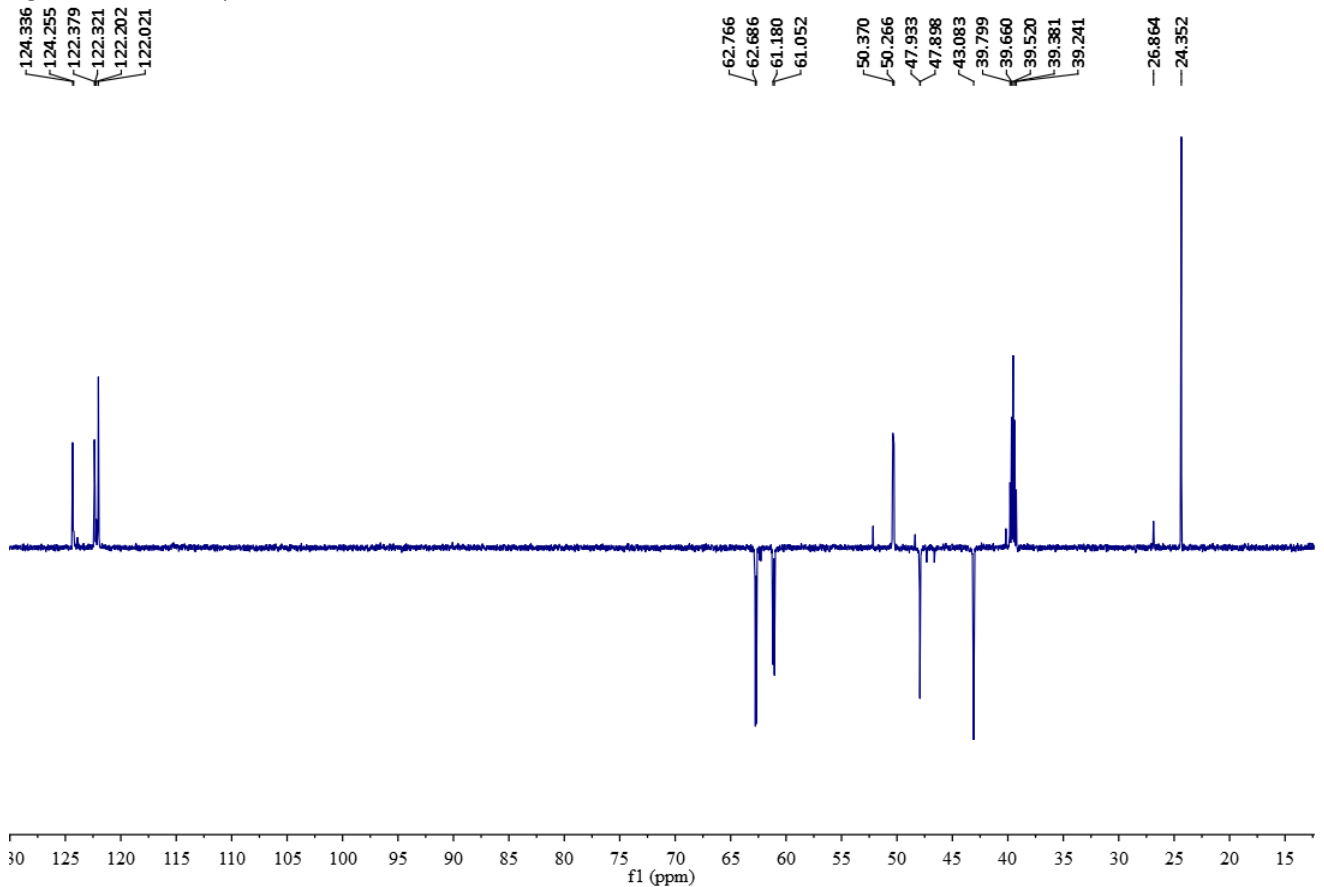


Figure S45. DEPT 135 spectrum of **5** in $\text{DMSO-}d_6$.

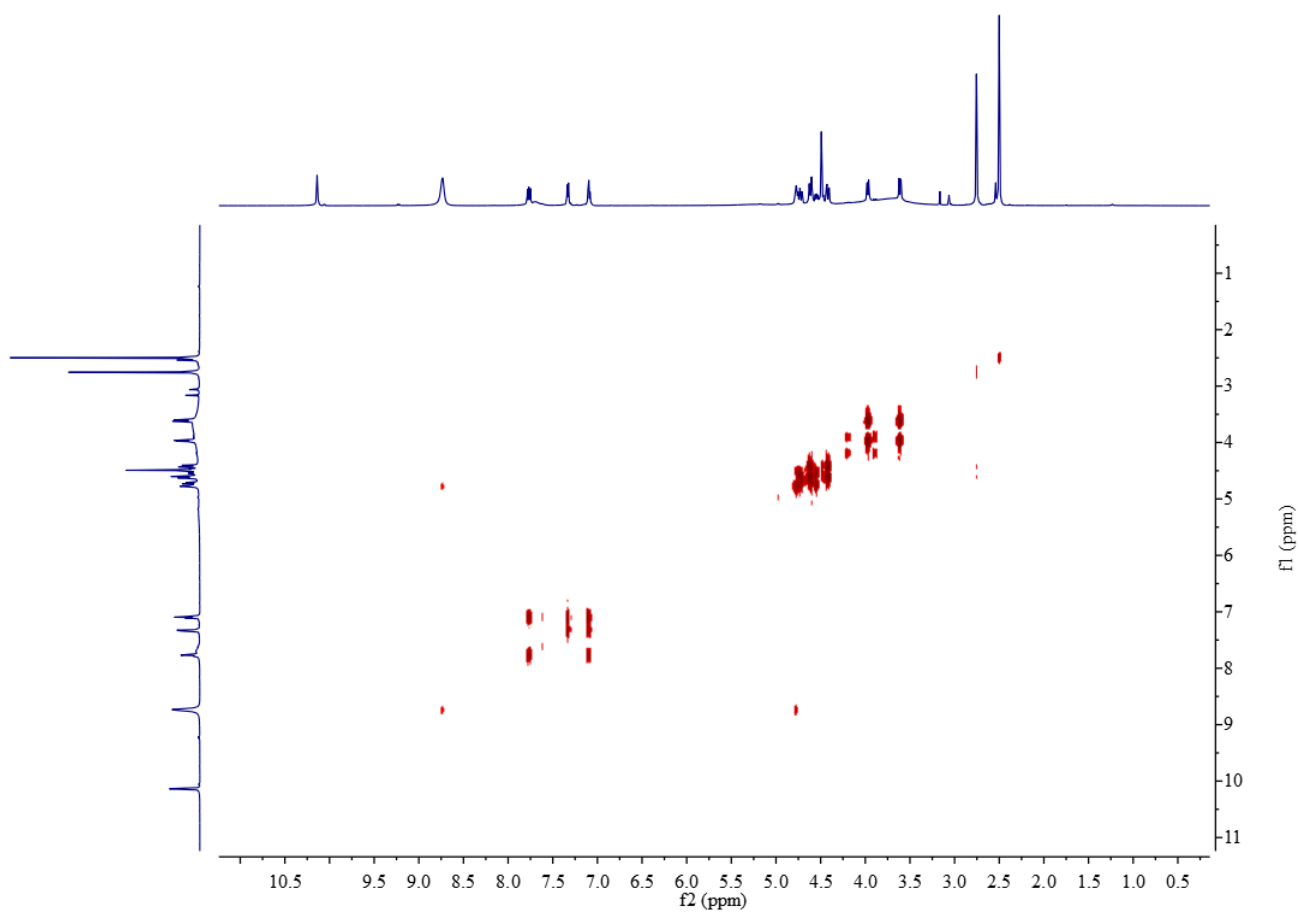


Figure S46. ^1H - ^1H COSY NMR spectrum of **5** in $\text{DMSO-}d_6$.

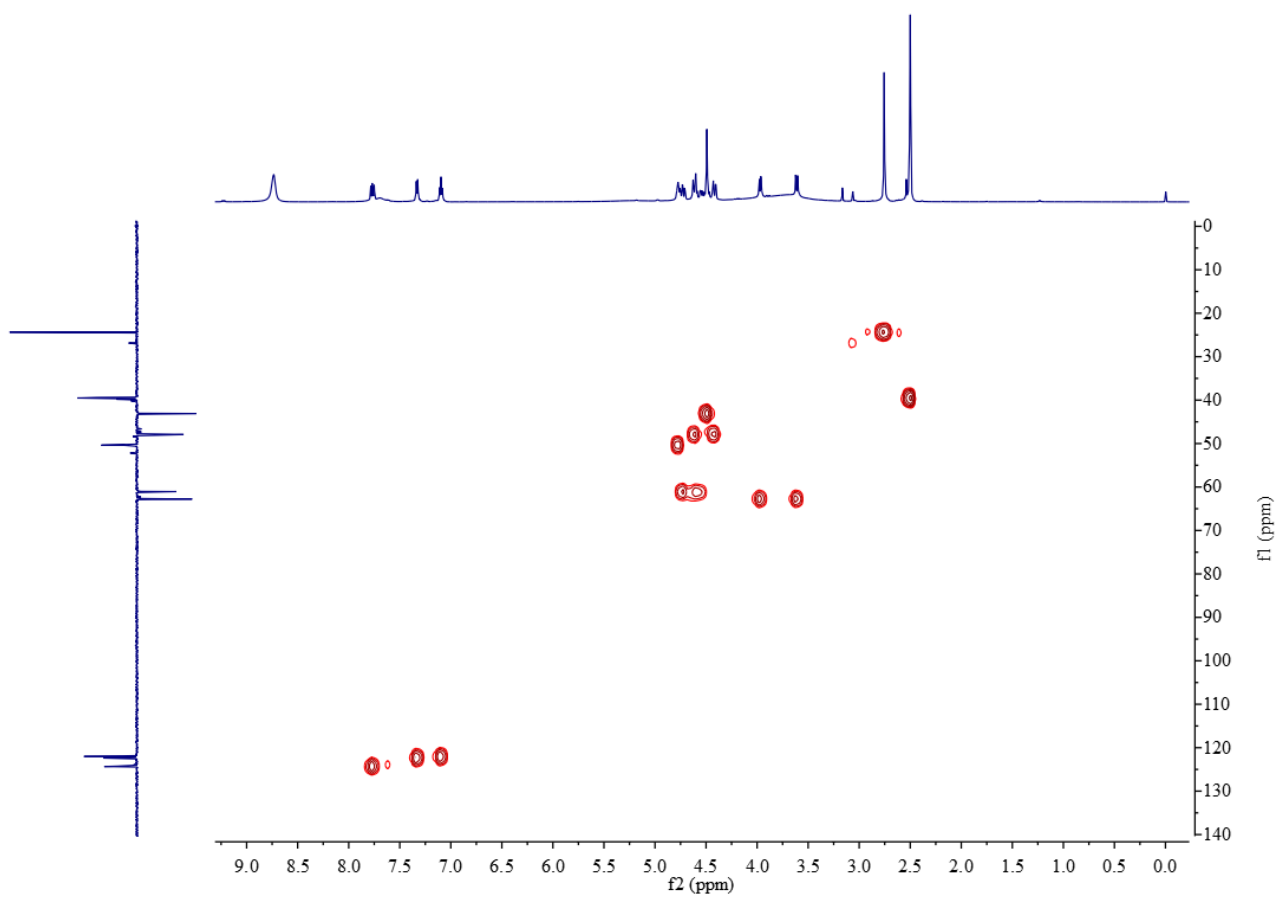


Figure S47. HSQC NMR spectrum of **5** in $\text{DMSO-}d_6$.

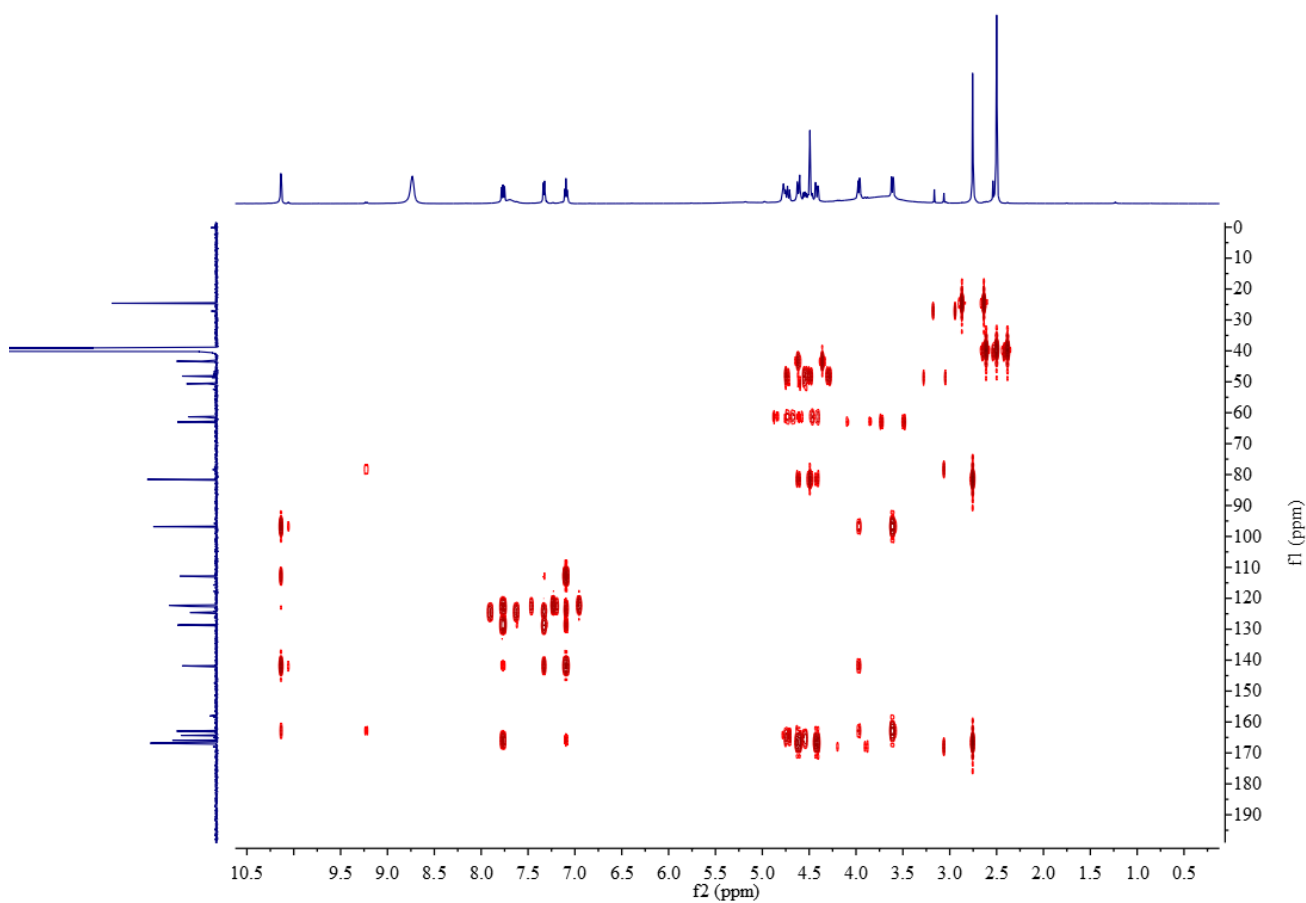


Figure S48. HMBC NMR spectrum of **5** in DMSO- d_6 .

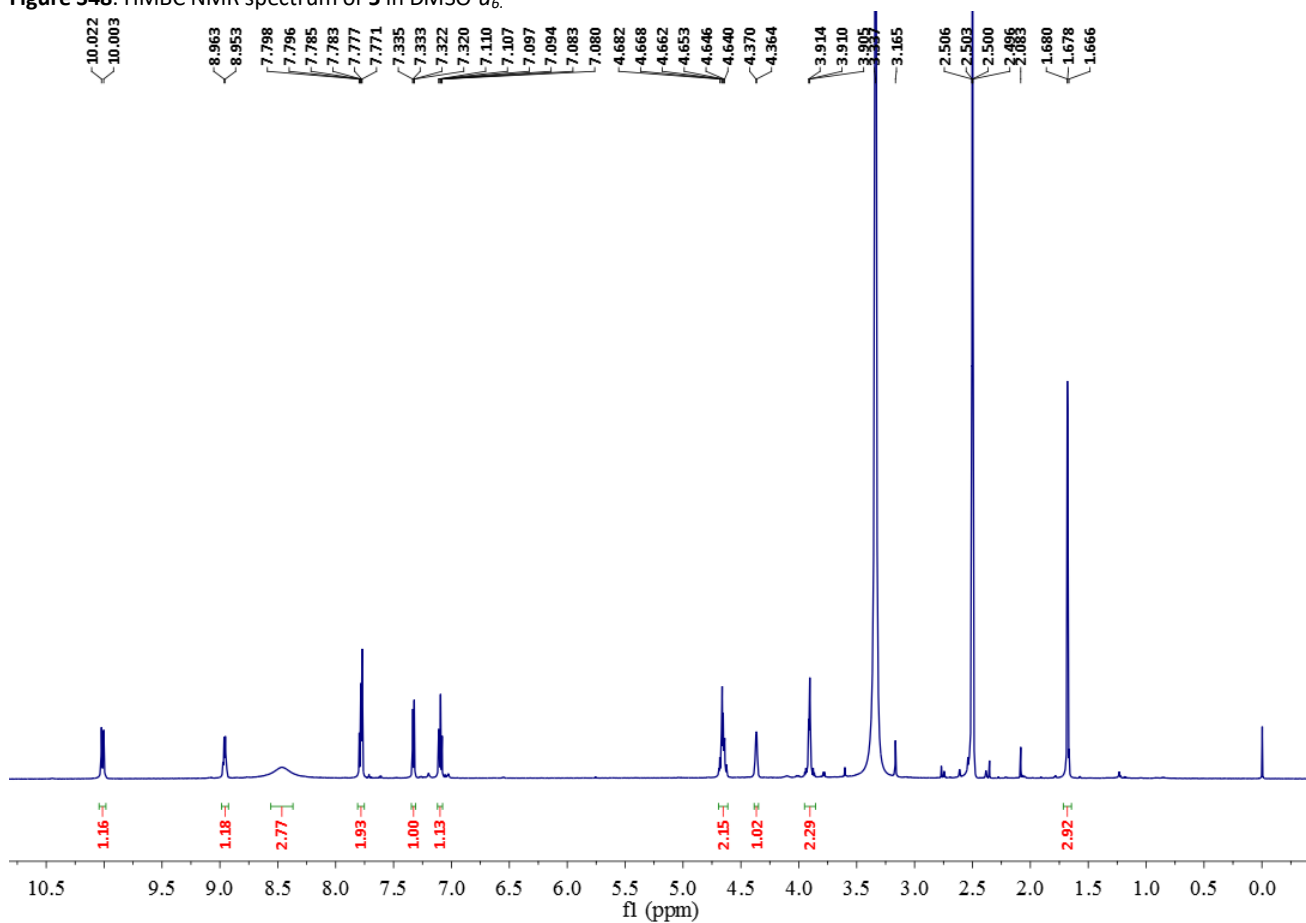


Figure S49. ^1H NMR spectrum of **6** in DMSO- d_6 at 600 MHz.

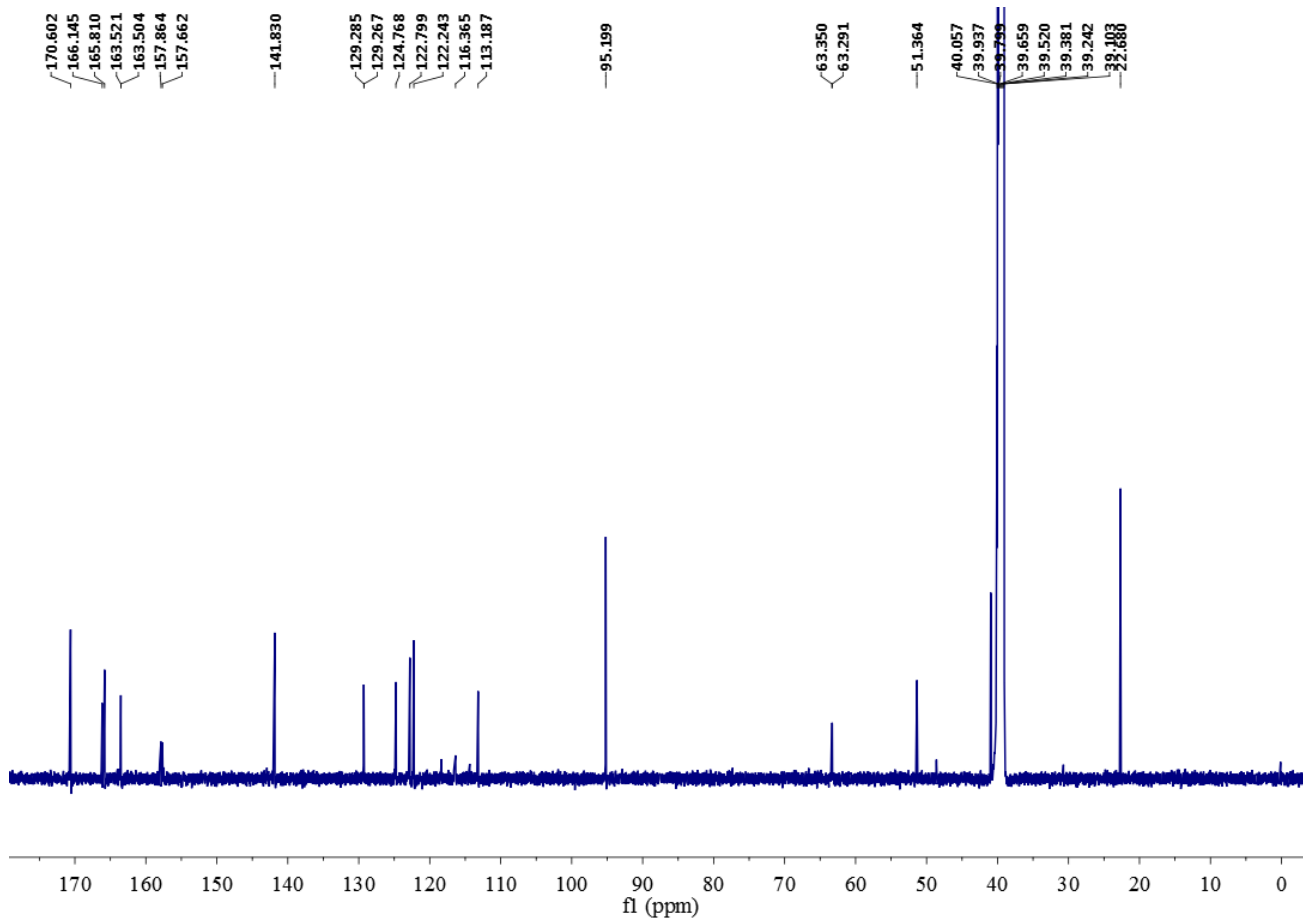


Figure S50. ^{13}C NMR spectrum of **6** in $\text{DMSO-}d_6$ at 150MHz.

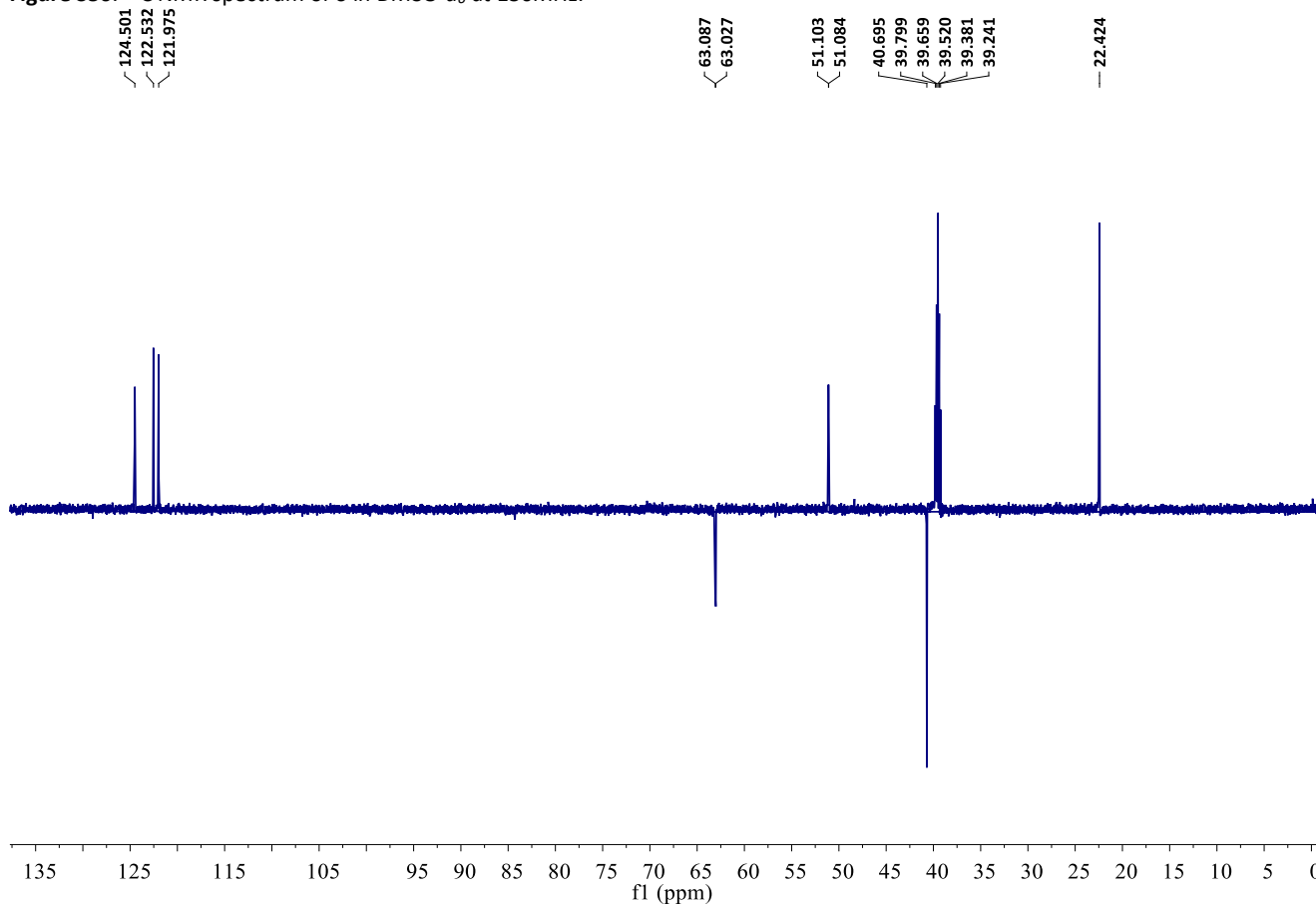


Figure S51. DEPT 135 spectrum of **6** in $\text{DMSO-}d_6$.

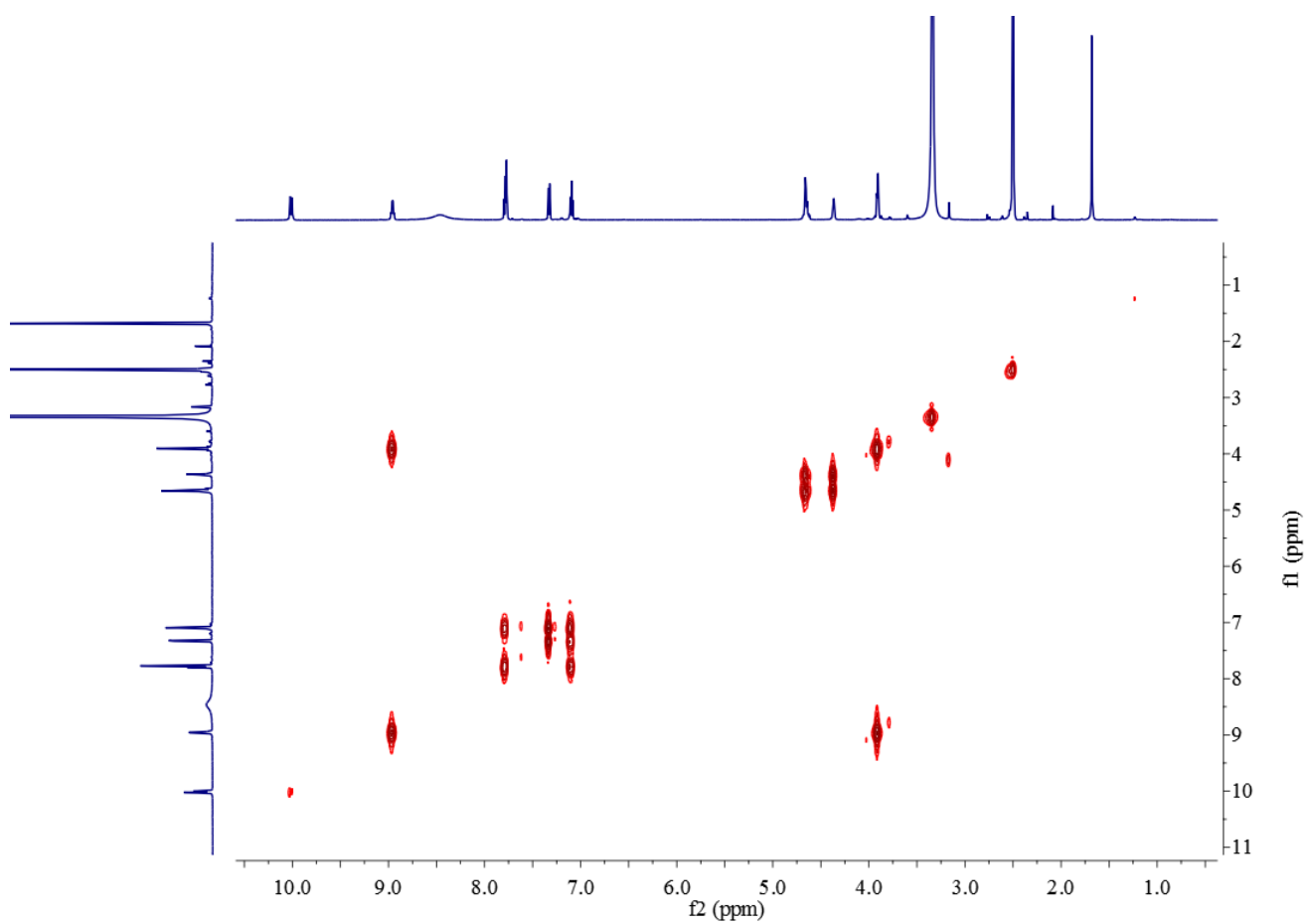


Figure S52. ^1H - ^1H COSY NMR spectrum of **6** in $\text{DMSO-}d_6$.

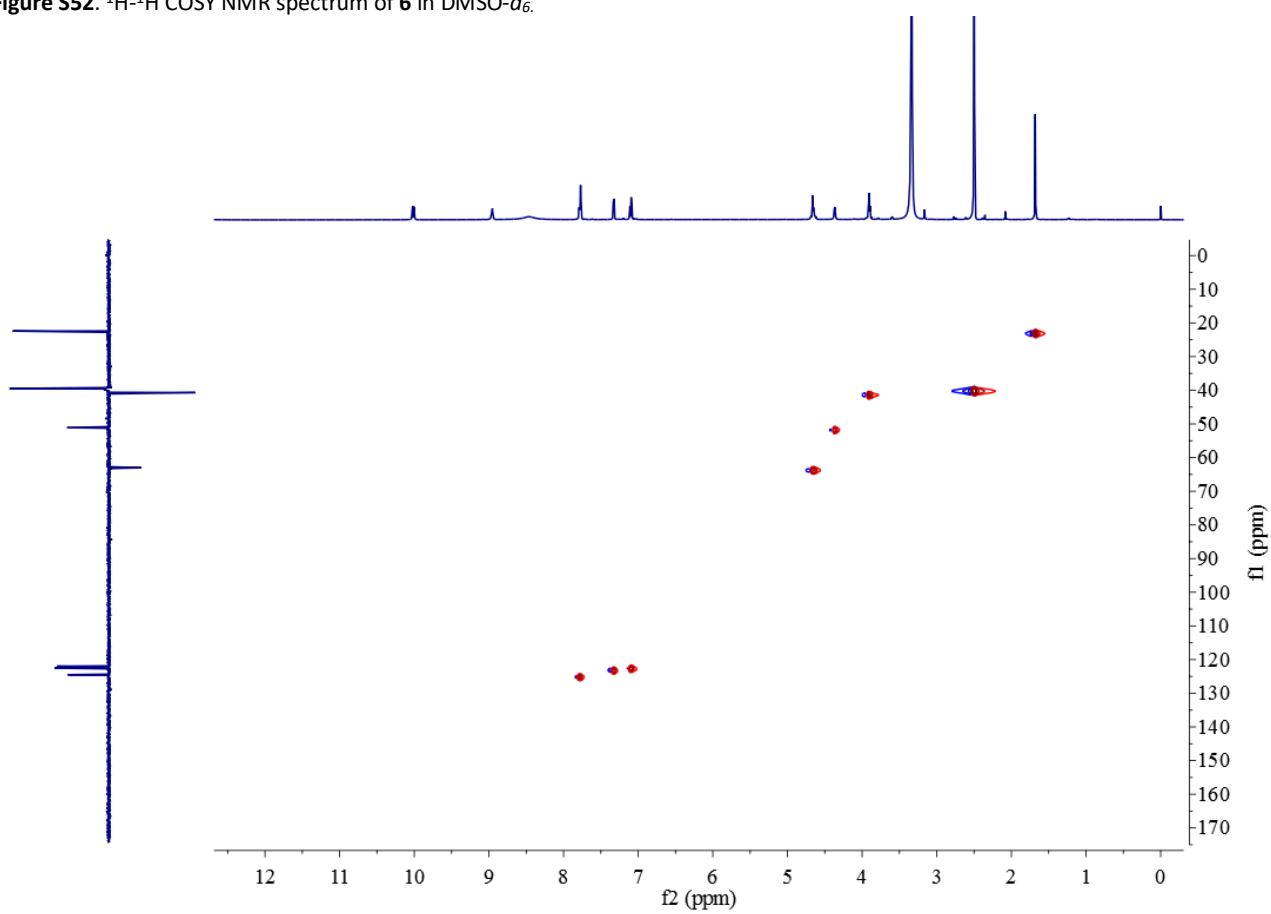


Figure S53. HSQC NMR spectrum of **6** in $\text{DMSO-}d_6$.

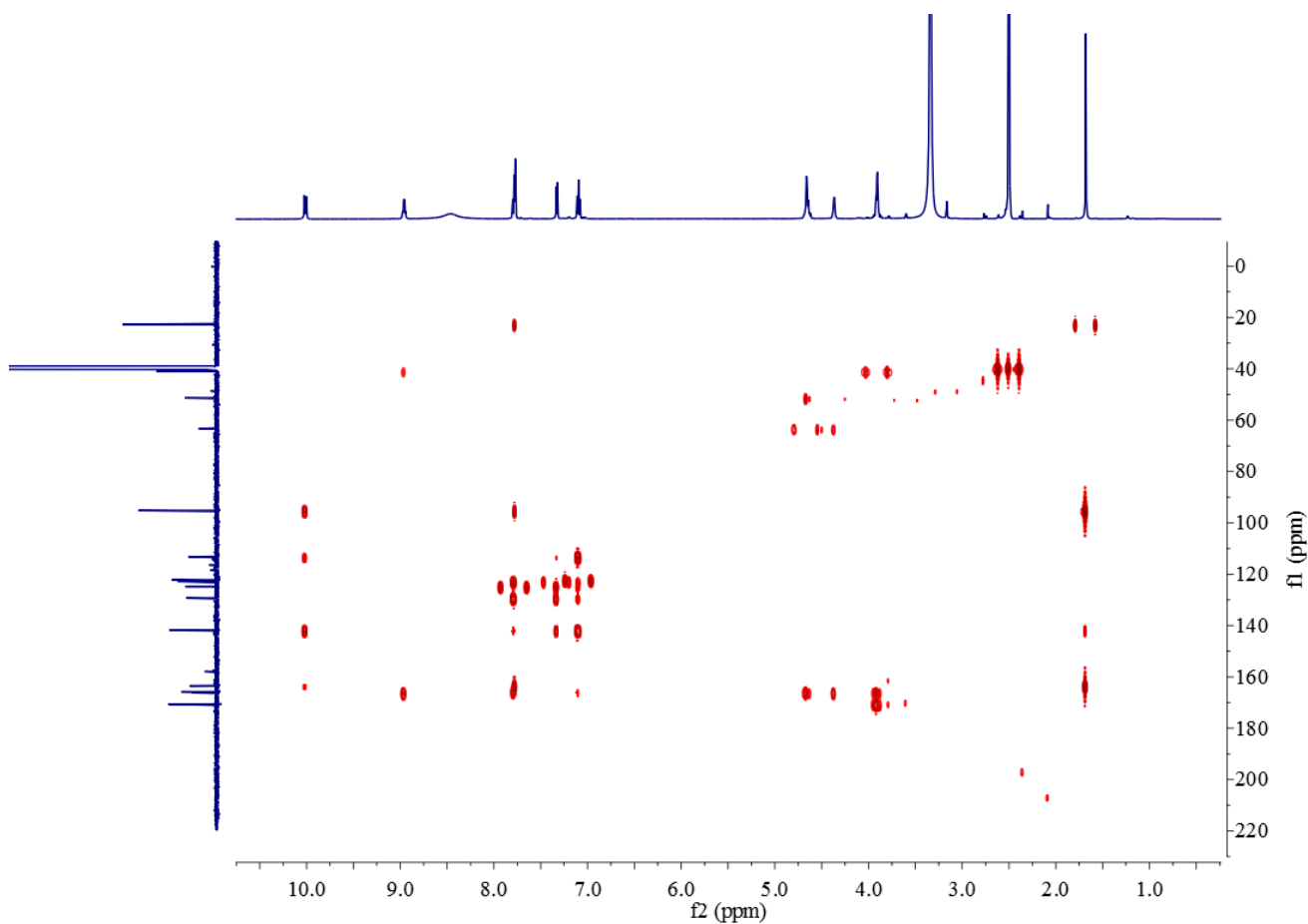


Figure S54. HMBC NMR spectrum of **6** in DMSO- d_6 .

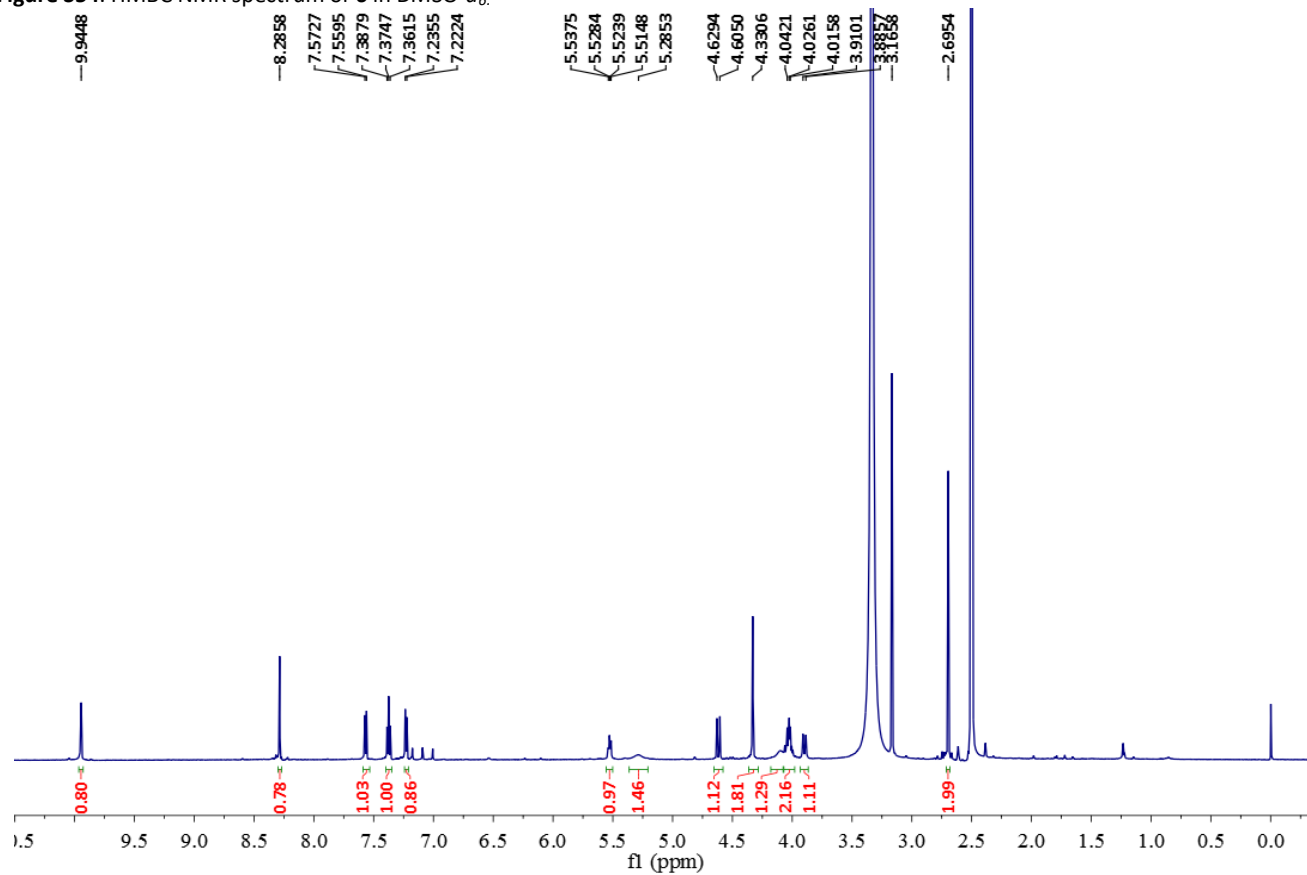


Figure S55. ^1H NMR spectrum of **7** in DMSO- d_6 at 600 MHz.

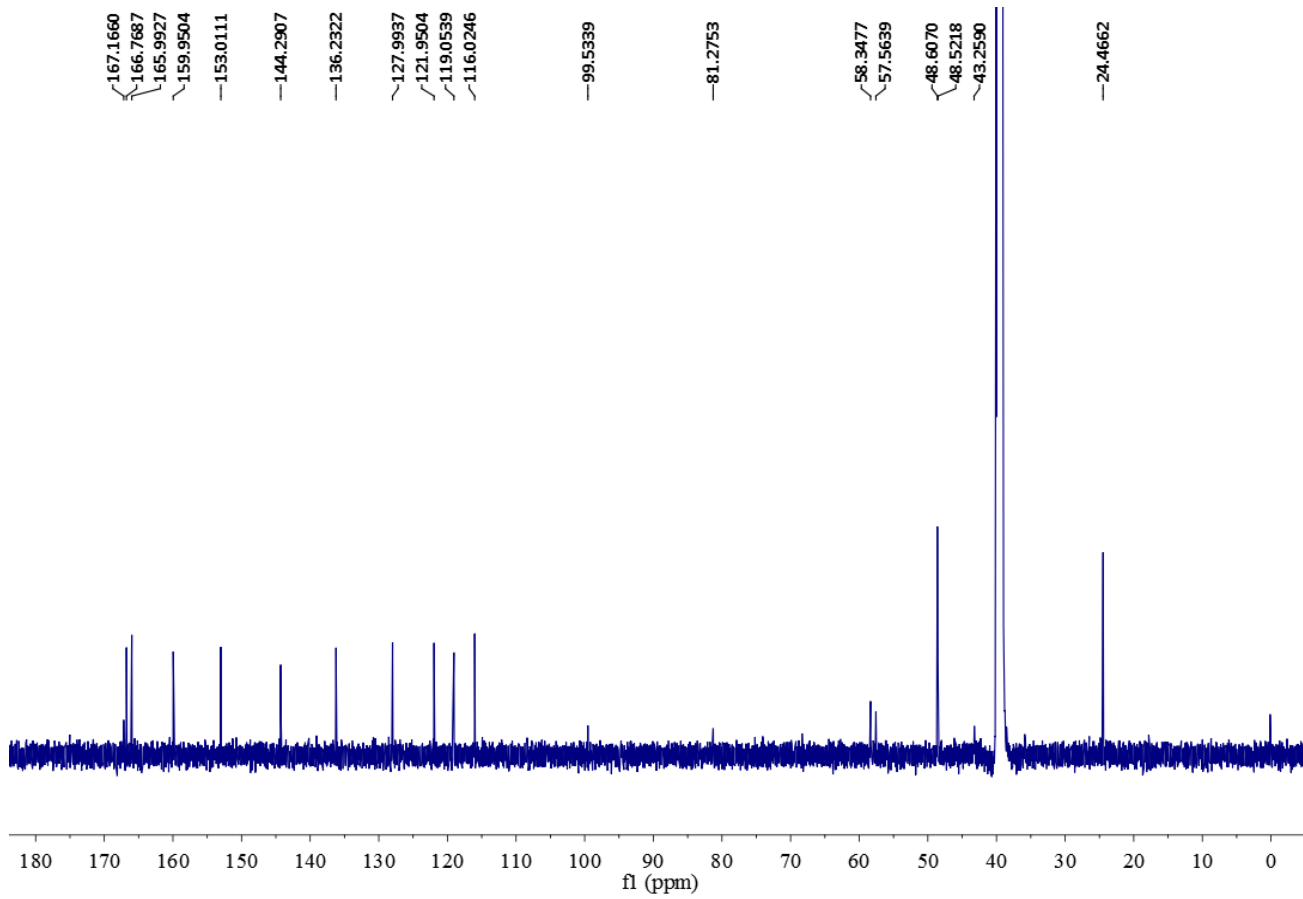


Figure S56. ^{13}C NMR spectrum of **7** in $\text{DMSO-}d_6$ at 150MHz.

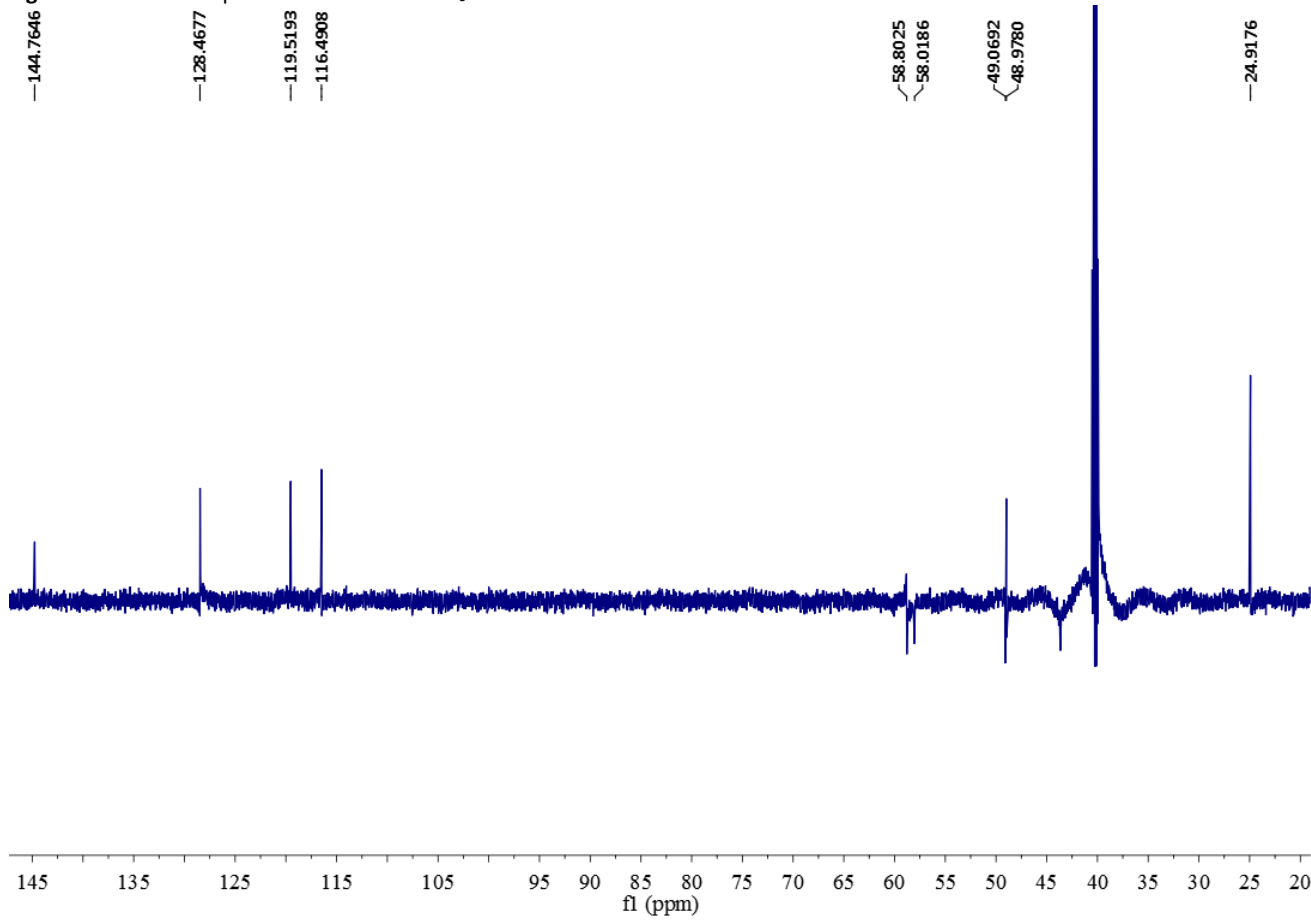


Figure S57. DEPT 135 spectrum of **7** in $\text{DMSO-}d_6$.

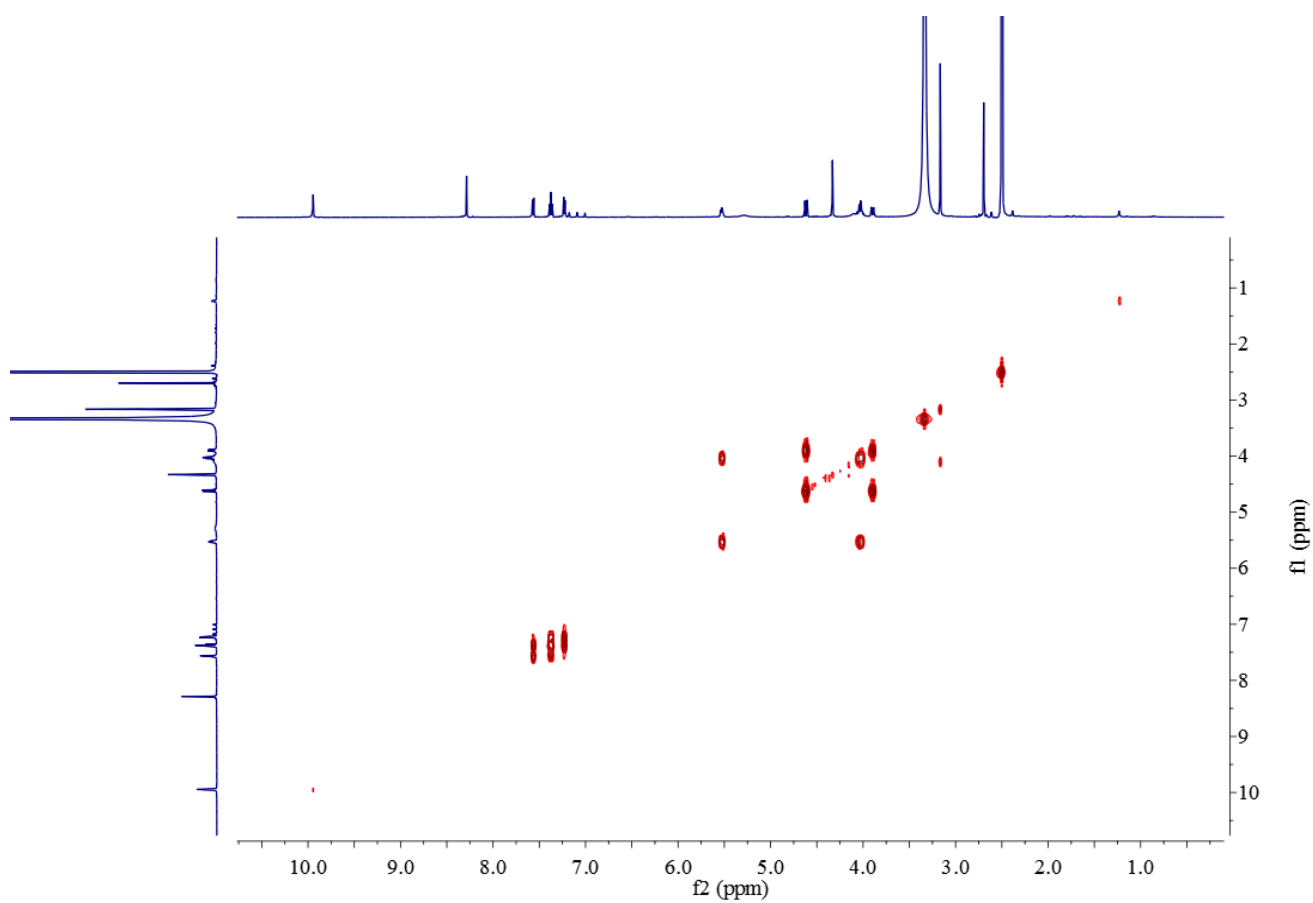


Figure S58. ^1H - ^1H COSY NMR spectrum of **7** in $\text{DMSO-}d_6$.

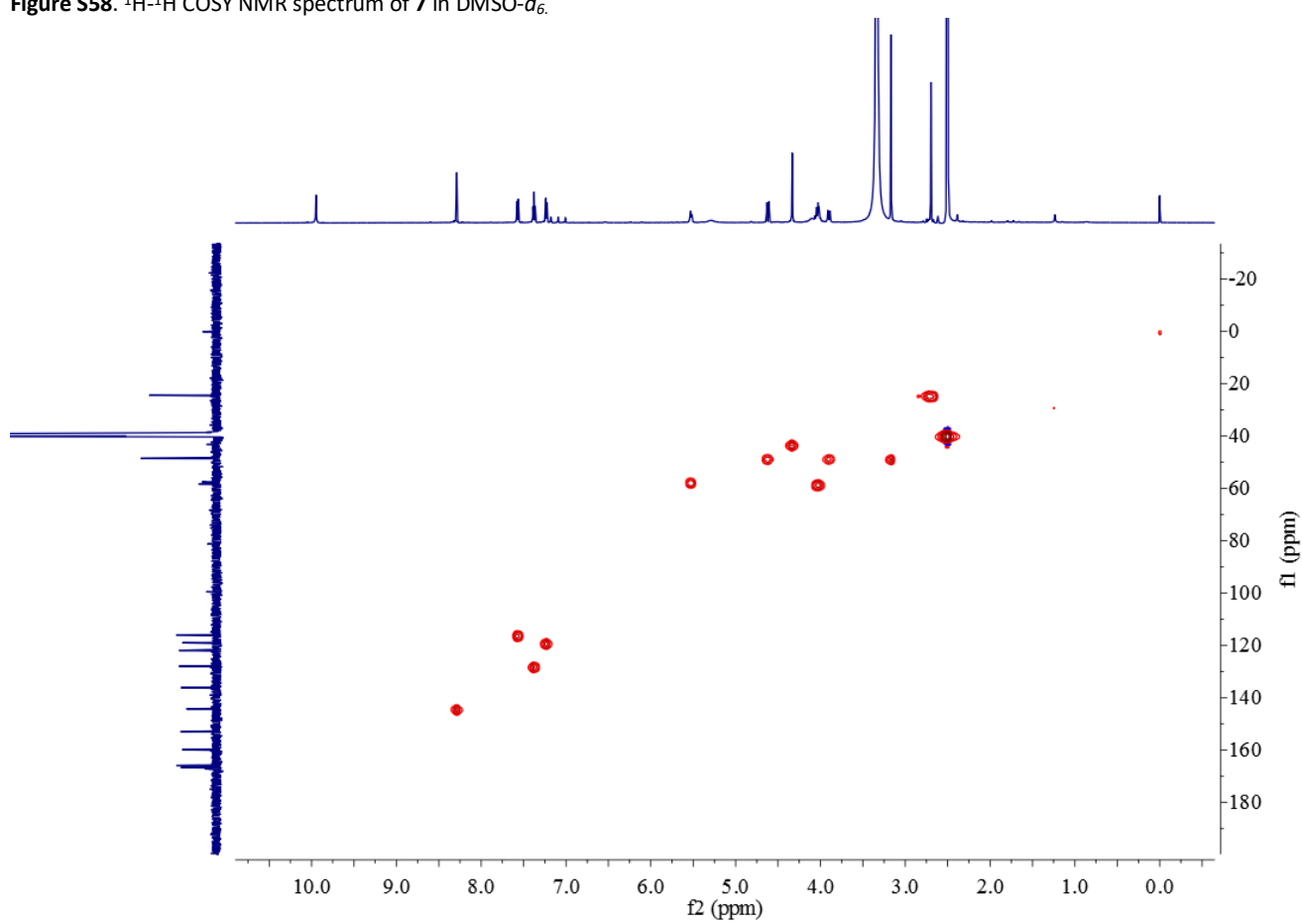


Figure S59. HSQC NMR spectrum of **7** in $\text{DMSO-}d_6$.

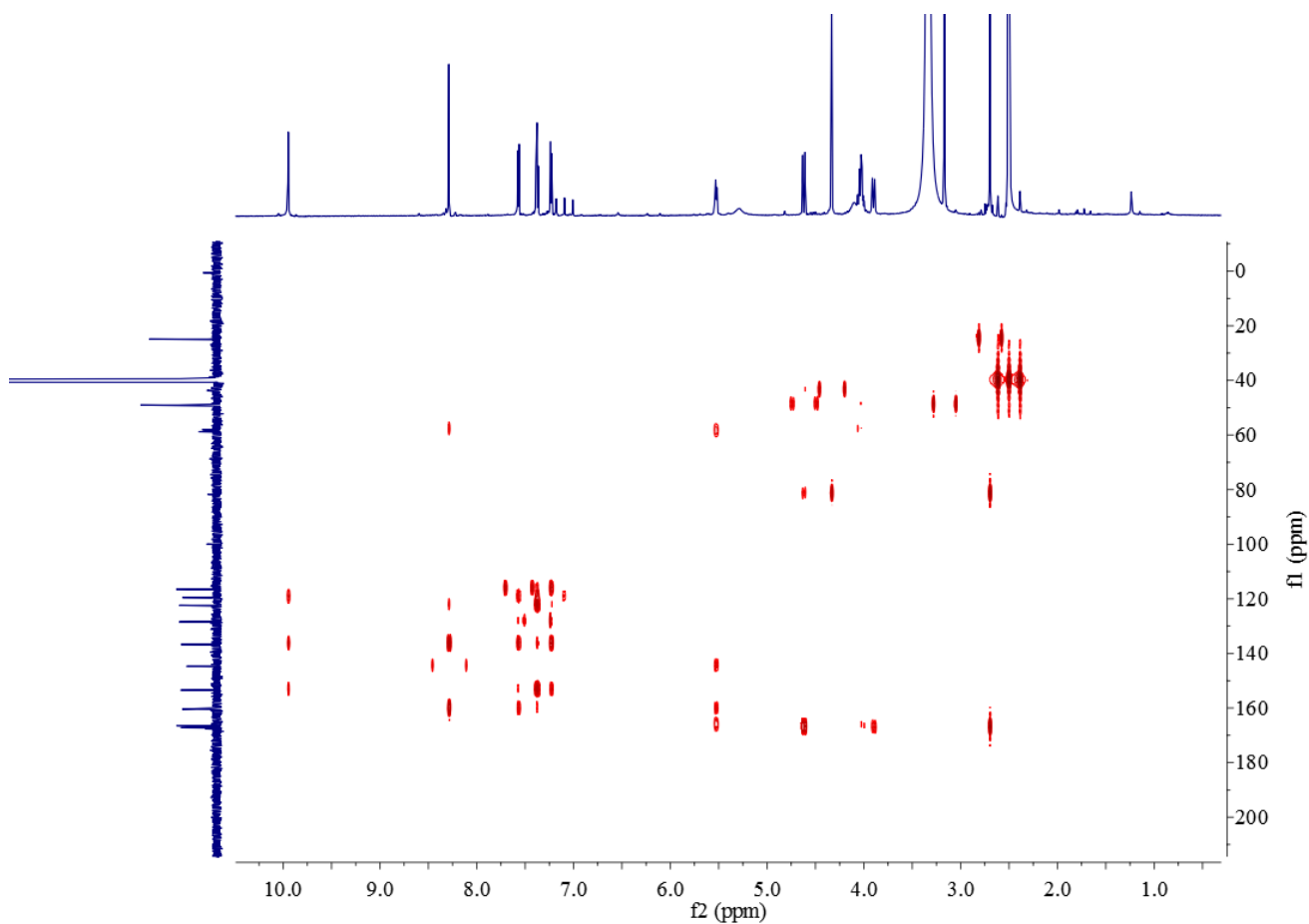


Figure S60. HMBC NMR spectrum of **7** in DMSO-*d*₆.

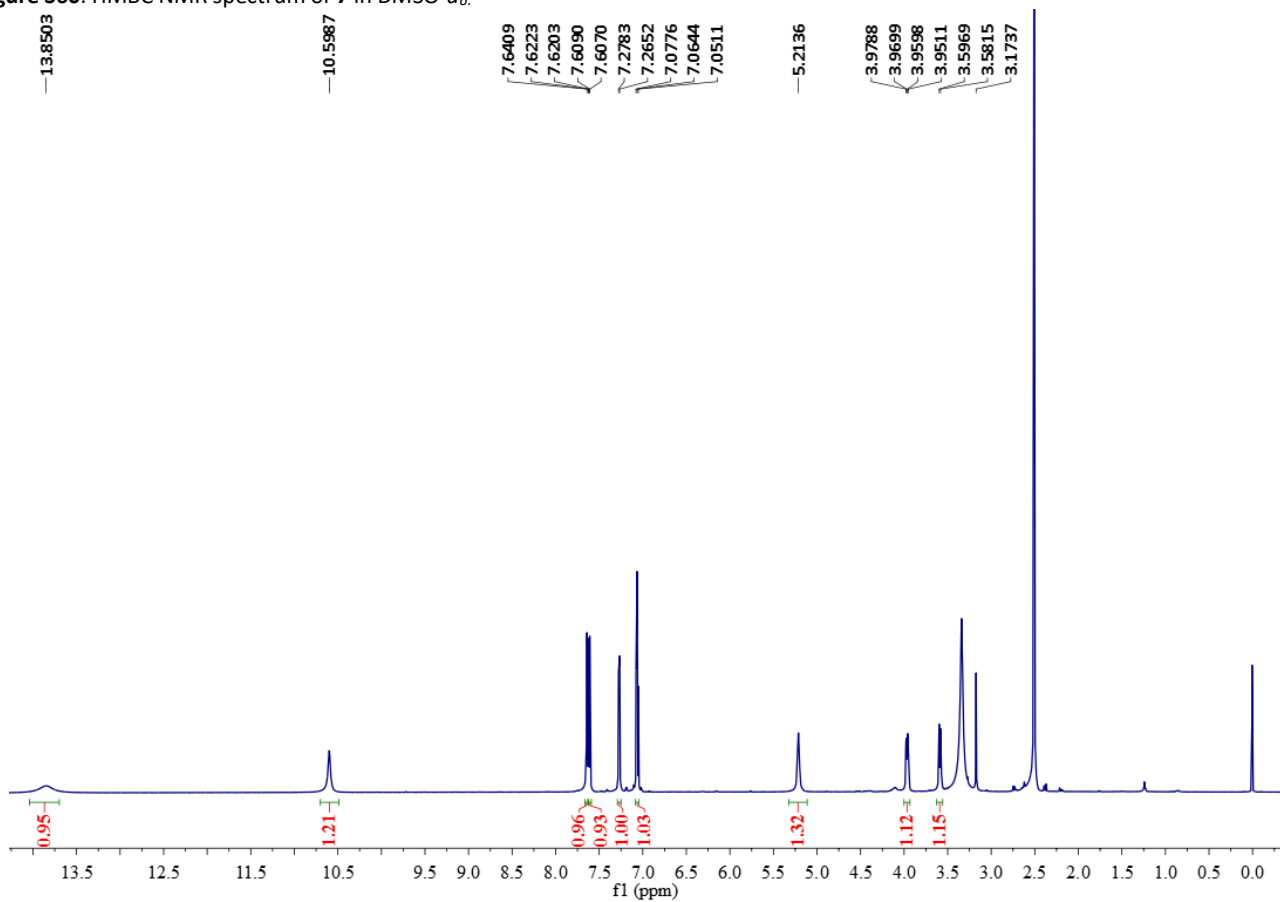


Figure S61. ¹H NMR spectrum of **8** in DMSO-*d*₆ at 600 MHz.

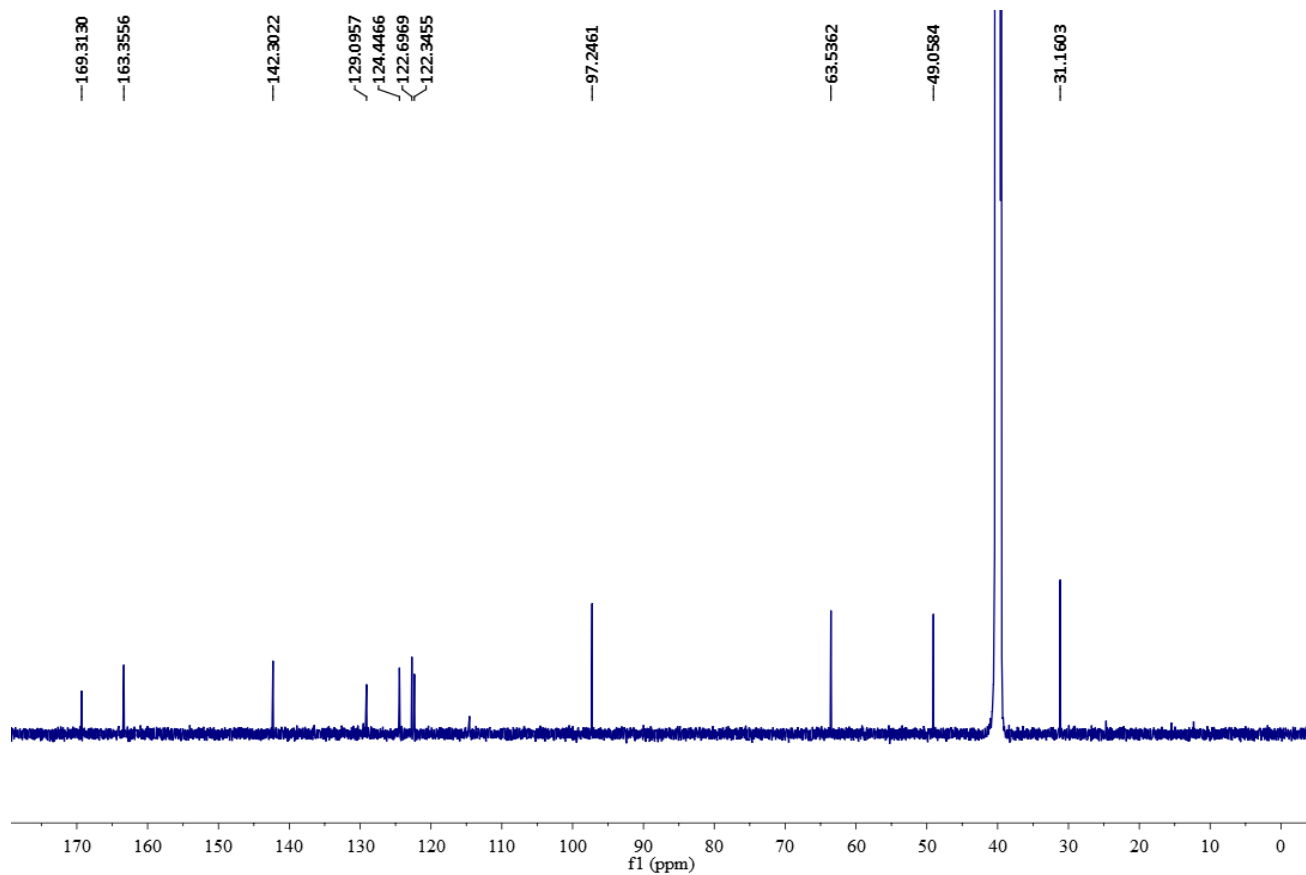


Figure S62. ^{13}C NMR spectrum of **8** in $\text{DMSO-}d_6$ at 150MHz.

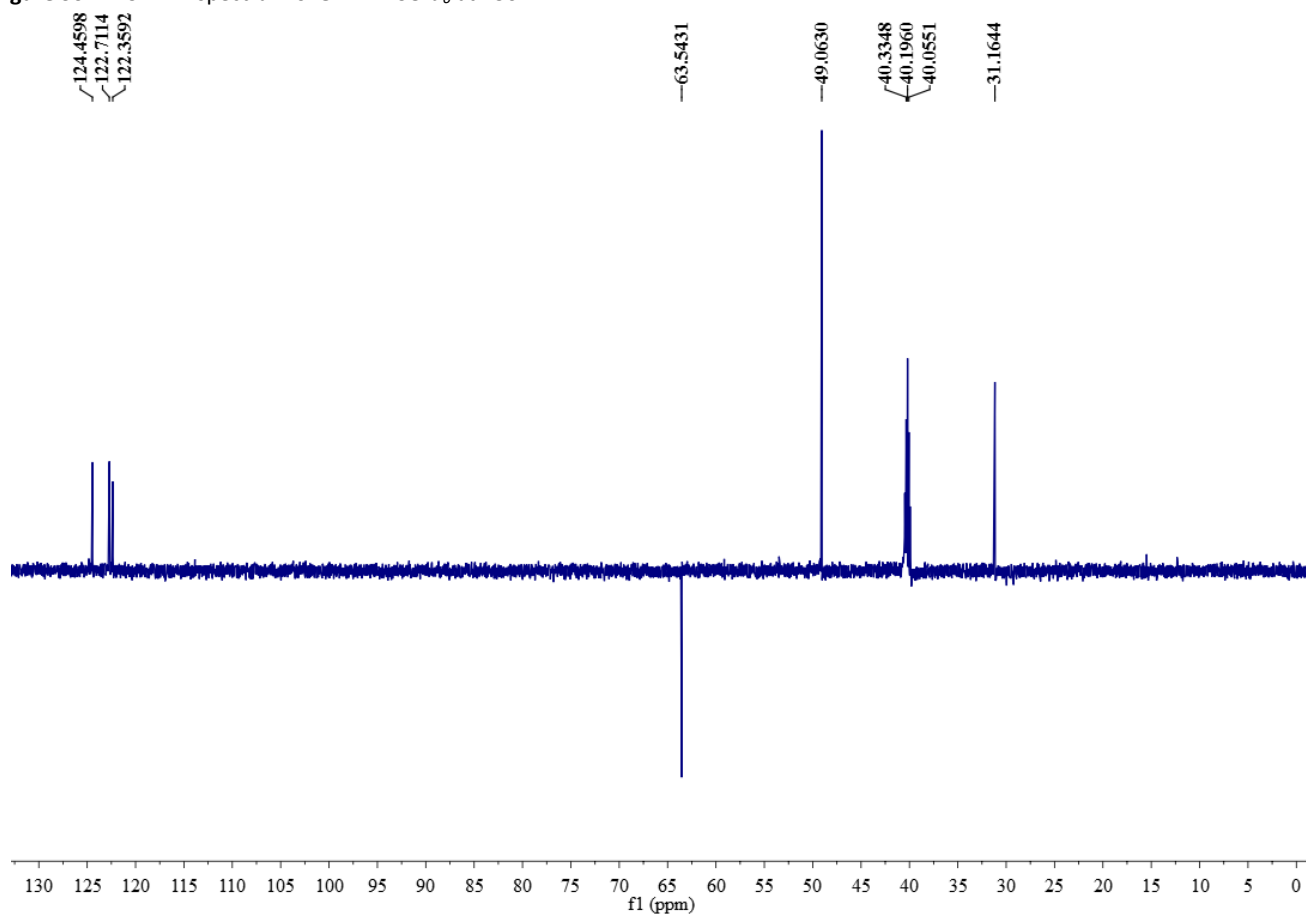


Figure S63. DEPT 135 spectrum of **8** in $\text{DMSO-}d_6$.

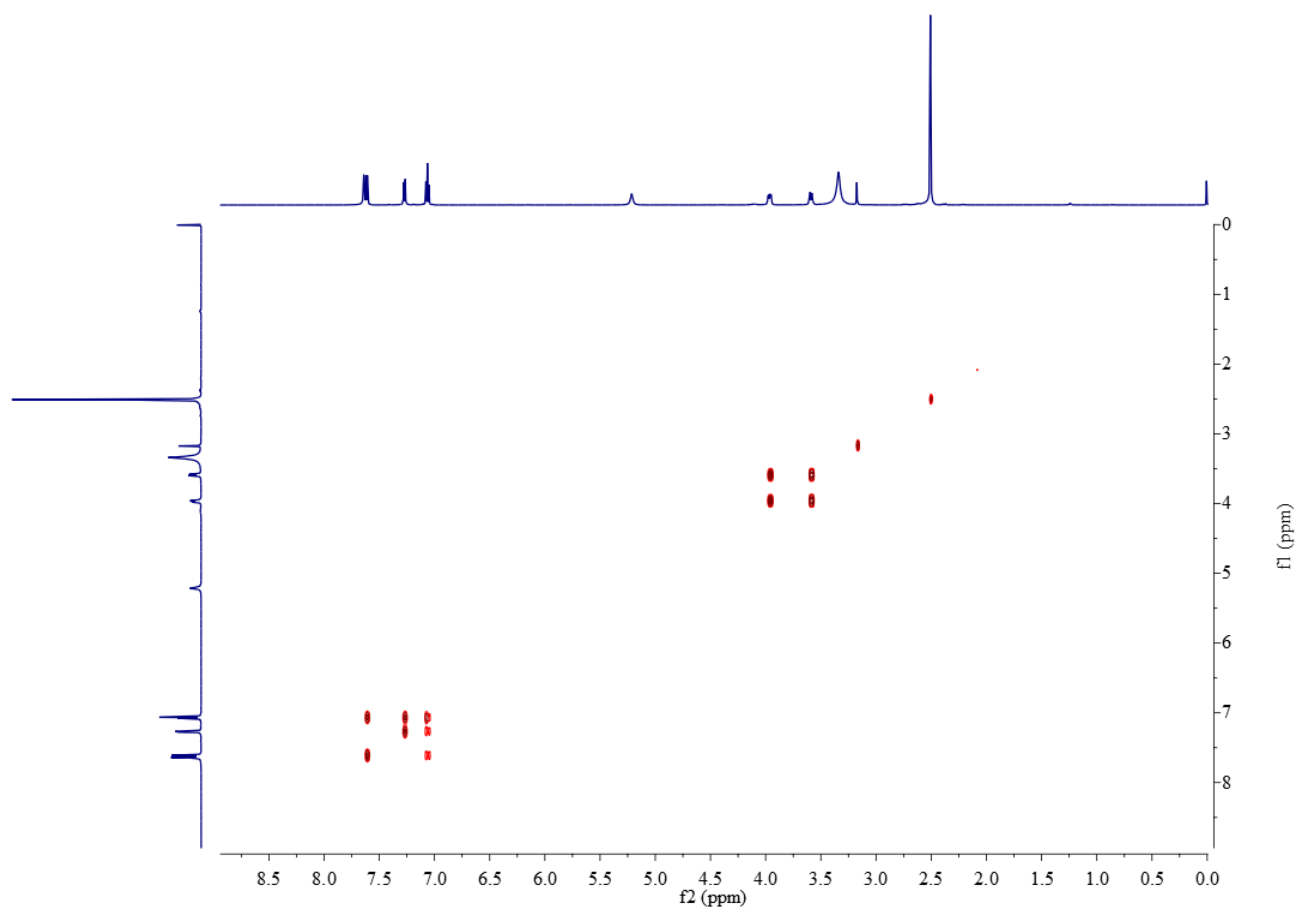


Figure S64. ^1H - ^1H COSY NMR spectrum of **8** in $\text{DMSO-}d_6$.

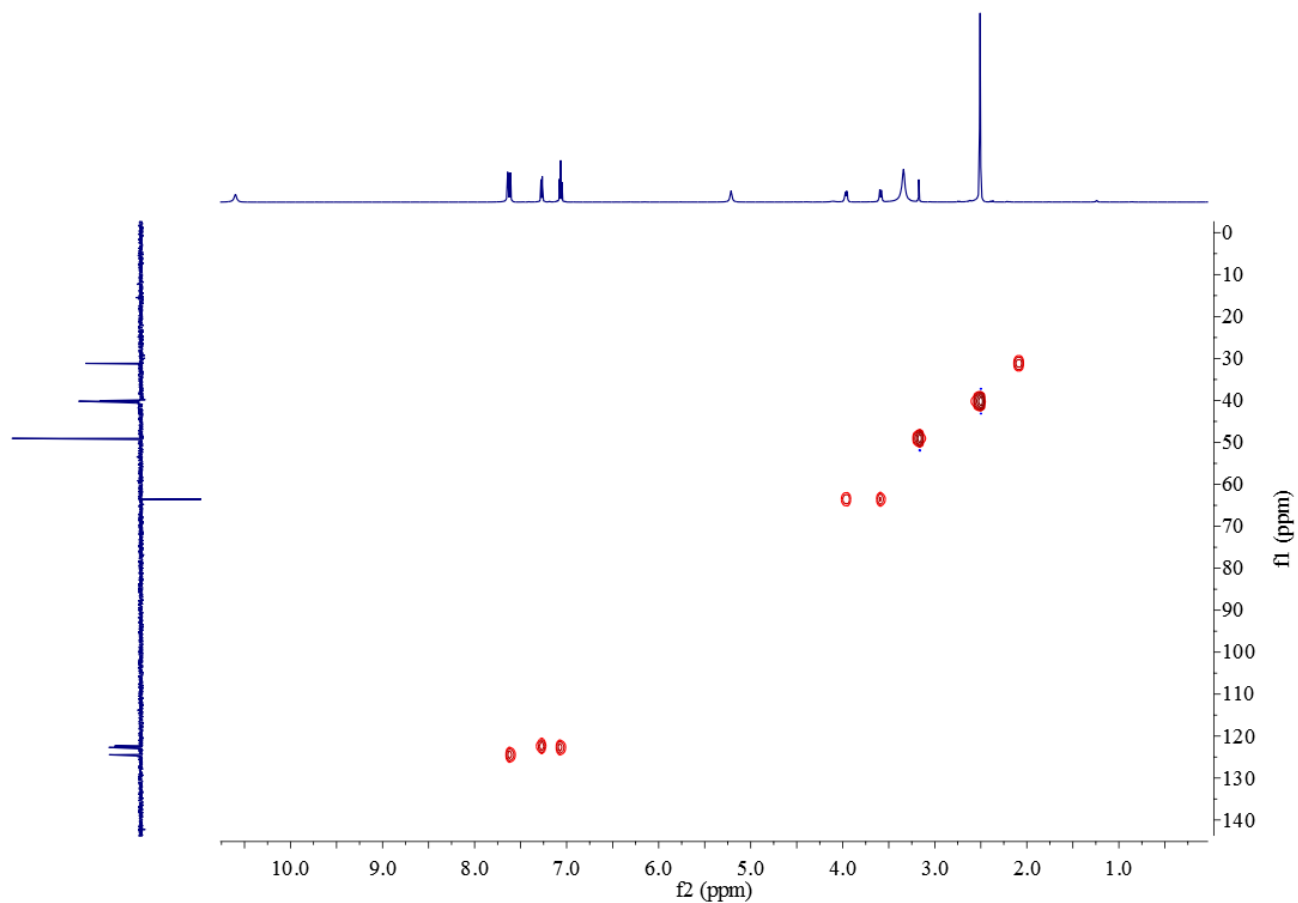


Figure S65. HSQC NMR spectrum of **8** in $\text{DMSO-}d_6$.

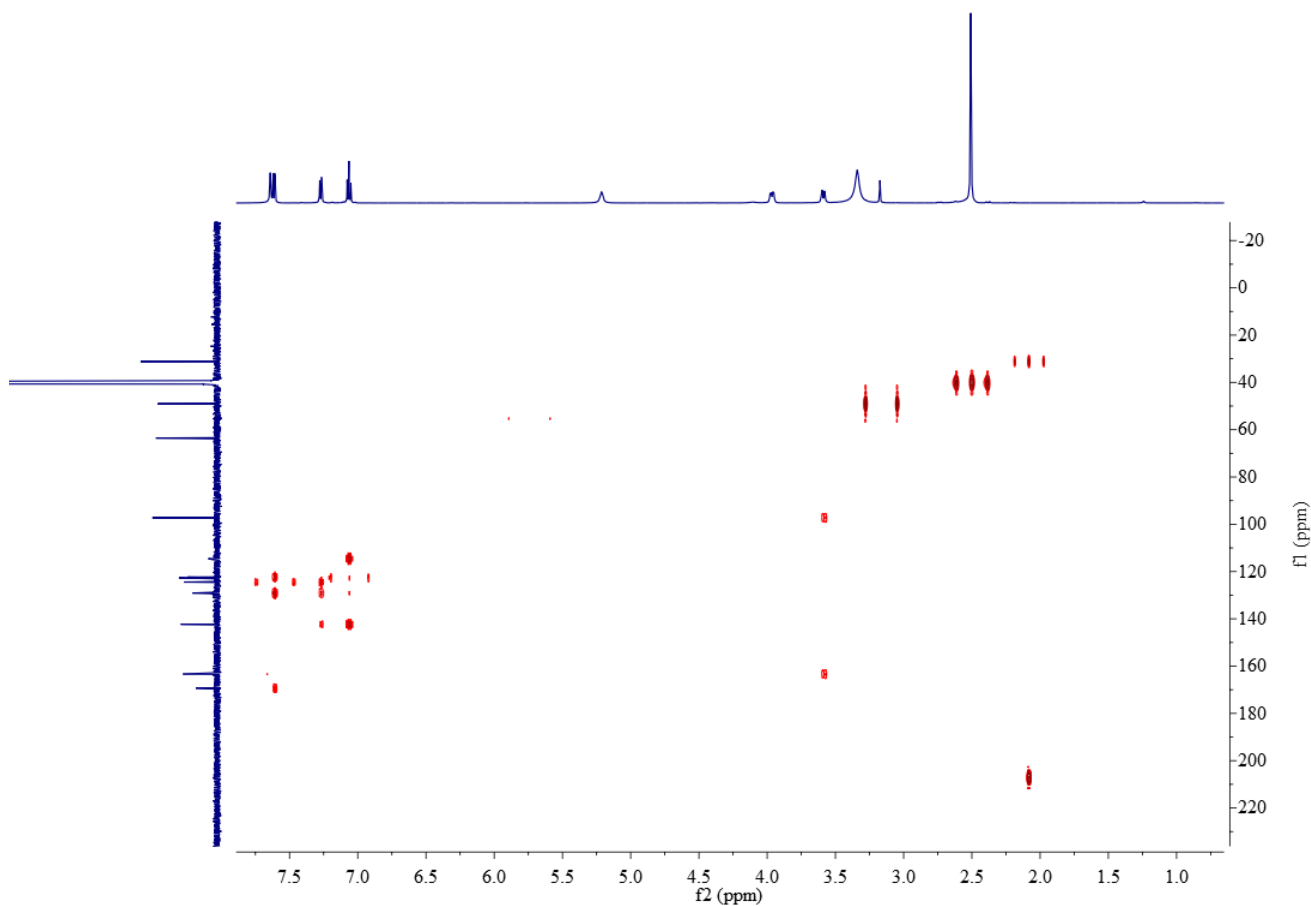


Figure S66. HMBC NMR spectrum of **8** in DMSO-*d*₆.

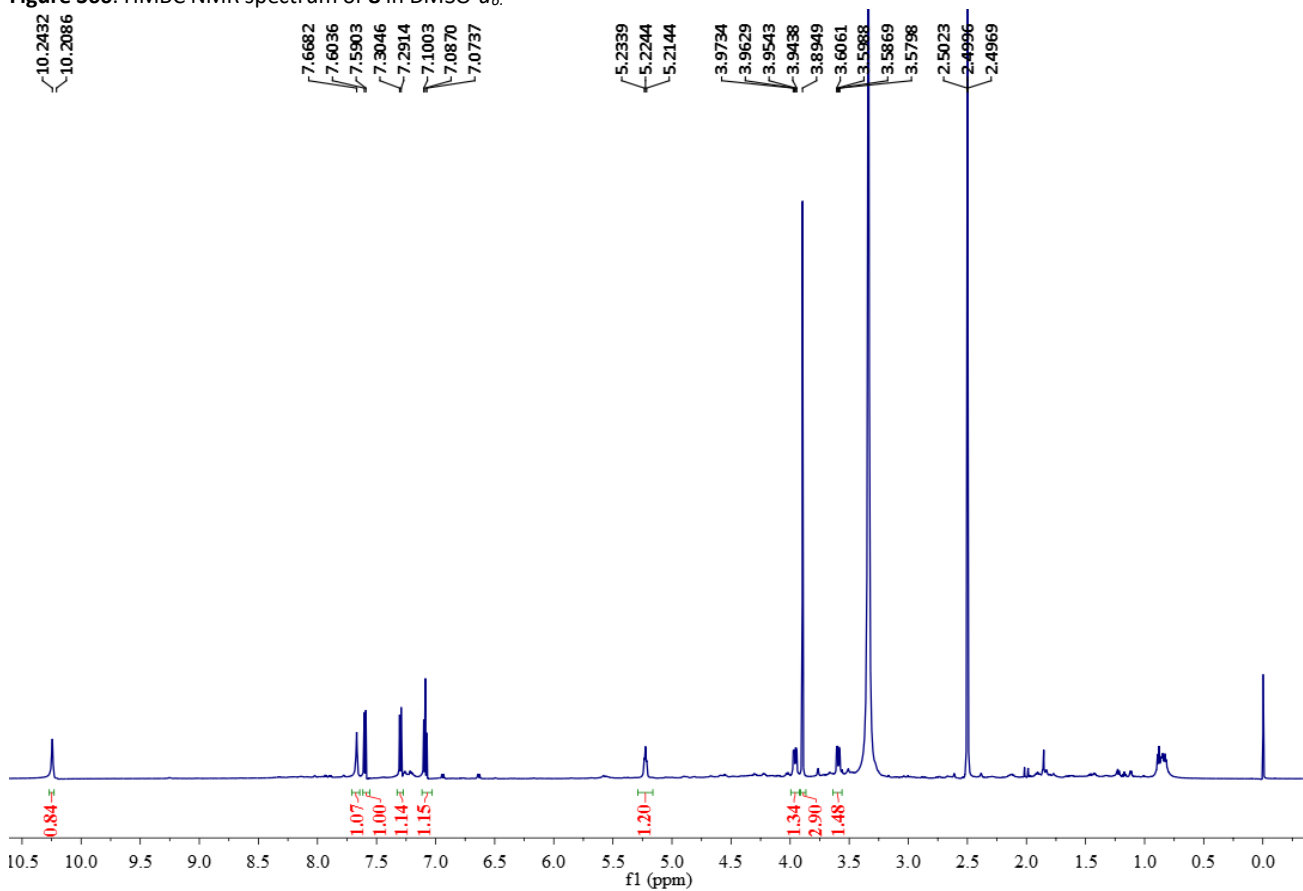


Figure S67. ¹H NMR spectrum of **9** in DMSO-*d*₆ at 600 MHz.

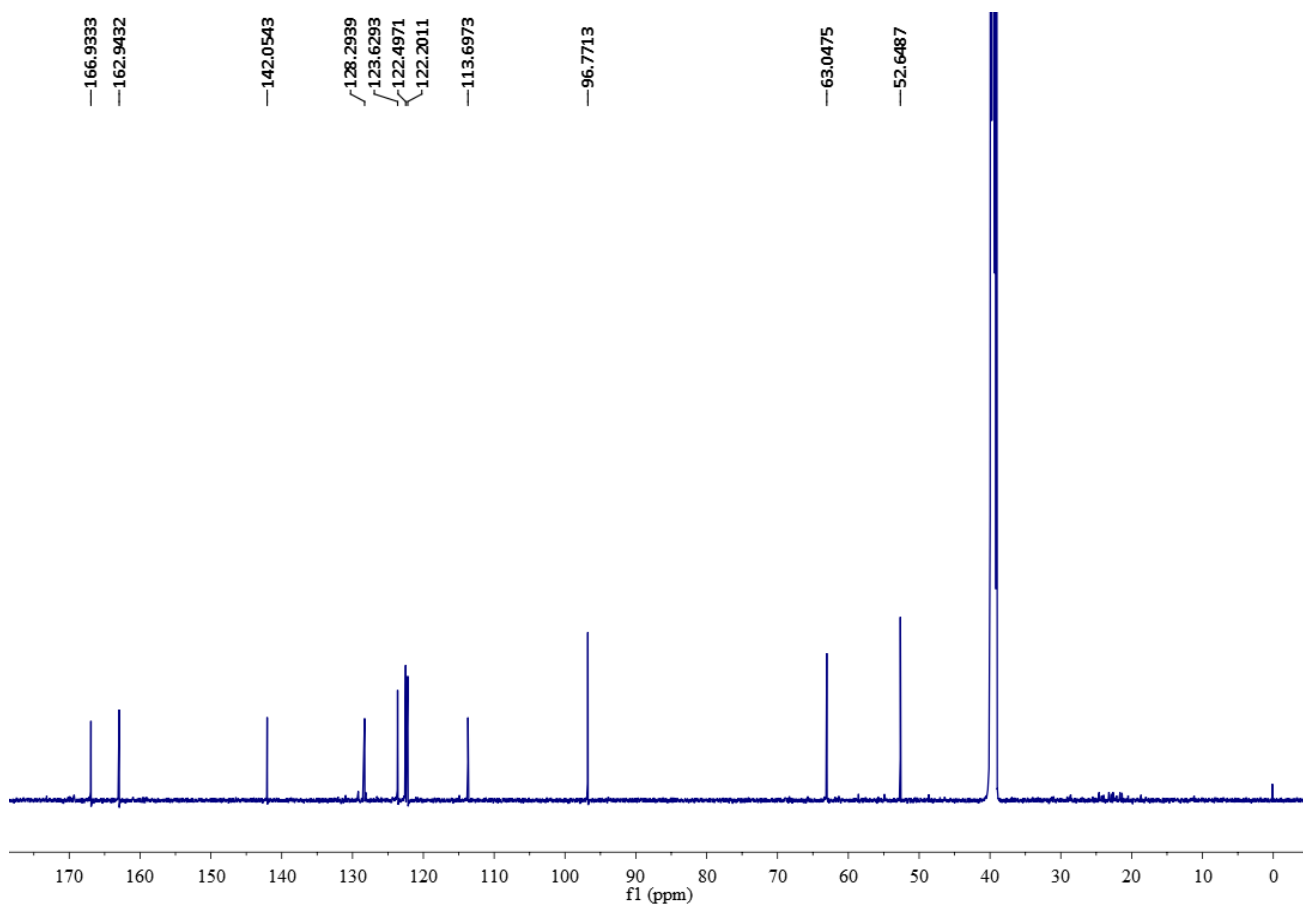


Figure S68. ^{13}C NMR spectrum of **9** in $\text{DMSO-}d_6$ at 150MHz.

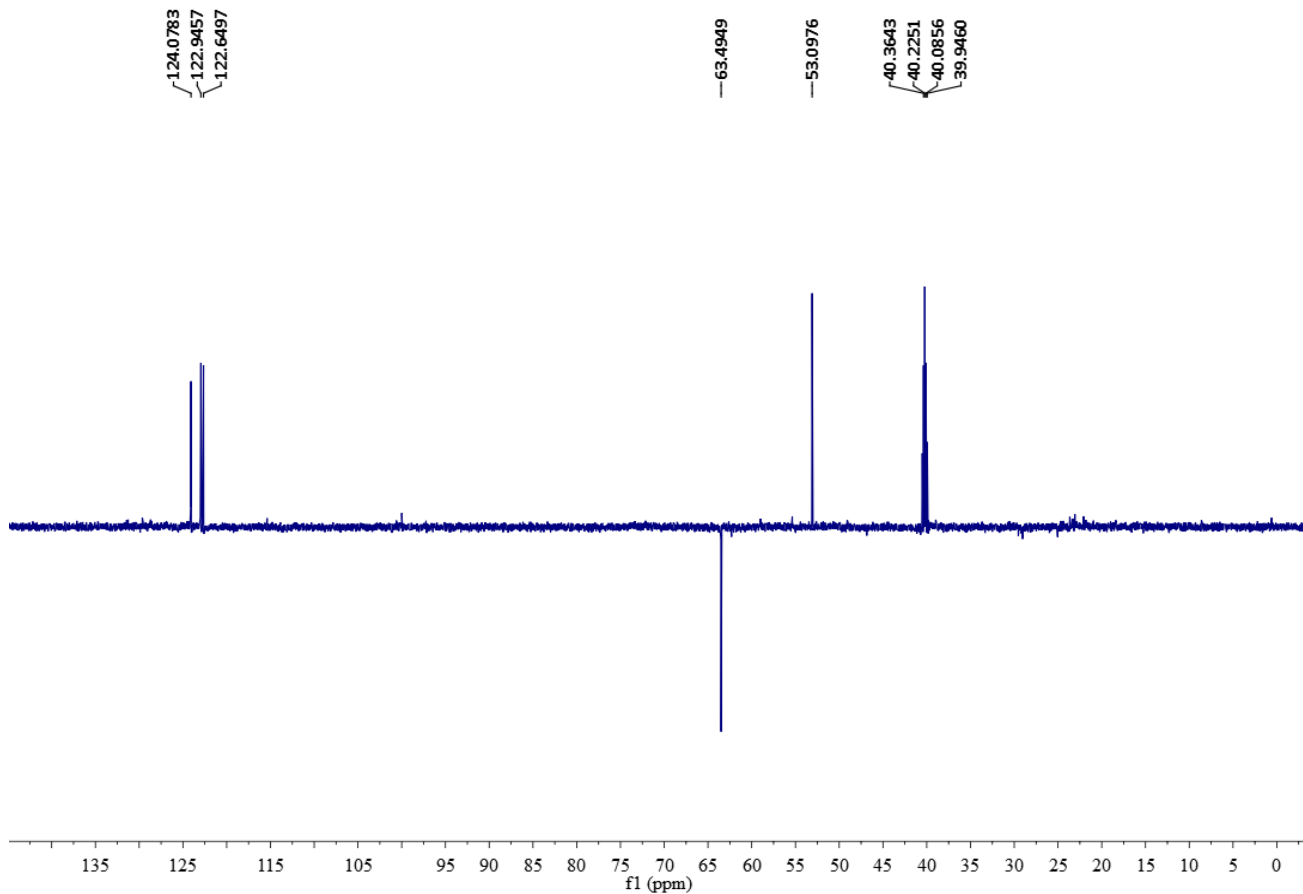


Figure S69. DEPT 135 spectrum of **9** in $\text{DMSO-}d_6$.

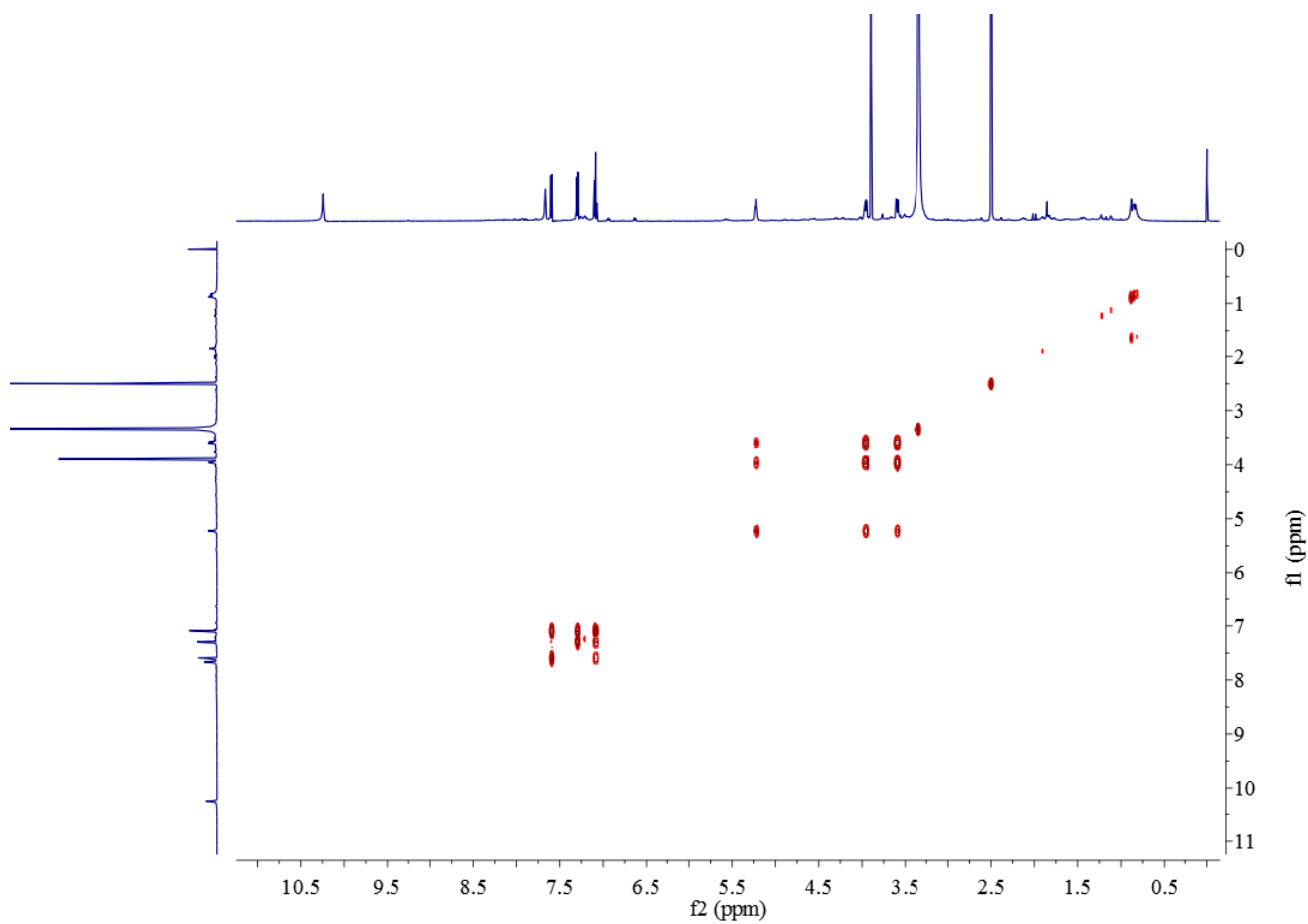


Figure S70. ^1H - ^1H COSY NMR spectrum of **9** in $\text{DMSO-}d_6$.

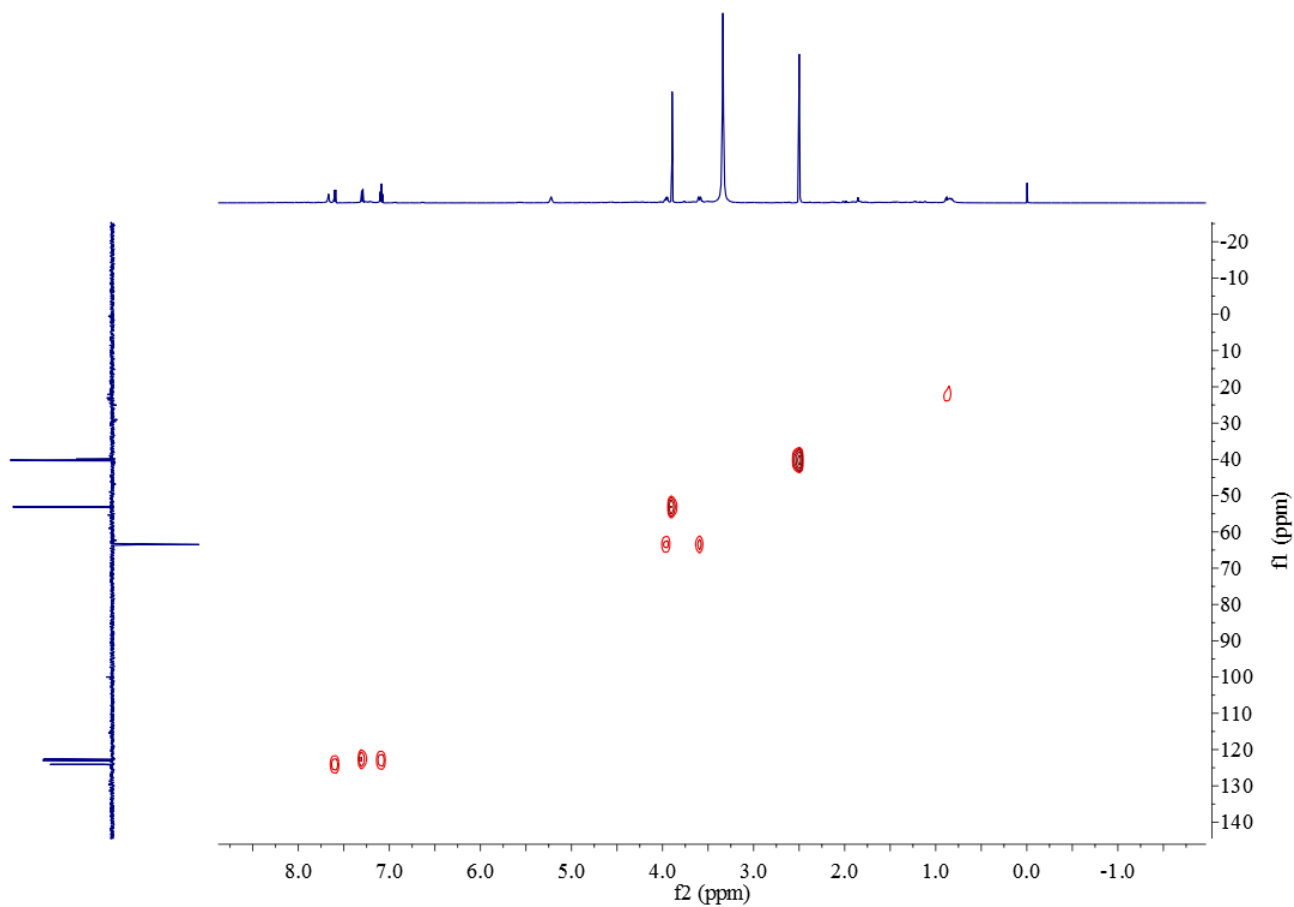


Figure S71. HSQC NMR spectrum of **9** in $\text{DMSO-}d_6$.

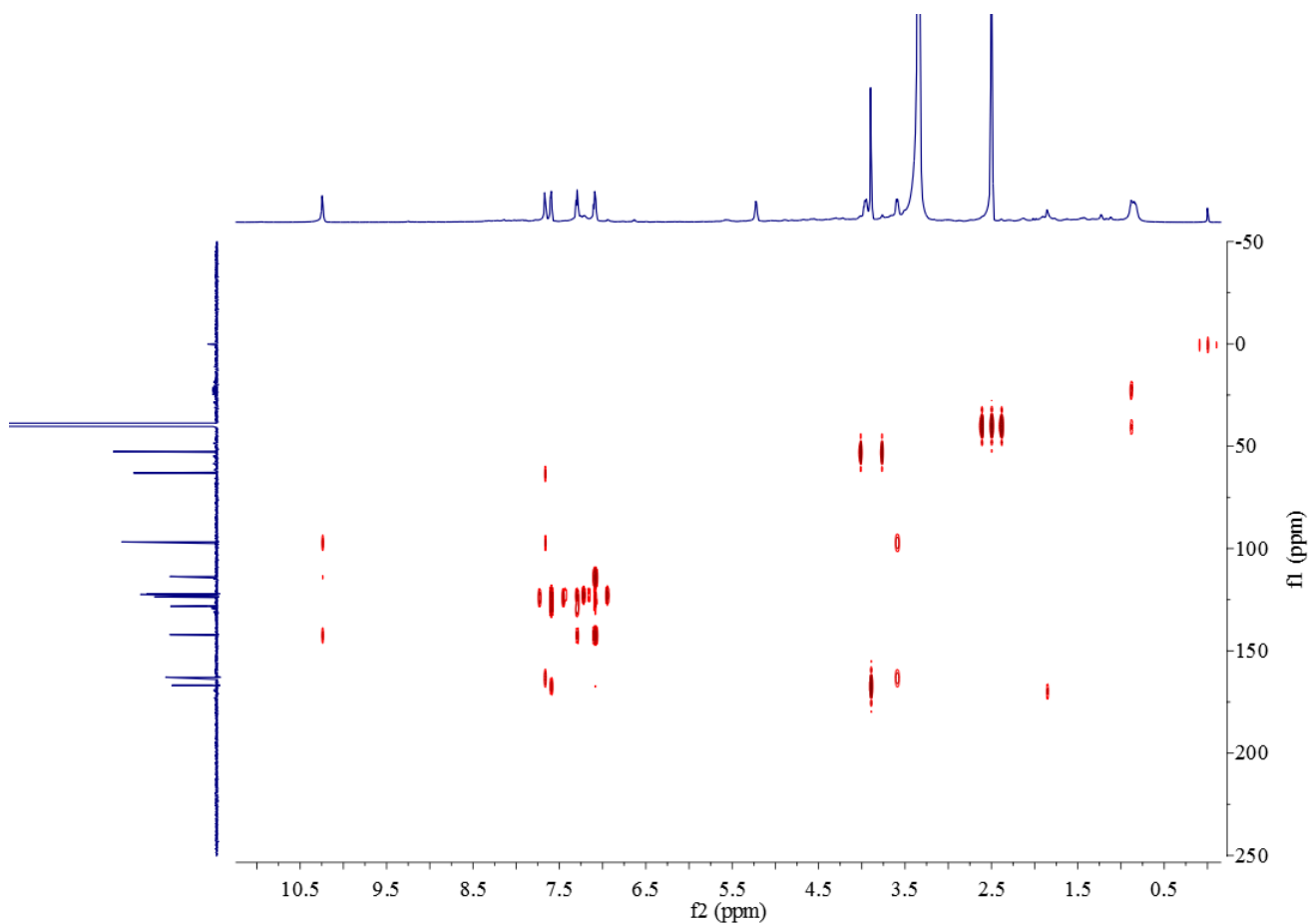


Figure S72. HMBC NMR spectrum of **9** in DMSO- d_6 .

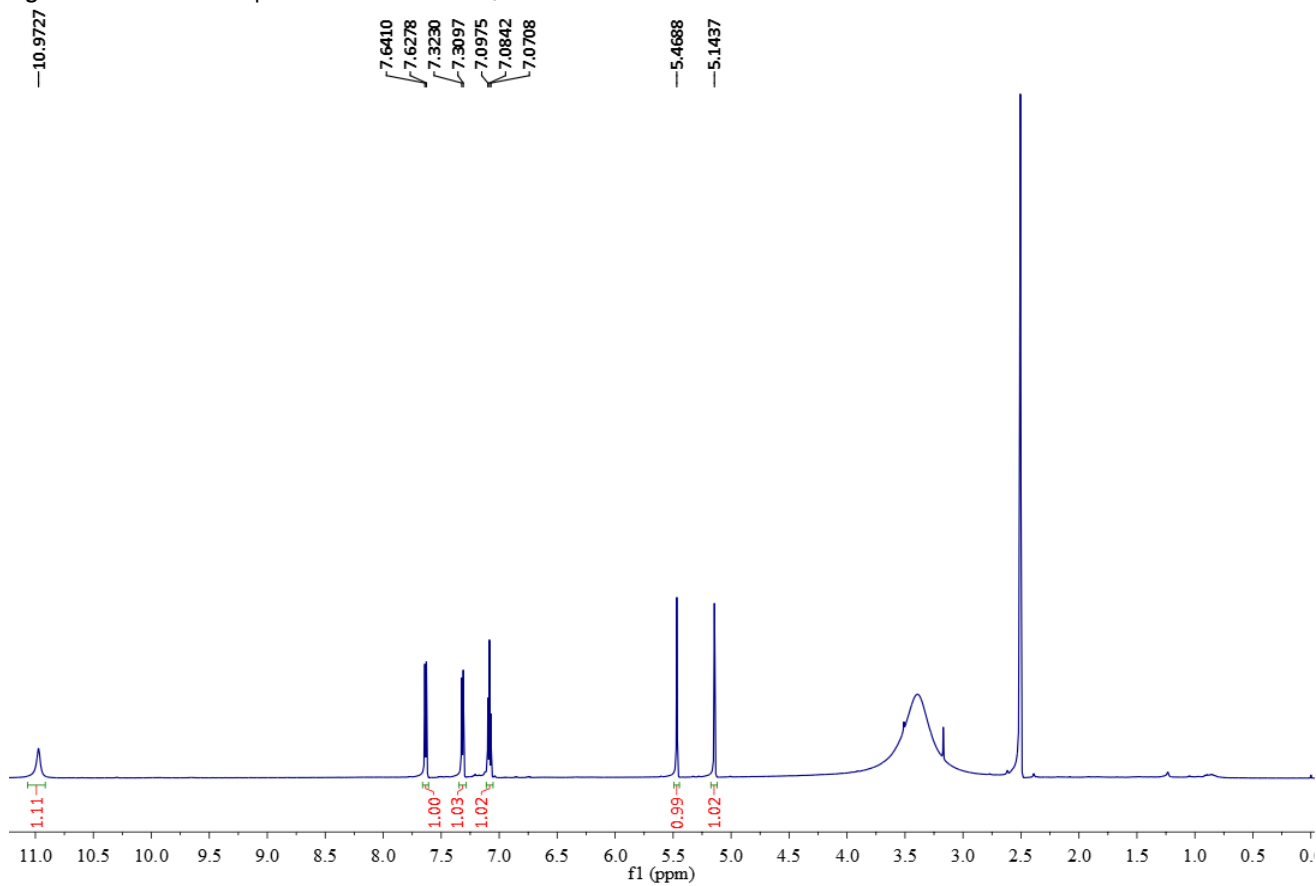


Figure S73. ^1H NMR spectrum of **10** in DMSO- d_6 at 600 MHz.

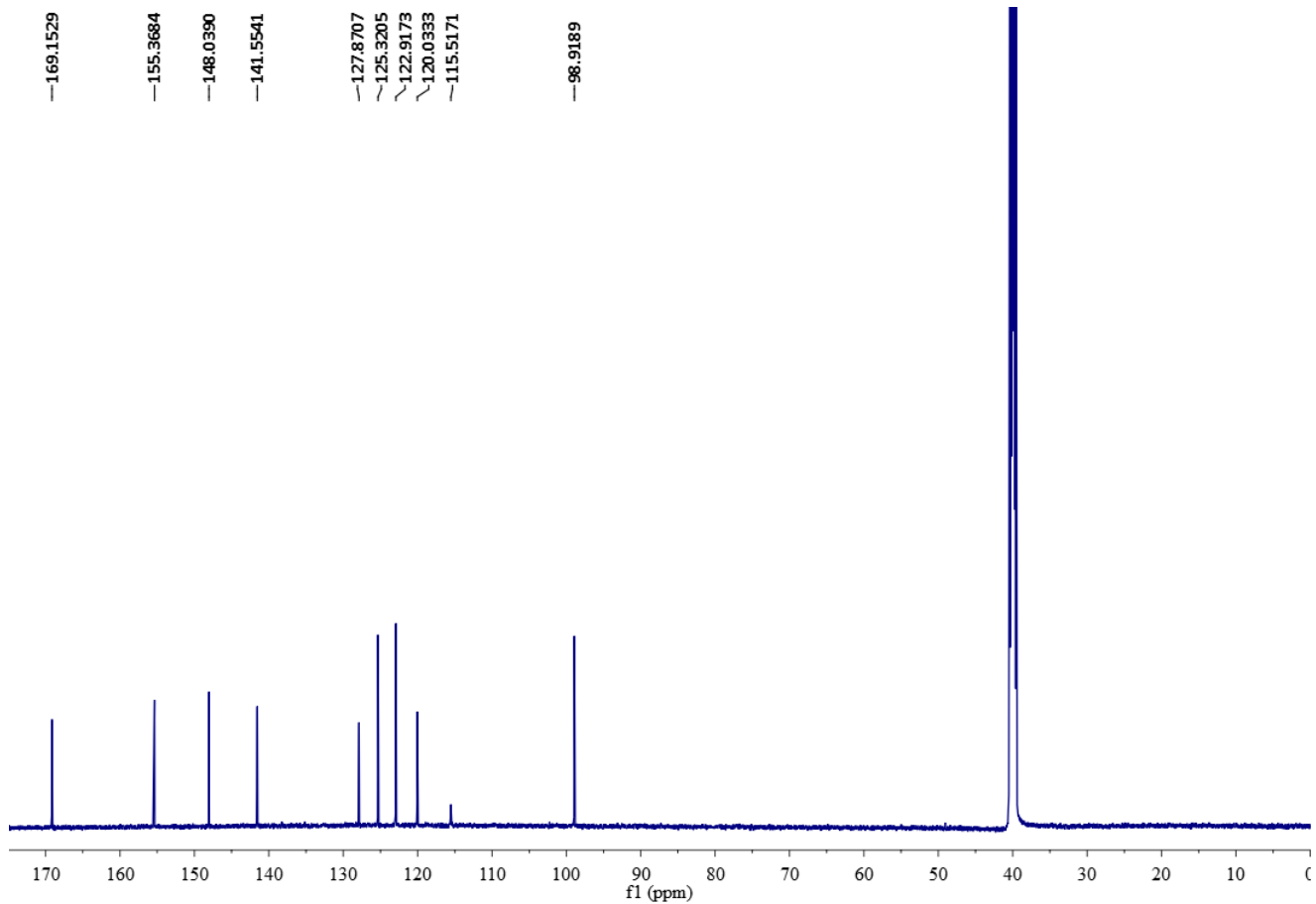


Figure S74. ¹³C NMR spectrum of **10** in DMSO-*d*₆ at 150MHz.

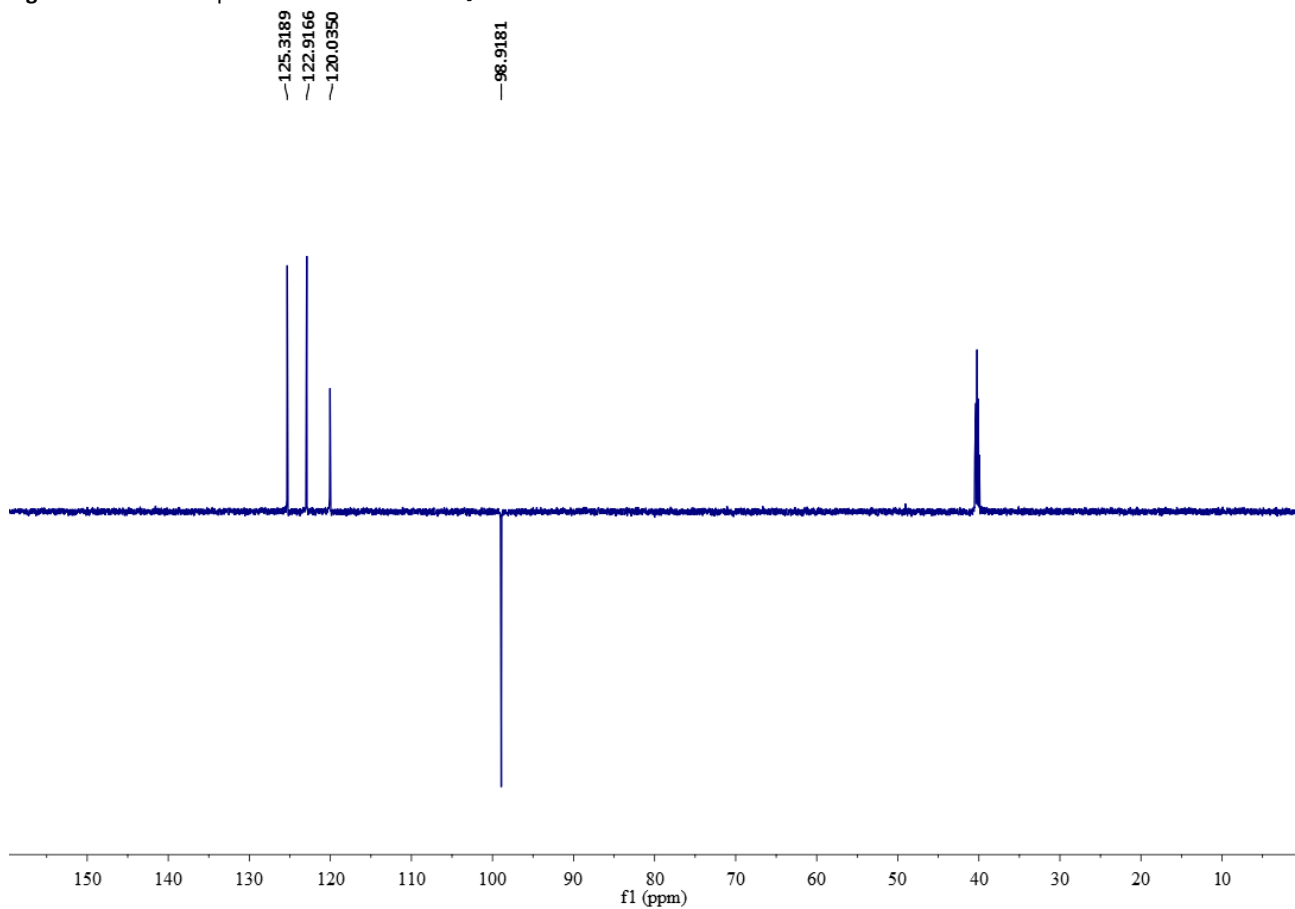


Figure S75. DEPT 135 spectrum of **10** in DMSO-*d*₆.

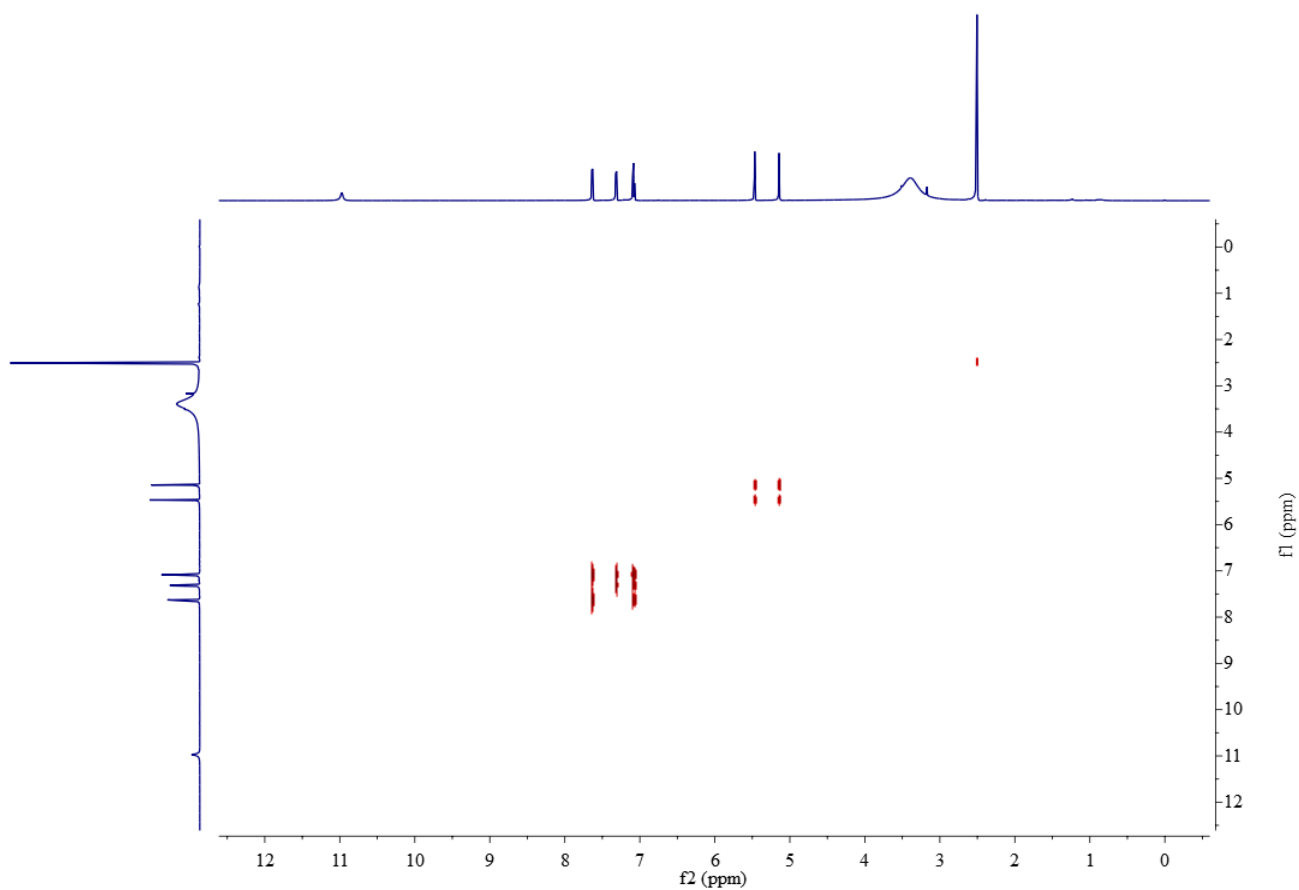


Figure S76. ^1H - ^1H COSY NMR spectrum of **10** in $\text{DMSO-}d_6$.

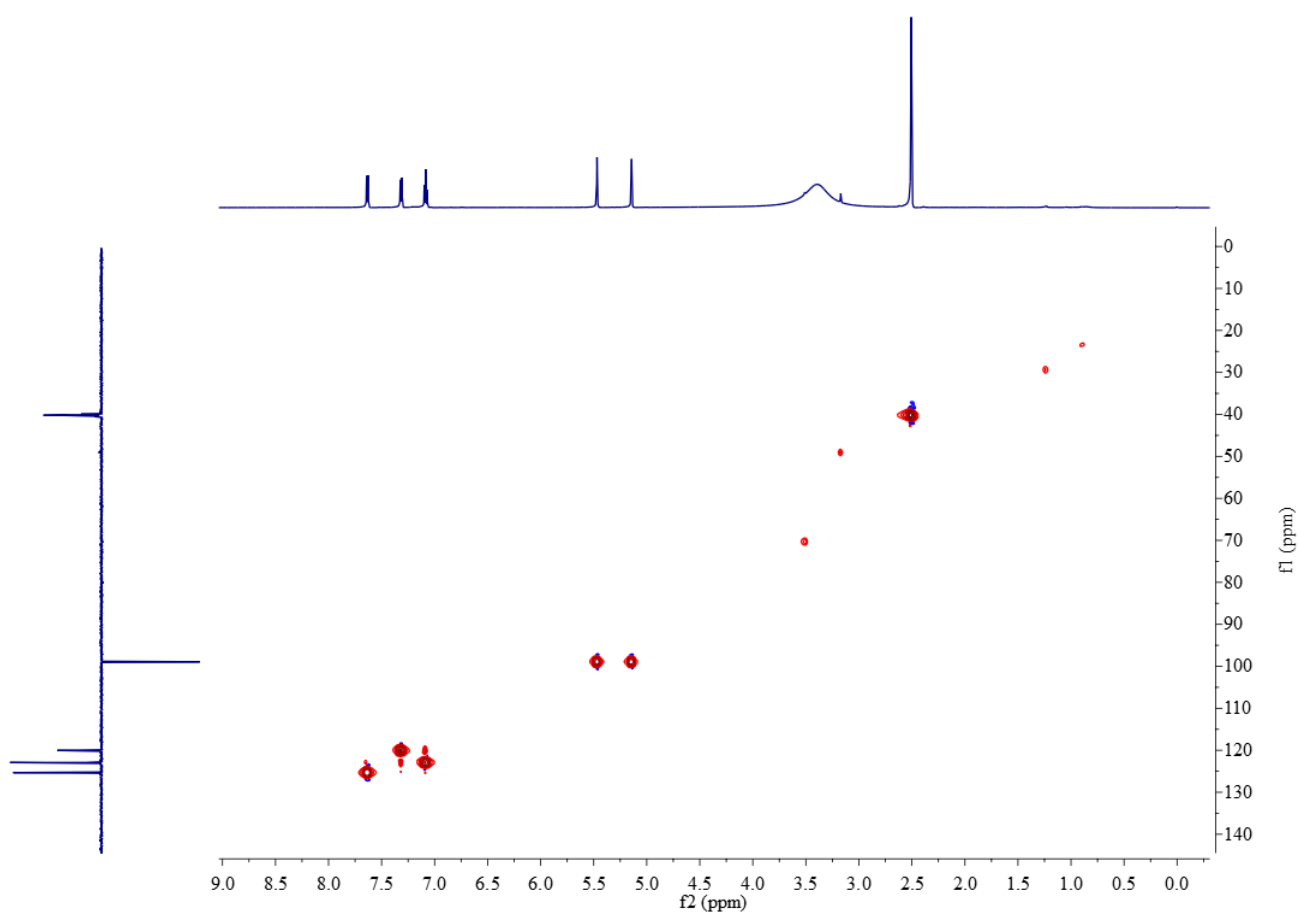


Figure S77. HSQC NMR spectrum of **10** in $\text{DMSO-}d_6$.

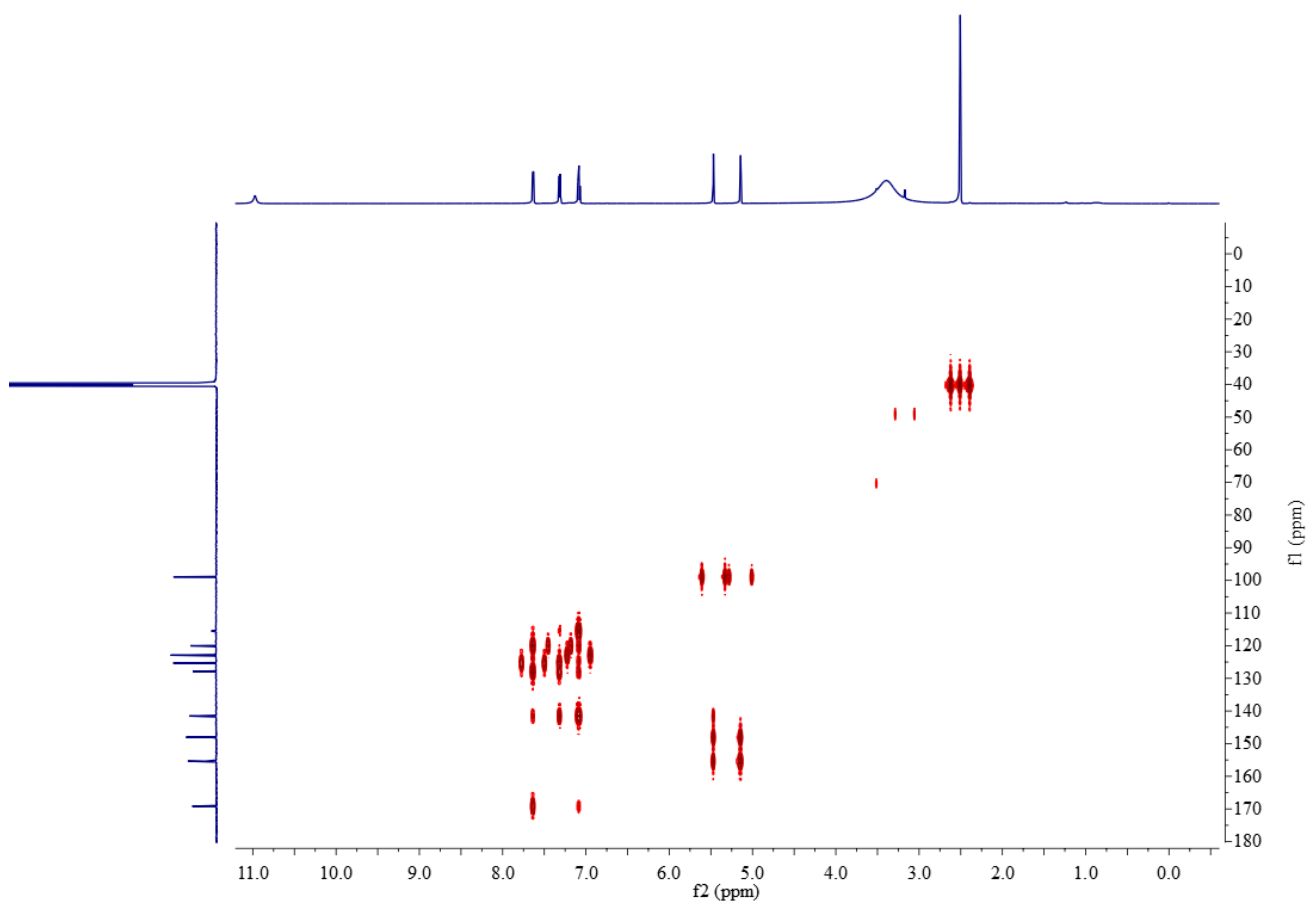


Figure S78. HMBC NMR spectrum of **10** in DMSO- d_6 .

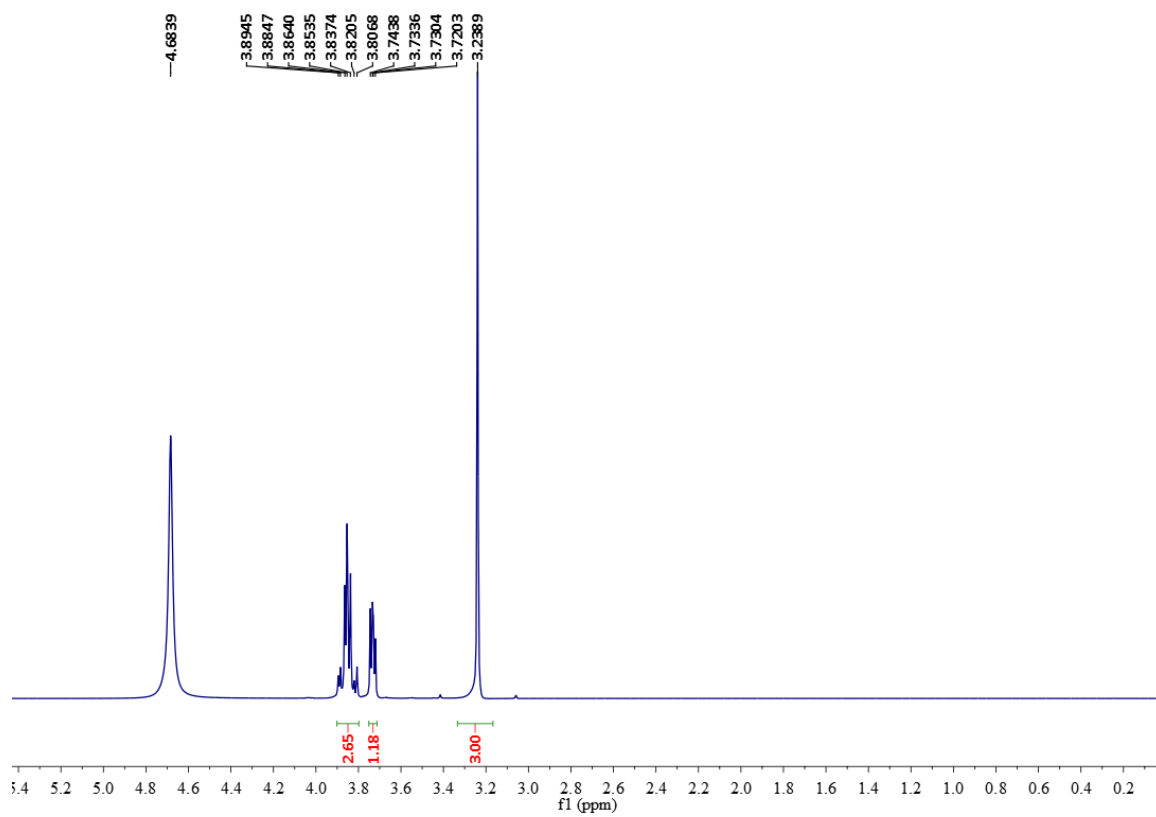


Figure S79. ^1H NMR spectrum of **12** in D_2O at 400 MHz.

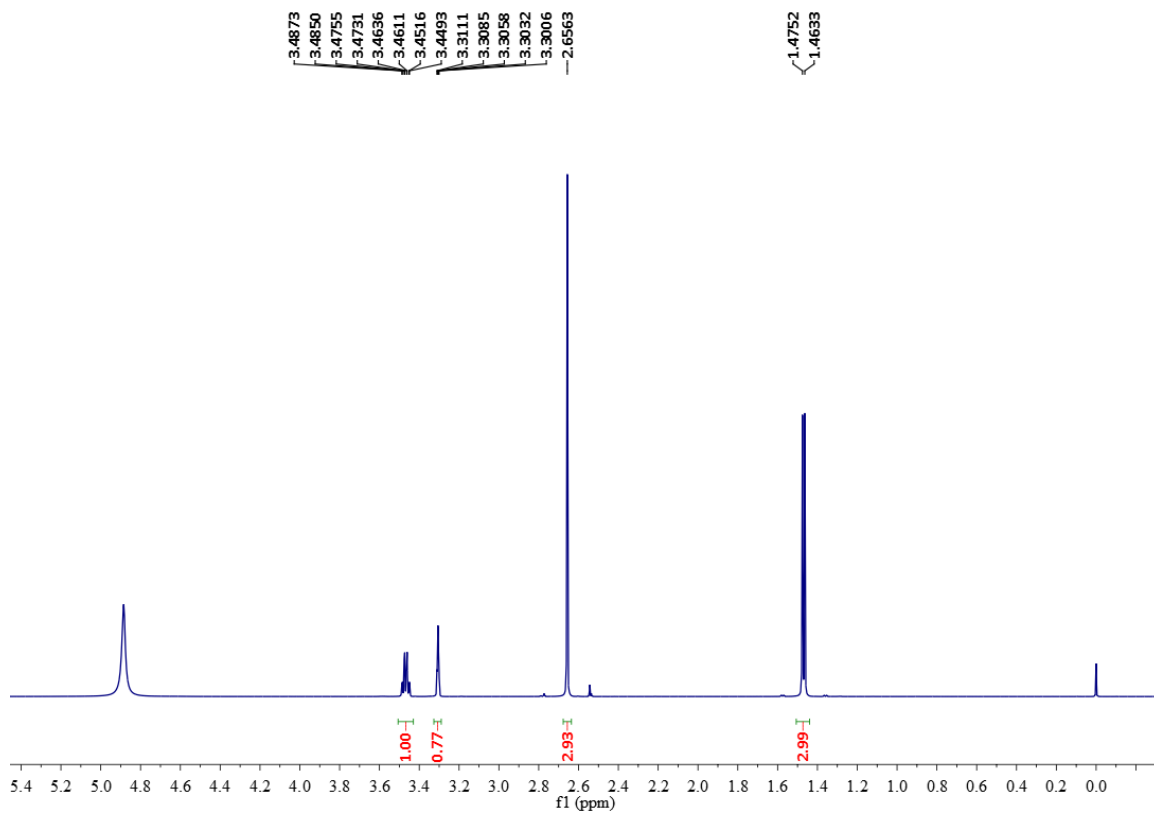


Figure S80. ^1H NMR spectrum of **13** in D_2O at 400 MHz.

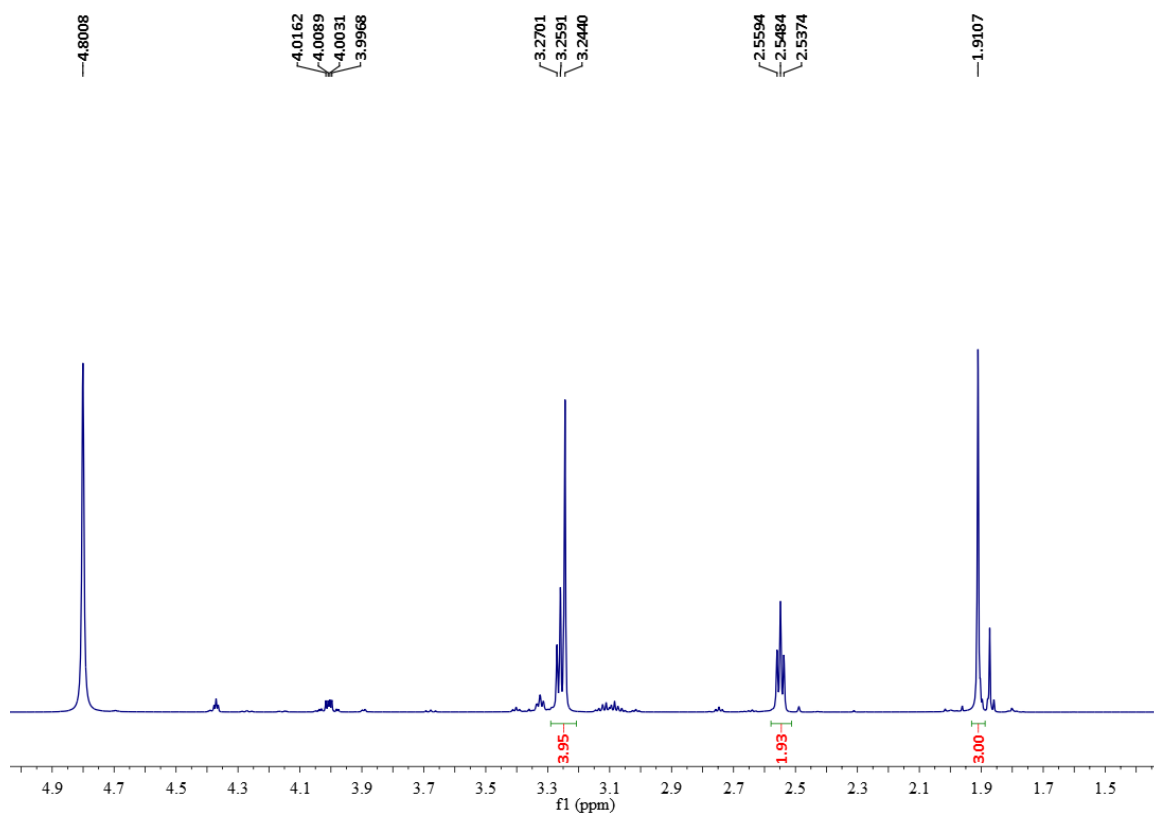


Figure S81. ^1H NMR spectrum of **15** in D_2O at 600 MHz.

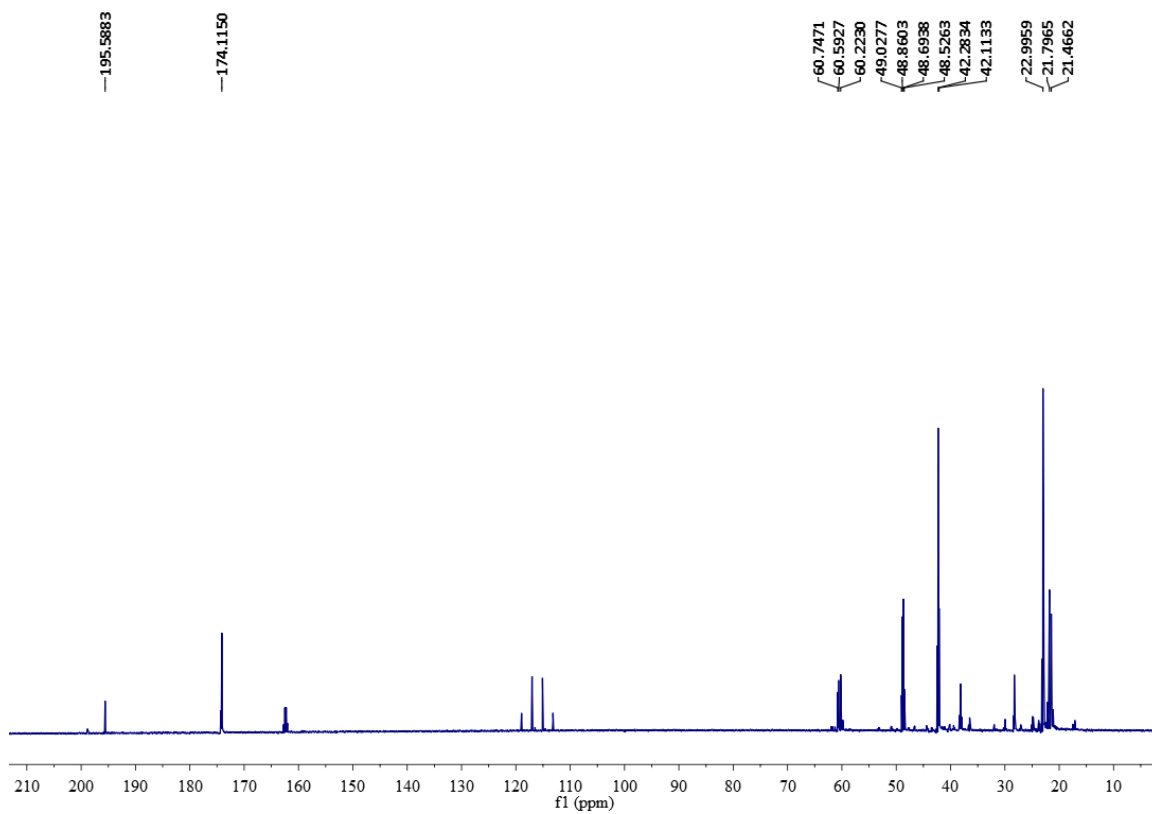


Figure S82. ¹³C NMR spectrum of **15** in D₂O at 150 MHz.

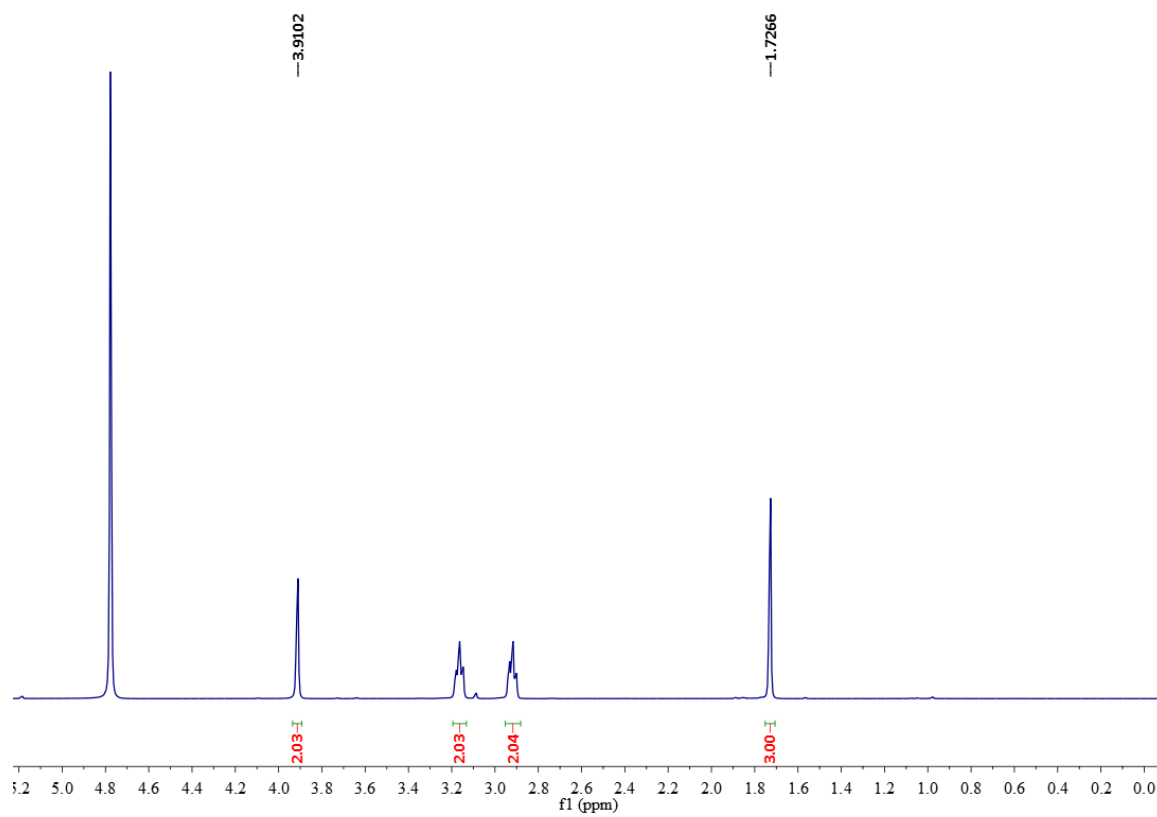


Figure S83. ¹H NMR spectrum of **16** in D₂O at 400 MHz.

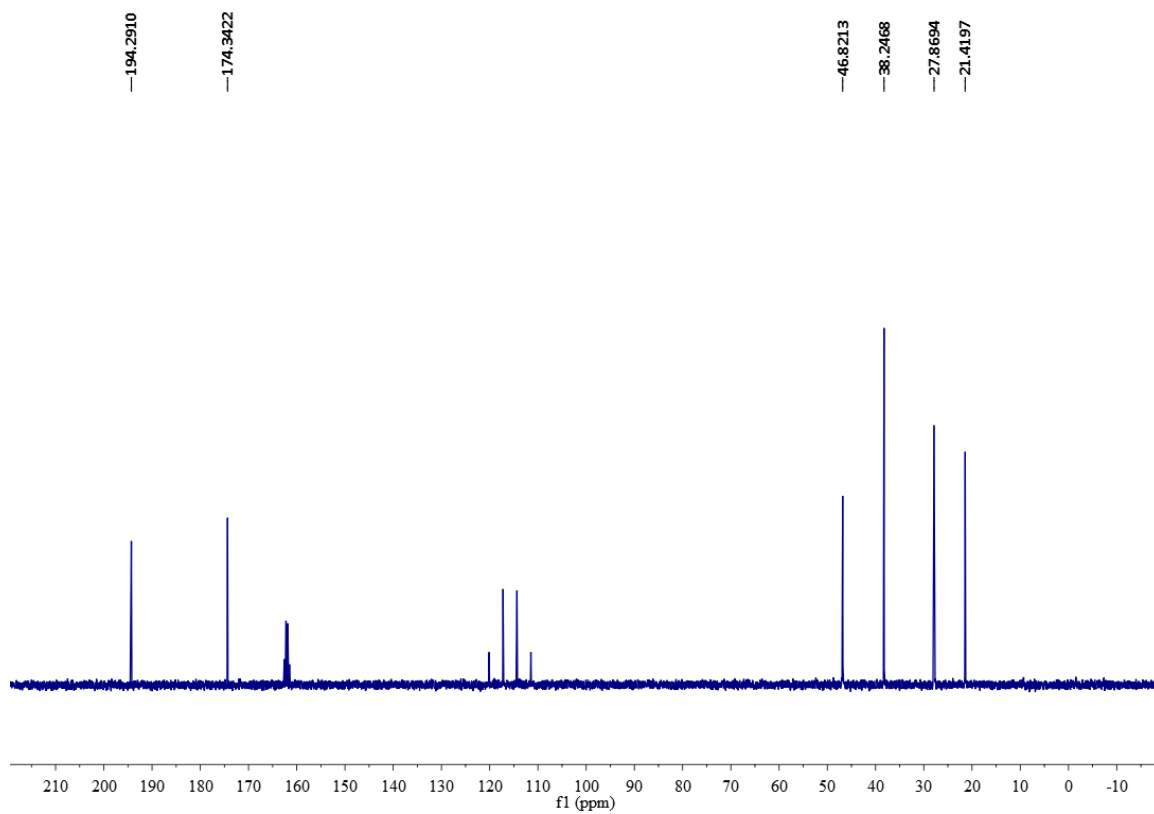


Figure S84. ^{13}C NMR spectrum of **16** in D_2O at 100 MHz.

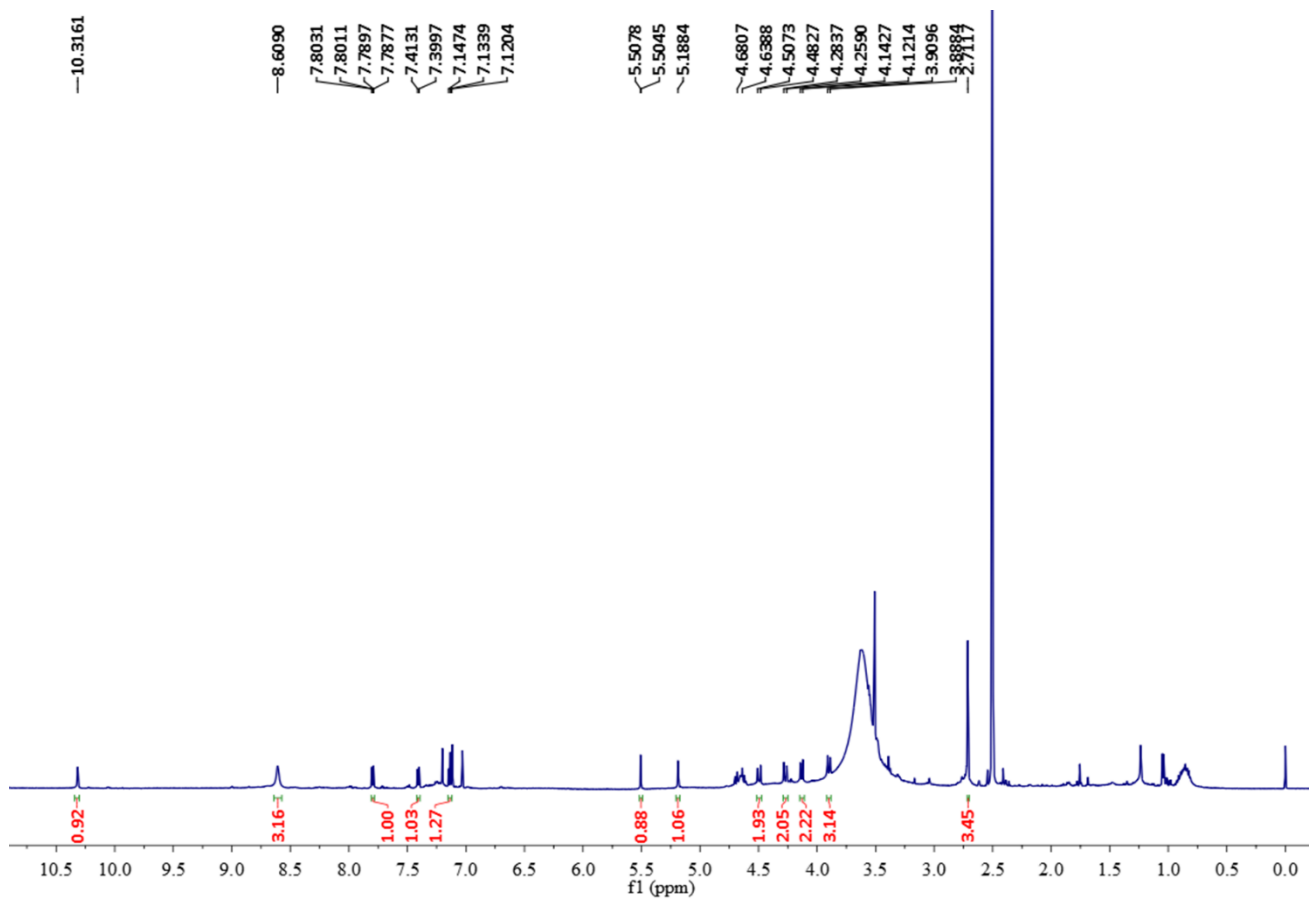


Figure S85. ^1H NMR spectrum of **17** in $\text{DMSO}-d_6$ at 600 MHz.

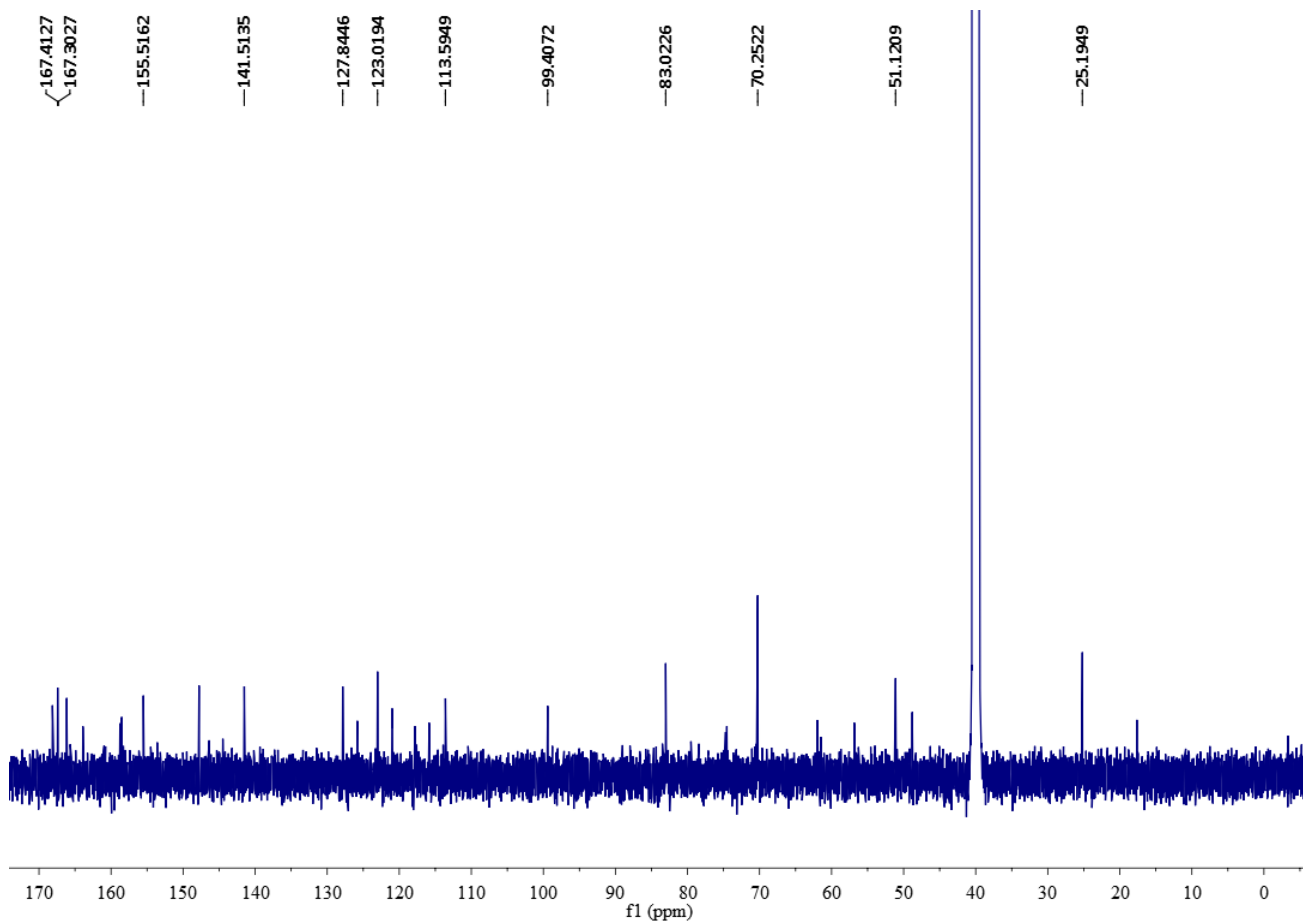


Figure S86. ^{13}C NMR spectrum of **17** in $\text{DMSO-}d_6$ at 150MHz.

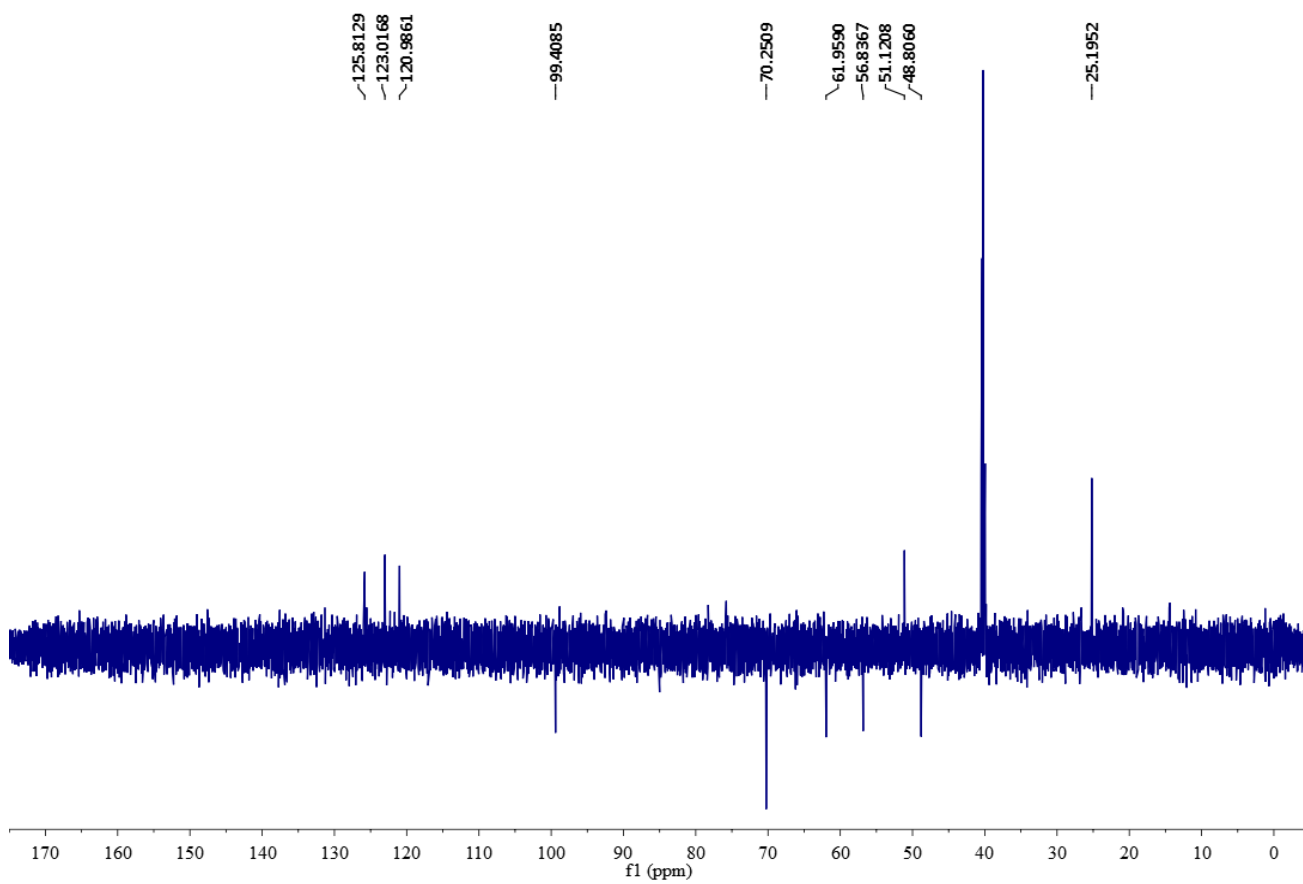


Figure S87. DEPT 135 spectrum of **17** in $\text{DMSO-}d_6$.

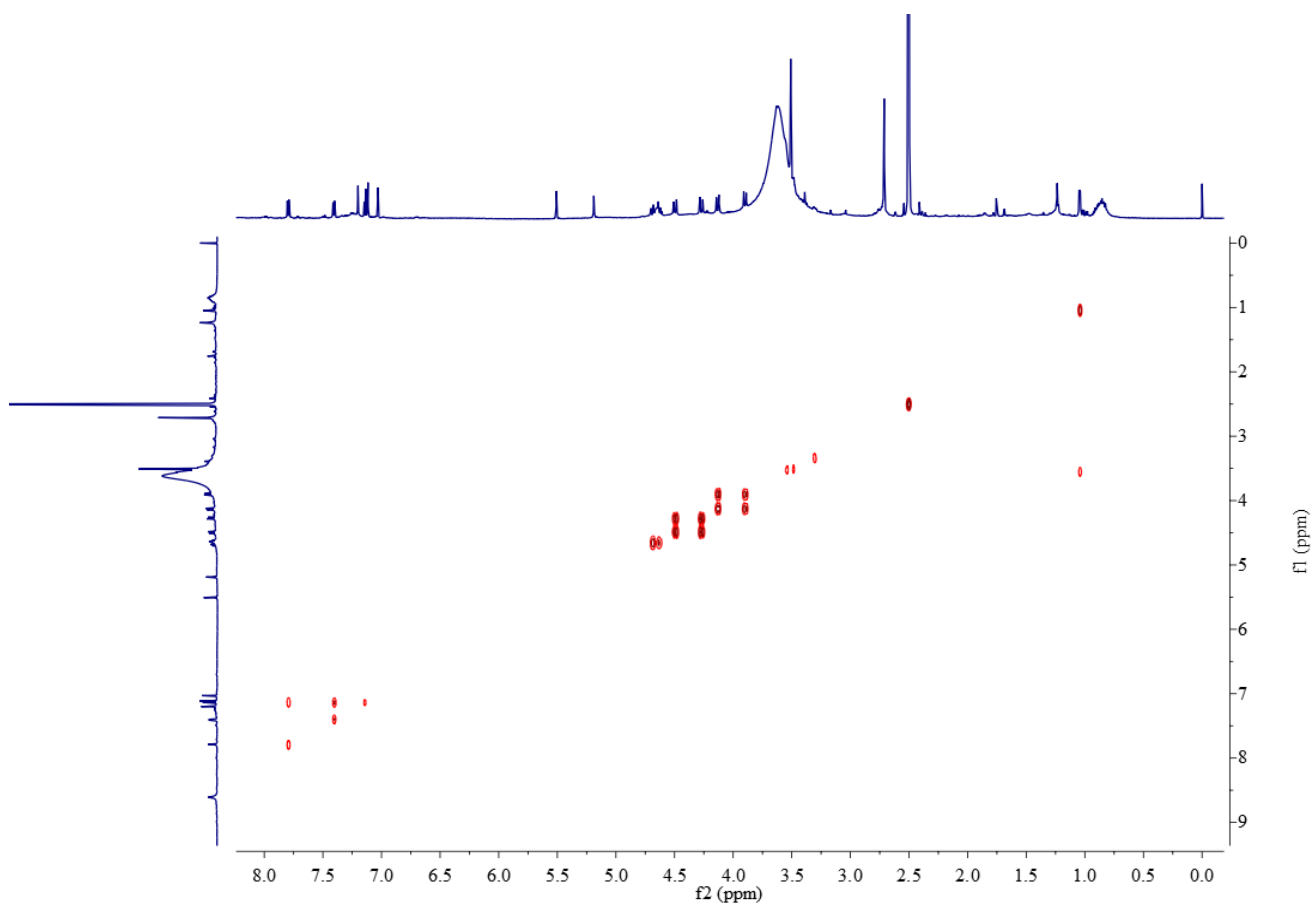


Figure S88. ^1H - ^1H COSY NMR spectrum of **17** in $\text{DMSO-}d_6$.

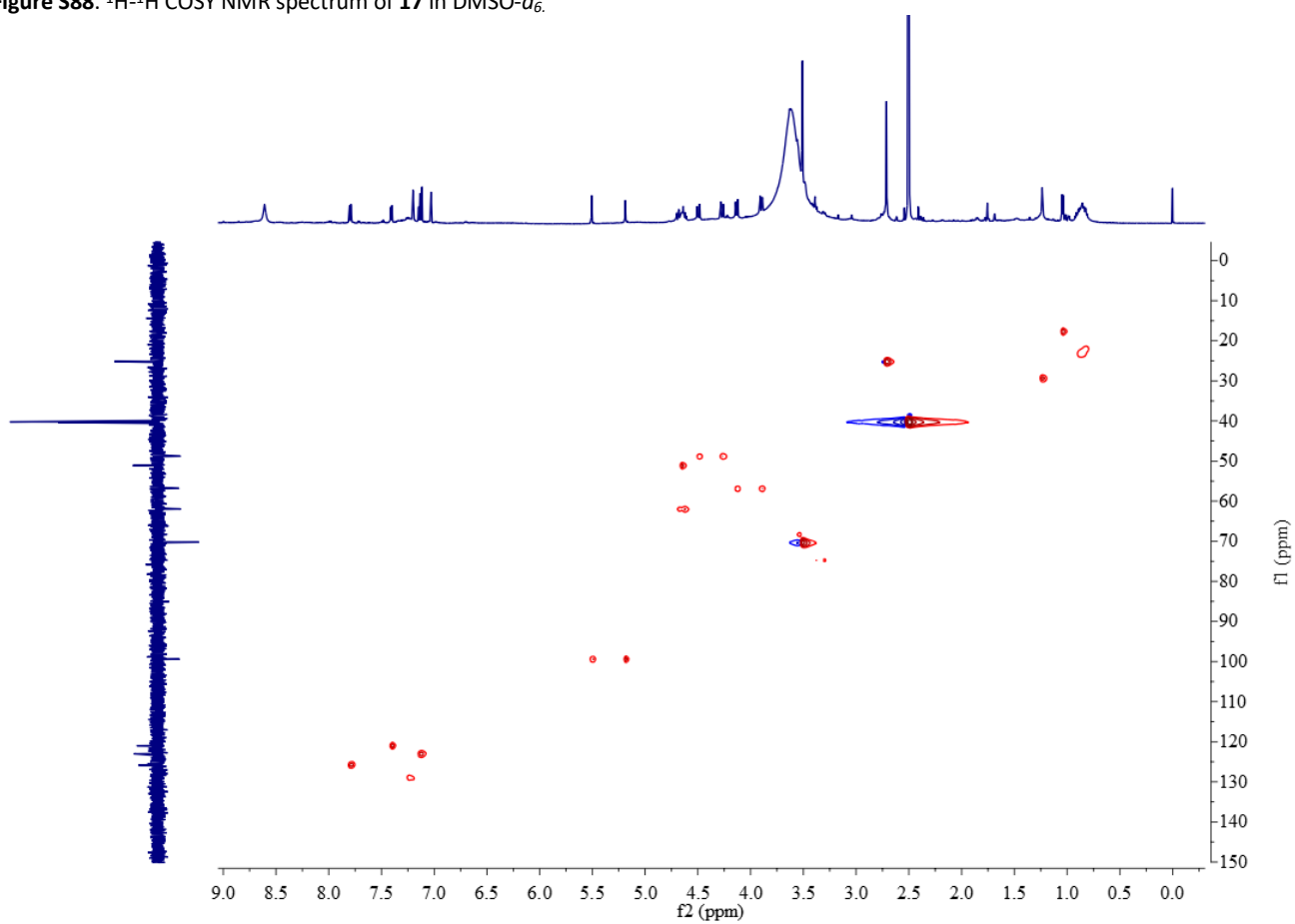


Figure S89. HSQC NMR spectrum of **17** in $\text{DMSO-}d_6$.

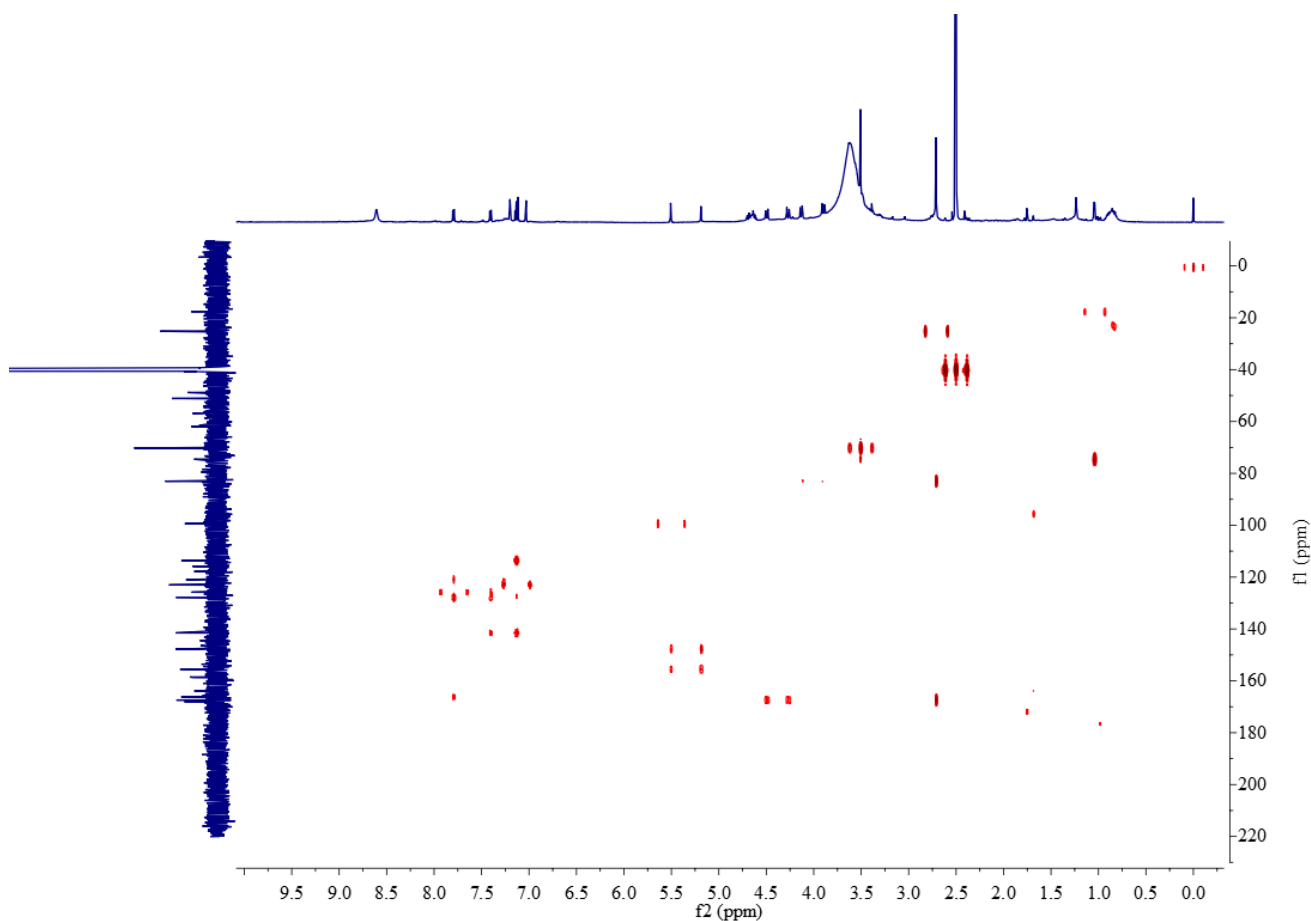


Figure S90. HMBC NMR spectrum of **17** in DMSO- d_6 .

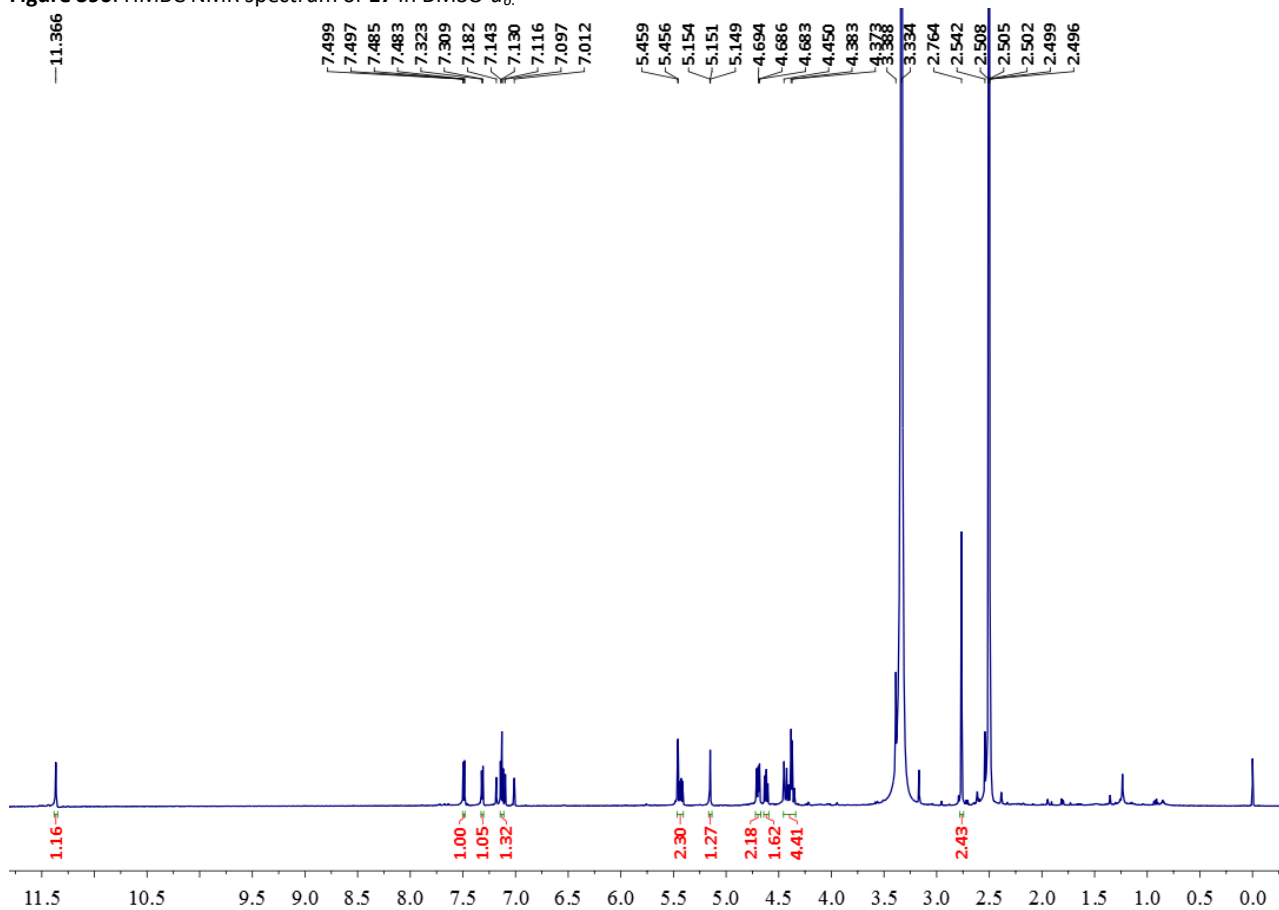


Figure S91. ^1H NMR spectrum of **18** in DMSO- d_6 at 600 MHz.

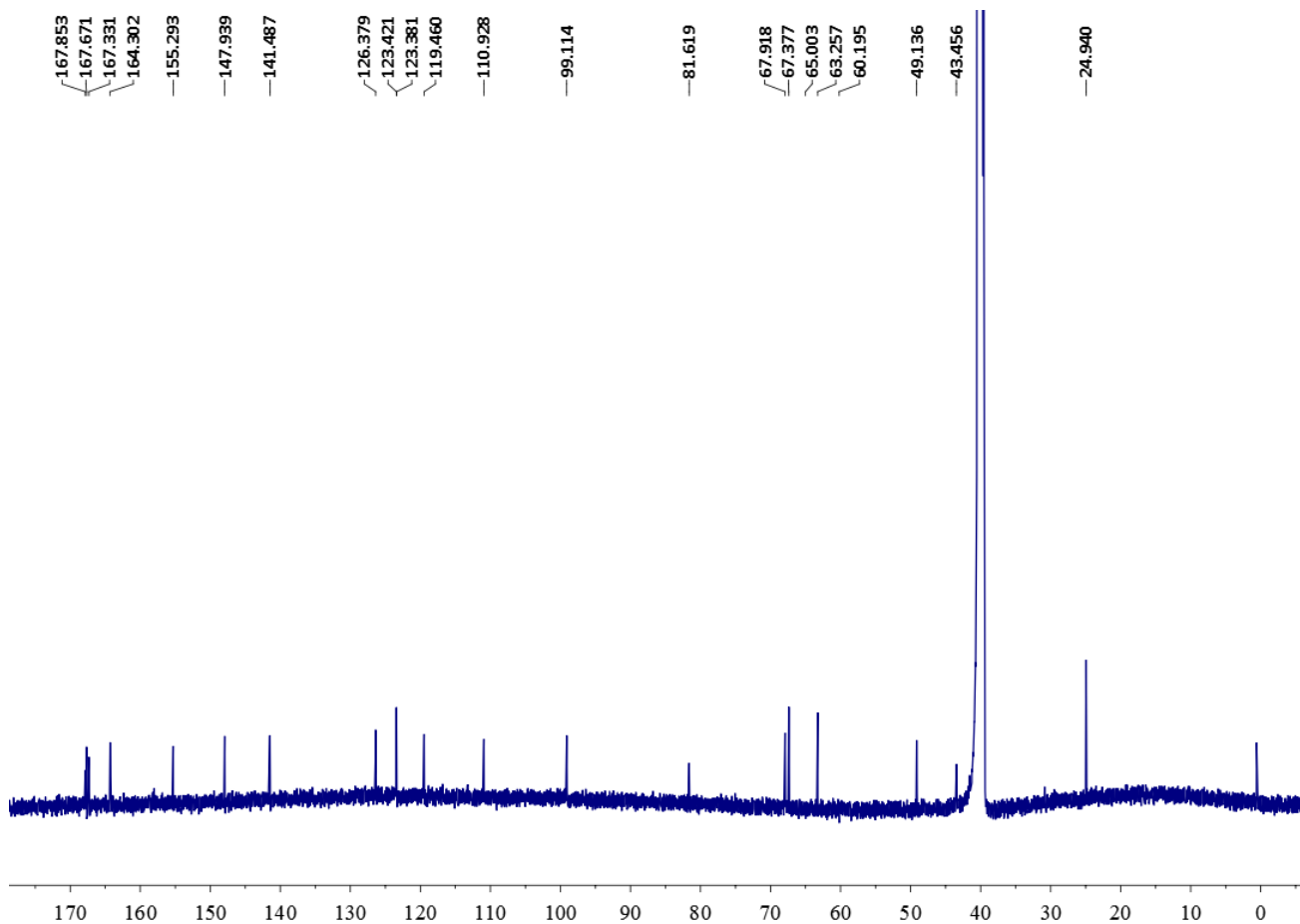


Figure S92. ^{13}C NMR spectrum of **18** in $\text{DMSO-}d_6$ at 150MHz.

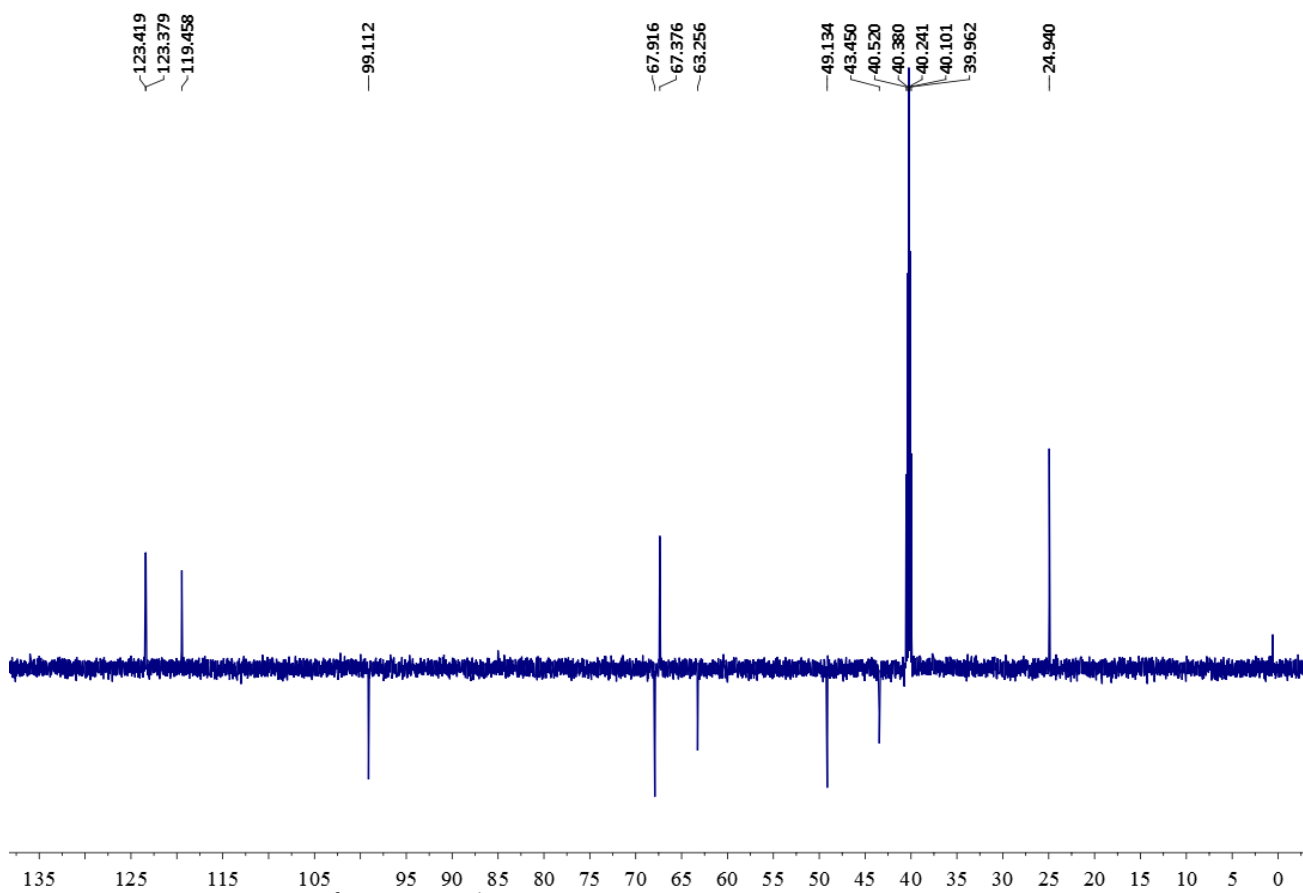


Figure S93. DEPT 135 spectrum of **18** in $\text{DMSO-}d_6$.

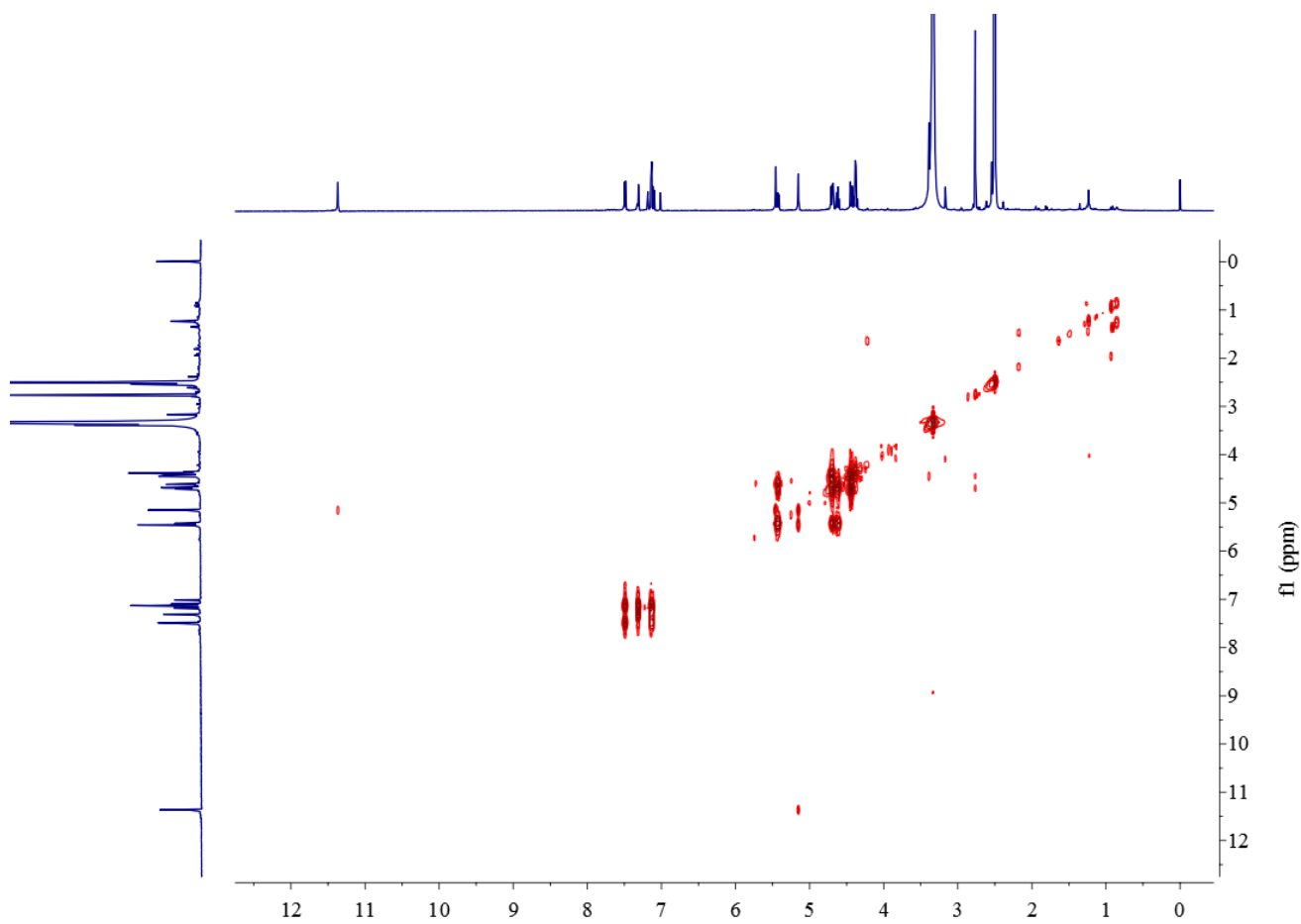


Figure S94. ^1H - ^1H COSY NMR spectrum of **18** in $\text{DMSO-}d_6$.

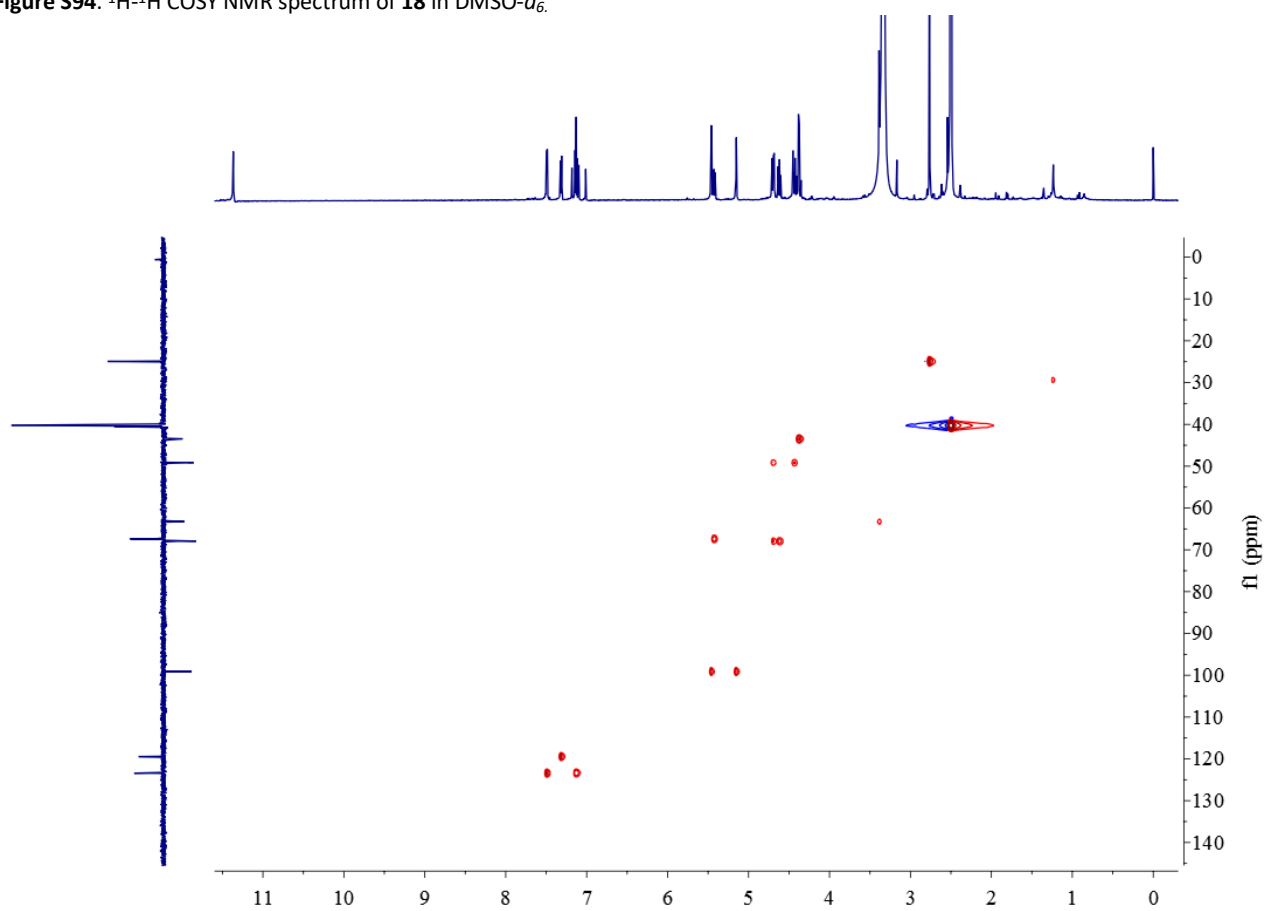


Figure S95. HSQC NMR spectrum of **18** in $\text{DMSO-}d_6$.

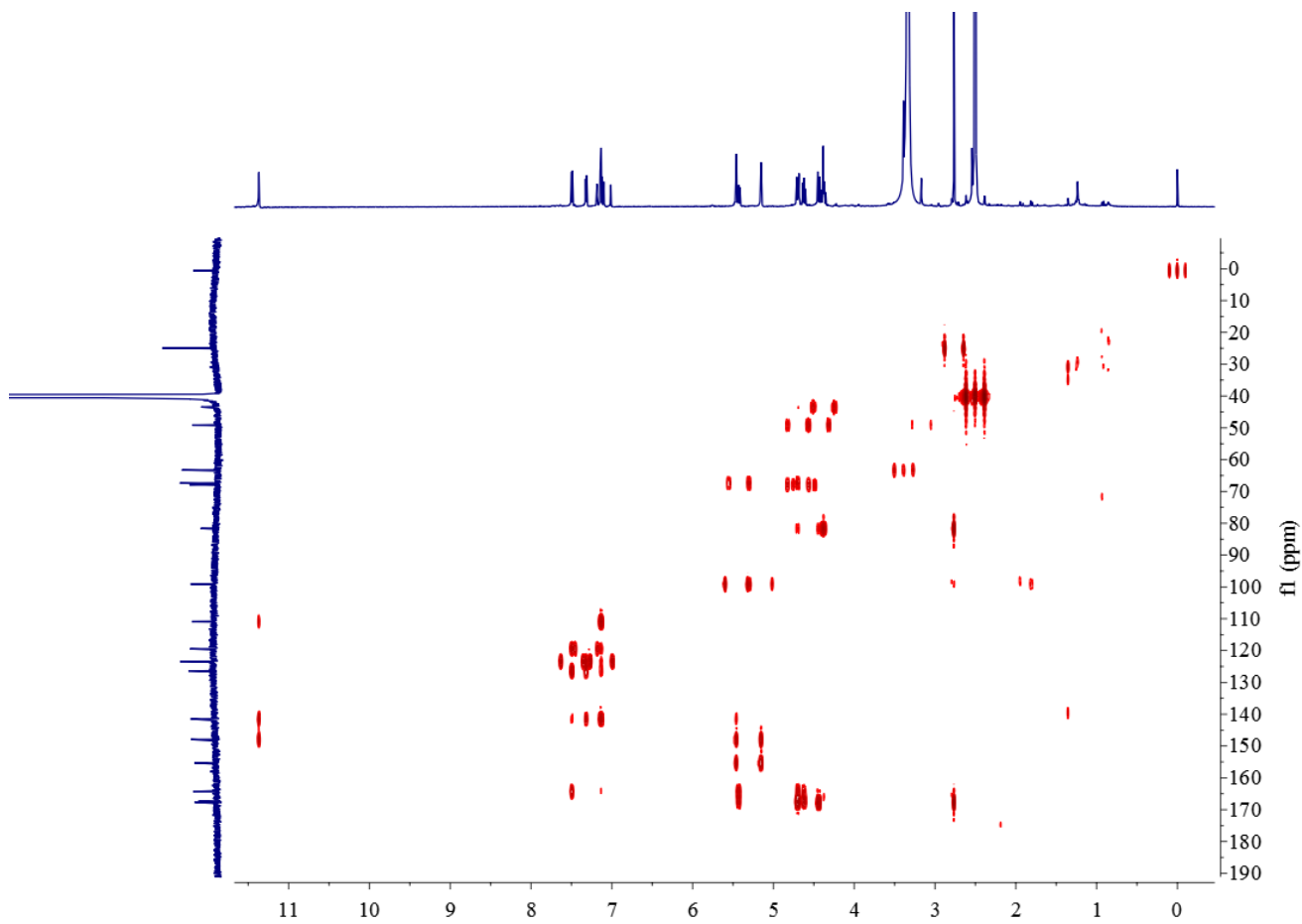


Figure S96. HMBC NMR spectrum of **18** in DMSO- d_6 .

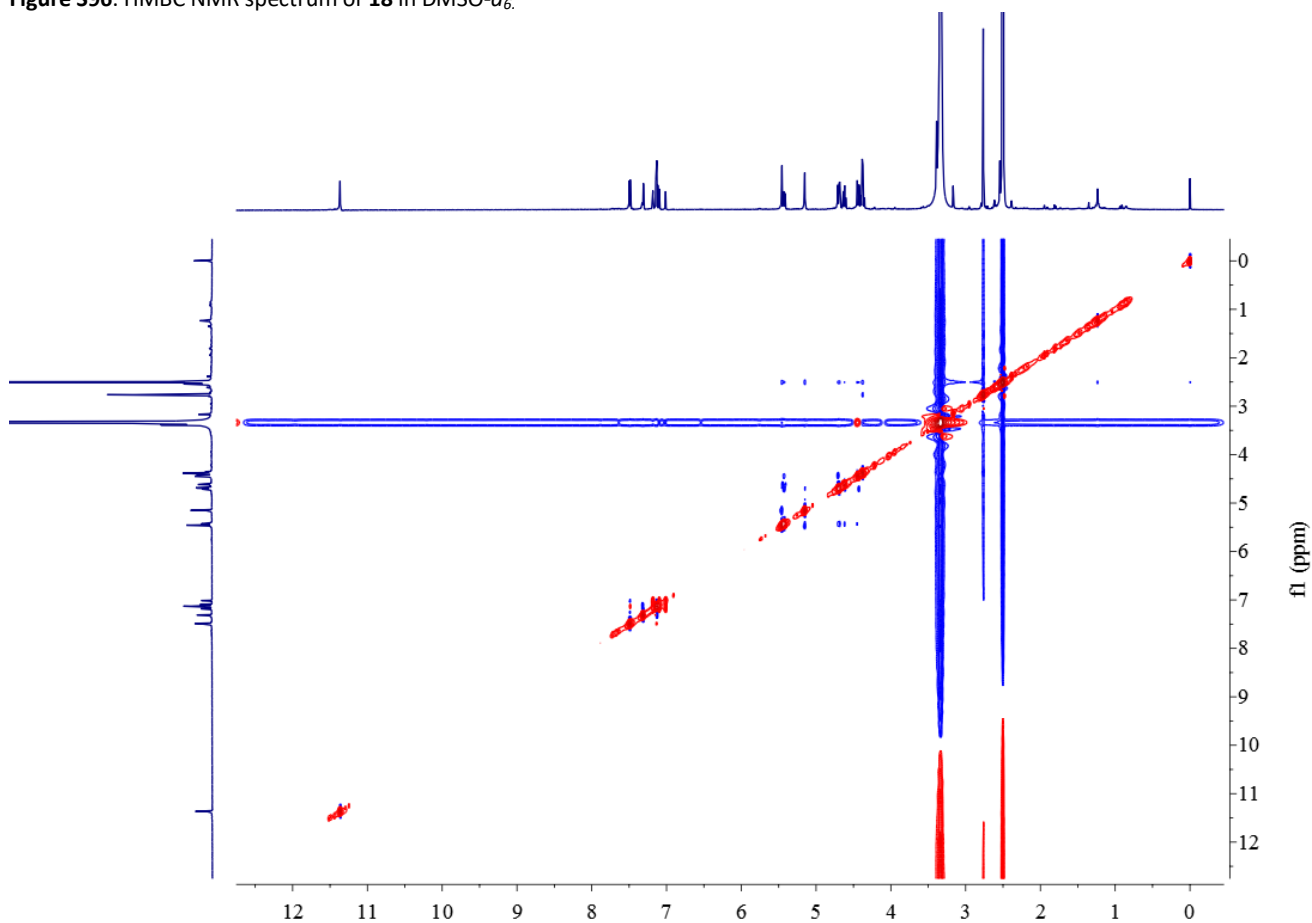


Figure S97. NOESY spectrum of **18** in DMSO- d_6 .

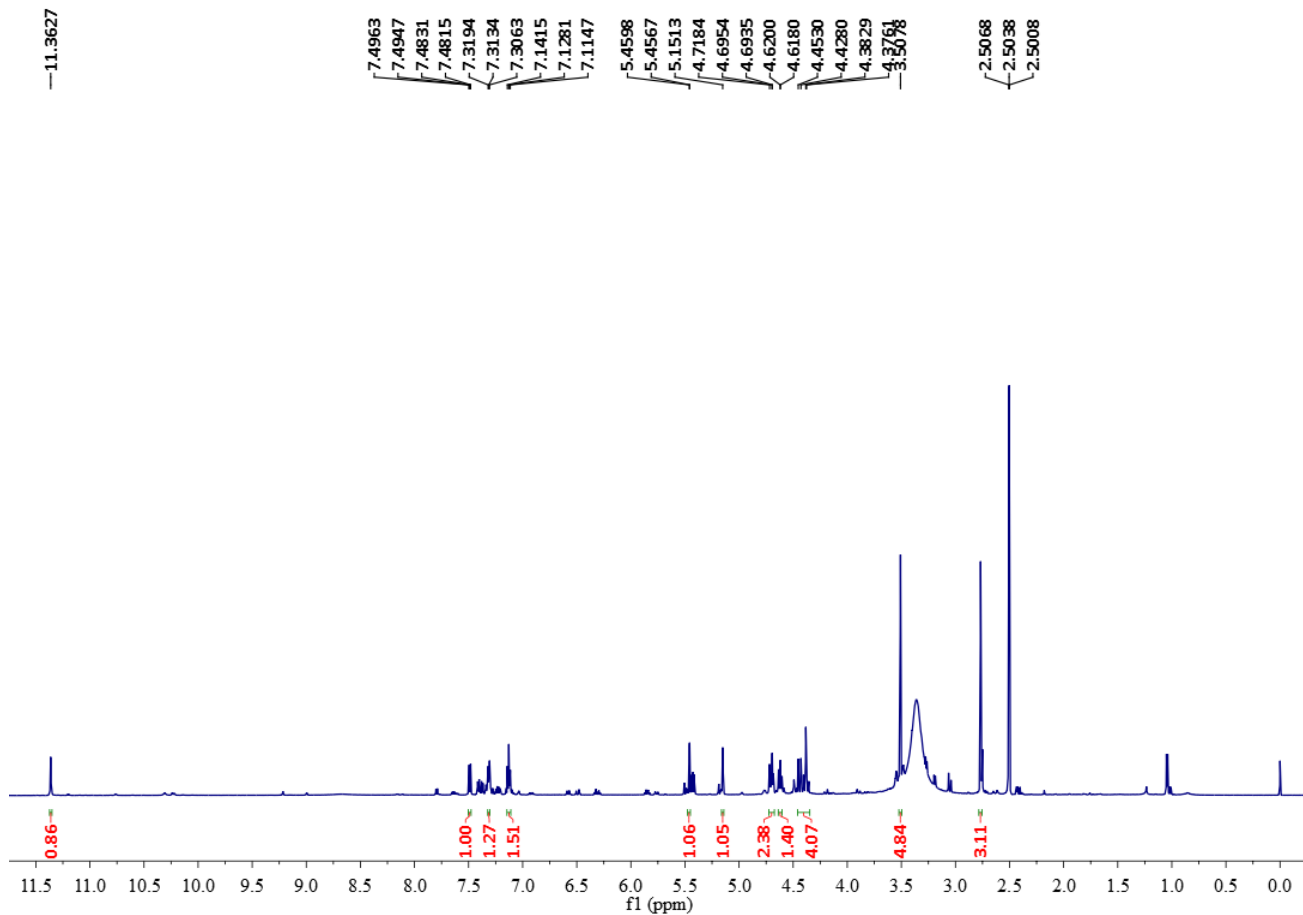


Figure S98. ^1H NMR spectrum of **19** in $\text{DMSO}-d_6$ at 600 MHz.

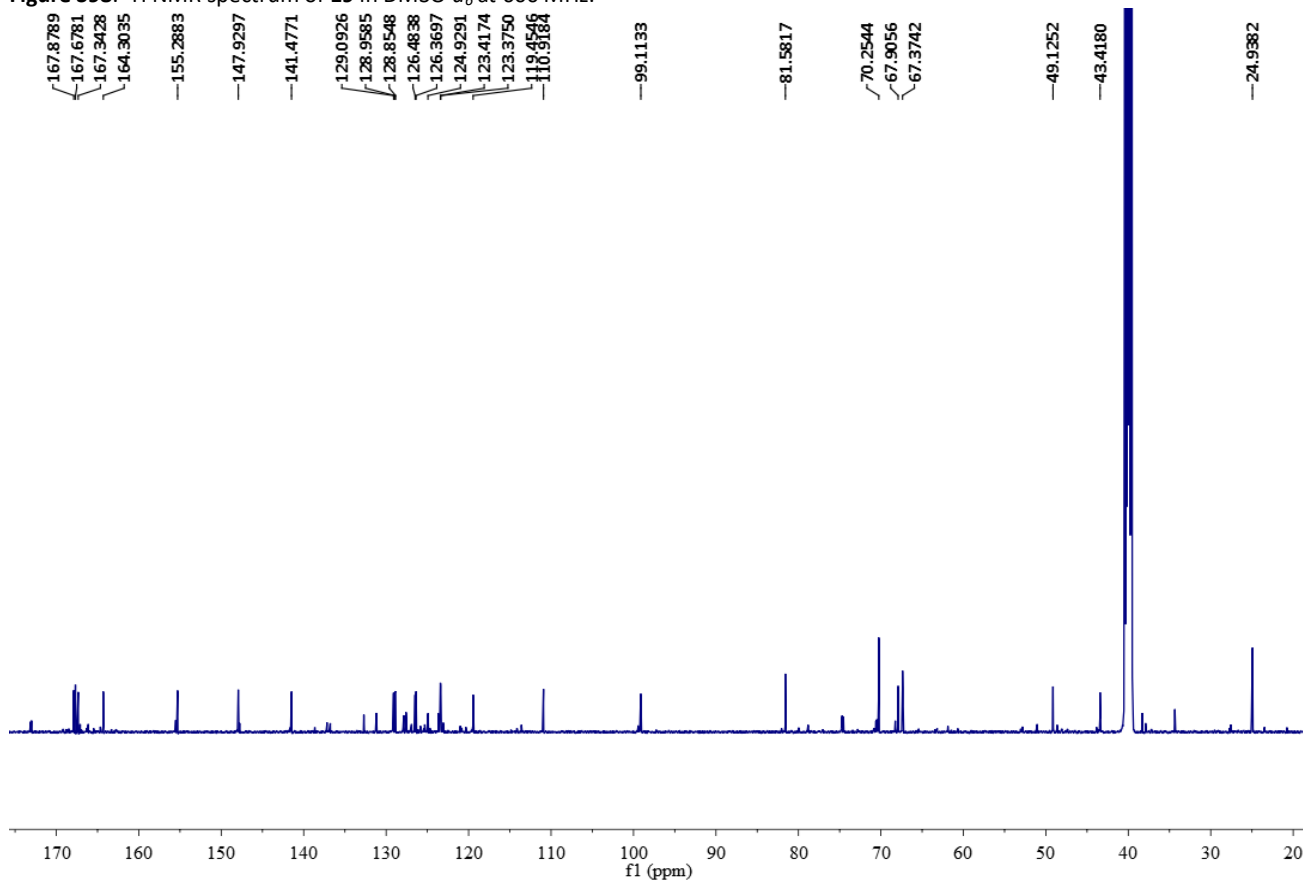


Figure S99. ^{13}C NMR spectrum of **19** in $\text{DMSO}-d_6$ at 150 MHz.

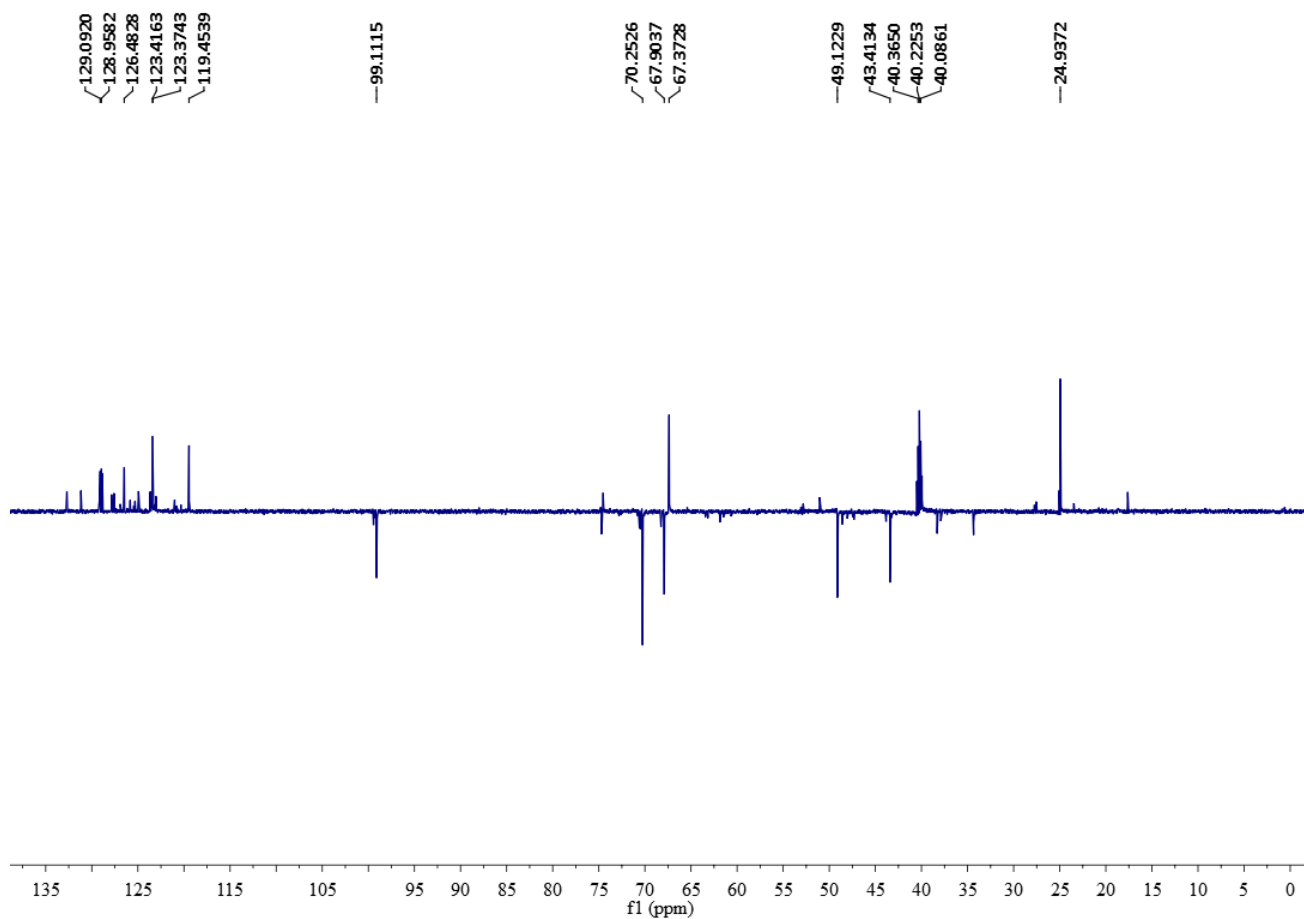


Figure S100. DEPT 135 spectrum of **19** in DMSO- d_6 .

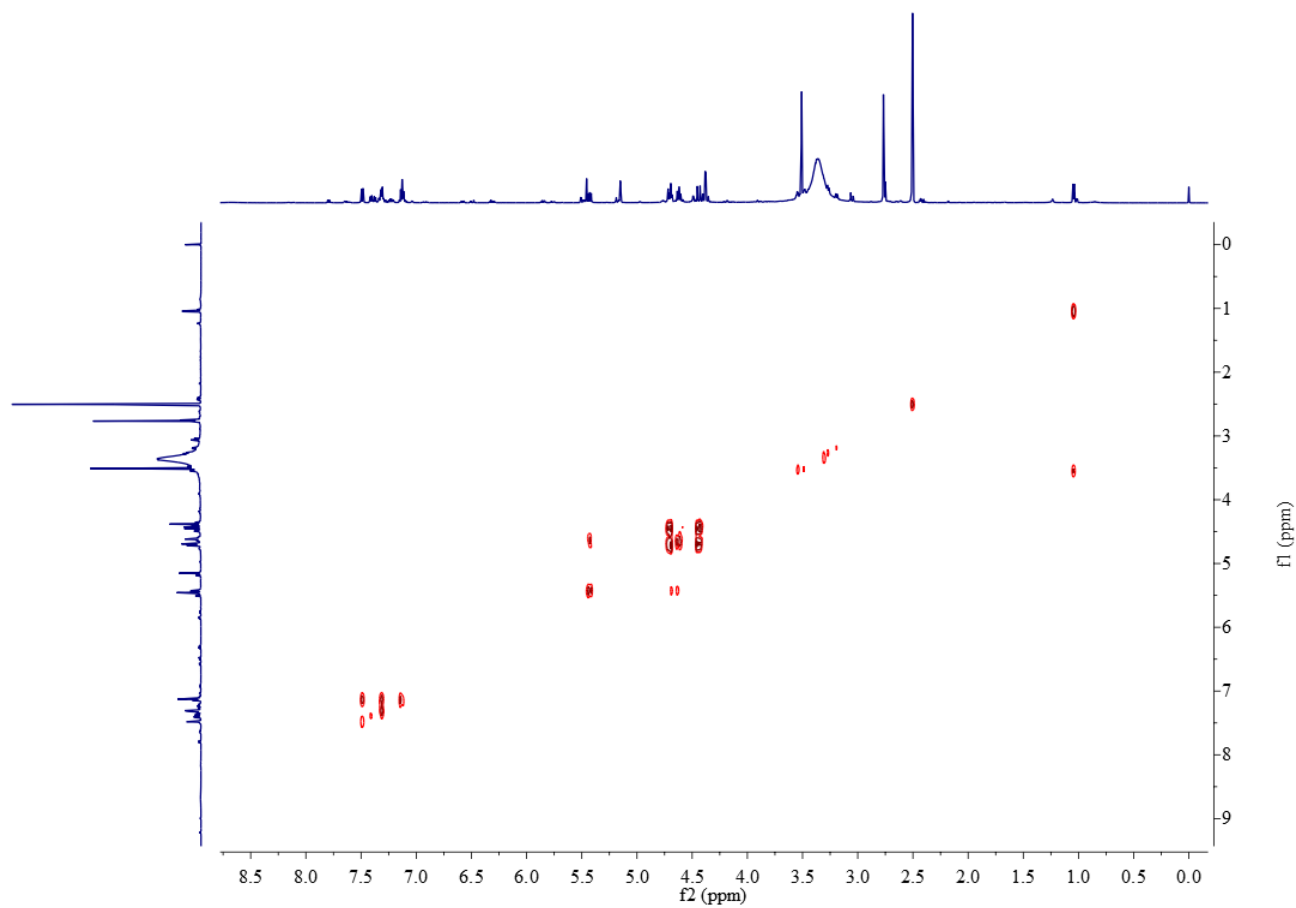


Figure S101. ^1H - ^1H COSY NMR spectrum of **19** in DMSO- d_6 .

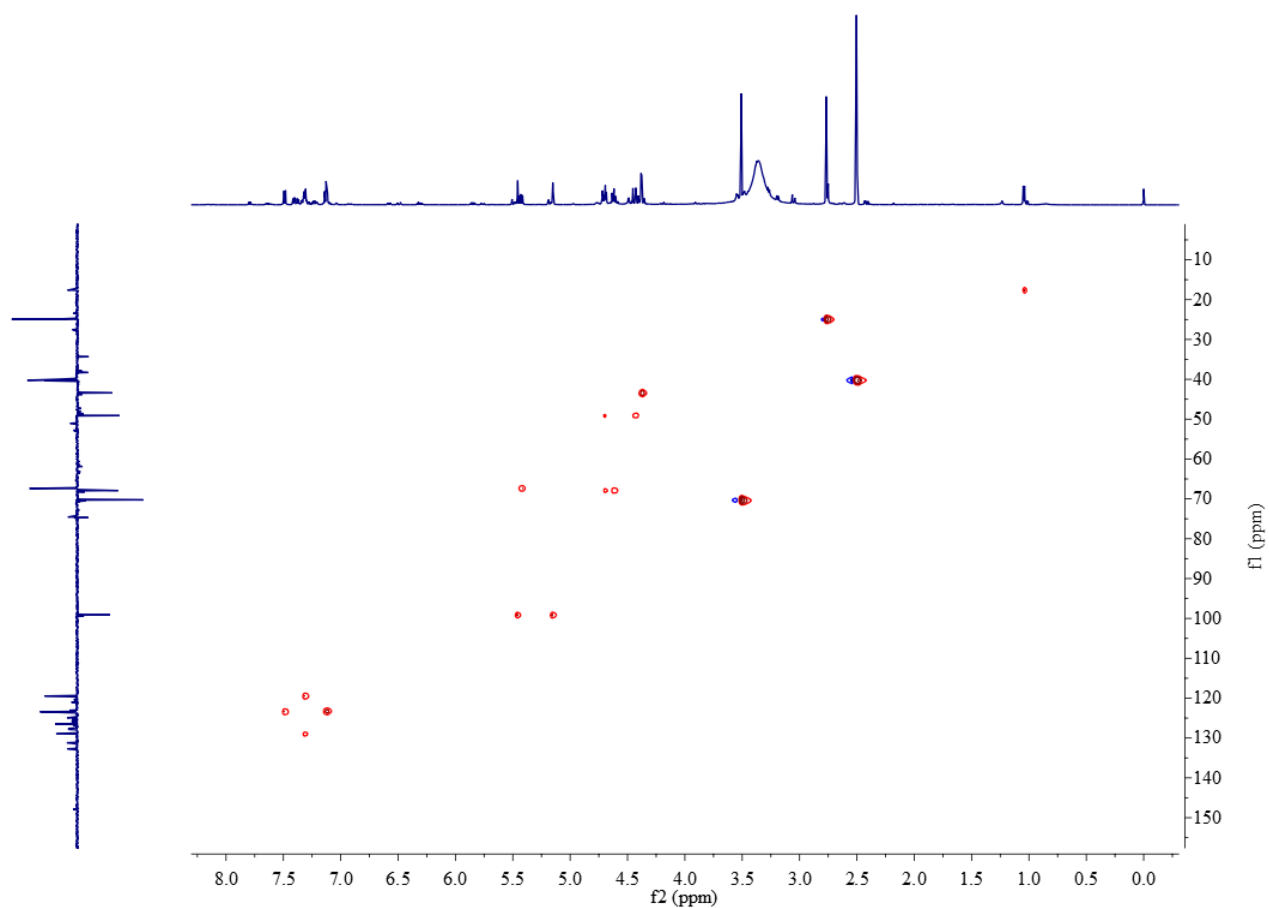


Figure S102. HSQC NMR spectrum of **19** in DMSO- d_6 .

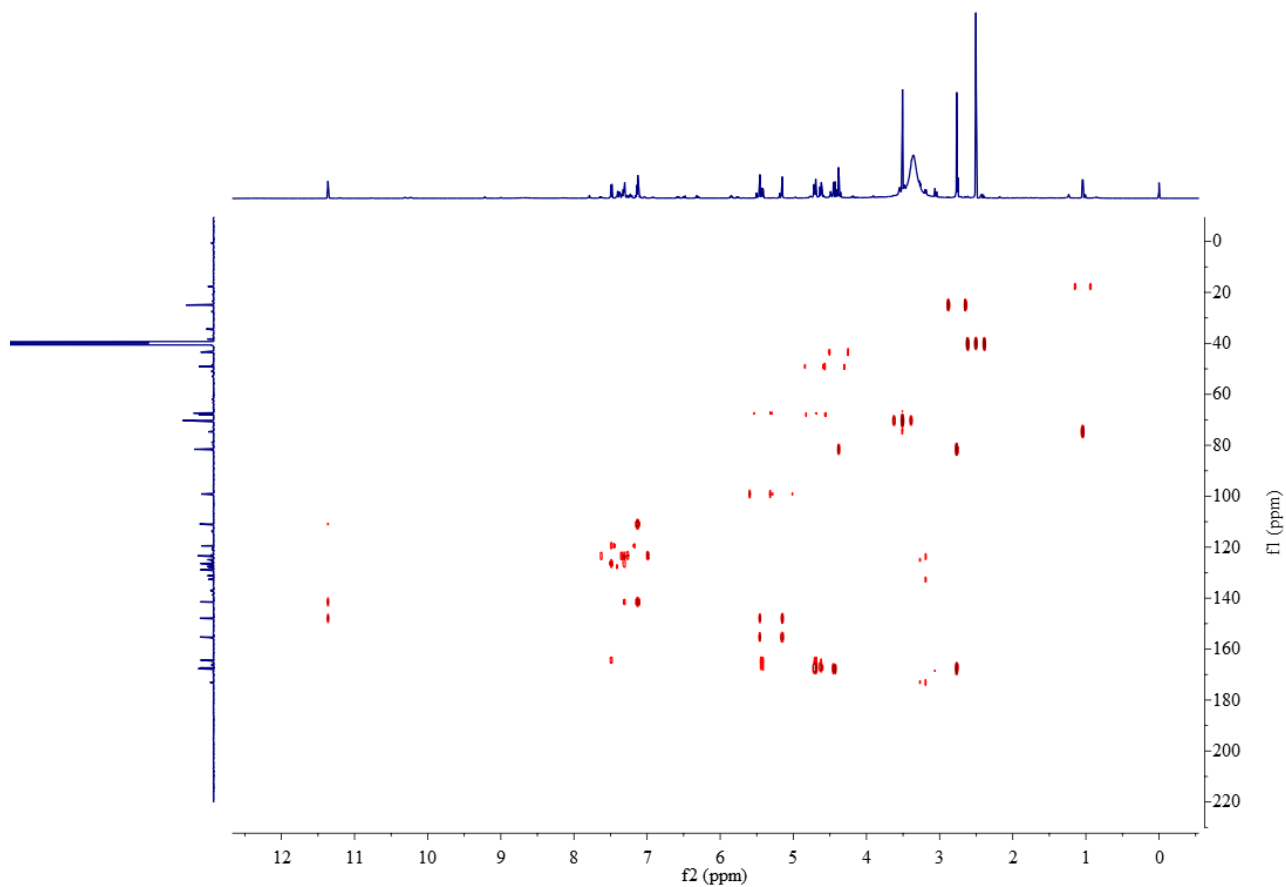


Figure S103. HMBC NMR spectrum of **19** in DMSO- d_6 .

References

- [1] M. Beye, A. Poch, C. Burgtorf, R. F. A. Moritz, H. Lehrach, *Genomics* **1998**, *49*, 317.
- [2] D. A. Hopwood, M. J. Bibb, K. F. Chater, T. Kieser, C. J. Bruton, H. M. Kieser, D. J. Lydiate, C. P. Smith, J. M. Ward, H. Schrempf, *Genetic Manipulation of Streptomyces-A Laboratory Manual*, Cold Spring Harbor Laboratory Press, New York **1985**.
- [3] M. D. Lalioti, J. K. Heath, *Nucleic Acids Res.* **2001**, *29*, 14-19.
- [4] J. Kottur, D. T. Nair, *Nucleic Acids Res.* **2018**, *46*, 5875–5885.
- [5] C. Sanchez, L. C. Du, D. J. Edwards, M. D. Toney, B. Shen, *Chem.Biol.* **2001**, *8*, 725-738.
- [6] S. G. Van Lanen, P. C. Dorrestein, S. D. Christenson, W. Liu, J. Ju, N. L. Kelleher, B. Shen, *J. Am. Chem. Soc.* **2005**, *127*, 11594-11595.
- [7] Y. Ling, X. Ye, H. Ji, Y. Zhang, Y. Lai, S. Peng, J. Tian, *Bioorg. Med. Chem.* **2010**, *18*, 3448–3456.
- [8] K. M. J. de Mattos-Shiple, C. Greco, D. M. Heard, G. Hough, N. P. Mulholland, J. L. Vincent, J. Micklefield, T. J. Simpson, C. L. Willis, R. J. Cox, A. M. Bailey, *Chem. Sci.*, **2018**, *9*, 4109–4117.
- [9] R. Fransson, A. N. McCracken, B. Chen, R. J. McMonigle, A. L. Edinger, S. Hanessian, *ACS Med. Chem. Lett.* **2013**, *4*, 969–973.
- [10] N. S. Guntaka, A. R. Healy, J. M. Crawford, S. B. Herzon, S. D. Bruner, *ACS Chem. Biol.* **2017**, *12*, 2598-2608.
- [11] L. Li, Z. Xu, J. Wu, Y. Zhang, X. He, T. M. Zabriskie, Z. Deng, *Chembiochem.* **2008**, *9*, 1286–1294.
- [12] M. D. Lalioti, J. K. Heath, *Nucleic Acids Res.* **2001**, *29*, e14.
- [13] A. M. A. Imam, G. P. Patrinos, M. de Krom, S. Bottardi, R. J. Janssens, E. Katsantoni, A. W. K. Wai, D. J. Sherratt, F. G. Grosveld, *Nuc. Acids Res.* **2000**, *28*, e65.
- [14] M.R. Green, J. Sambrook, *Molecular Cloning: A Laboratory Manual 4th edn* (Cold Spring Harbor Laboratory Press, **2012**).
- [15] M. Bierman, R. Logan, K. O'Brien, E. T. Seno, R. N. Rao, B. E. Schoner, *Gene* **1992**, *116*, 43–49.
- [16] Z. Zhao, T. Shi, M. Xu, N. L. Brock, Y. L. Zhao, Y. Wang, Z. Deng, X. Pang, M. Tao, *Org. Lett.* **2016**, *18*, 572–575.
- [17] M. Röttig, M. H. Medema, K. Blin, T. Weber, C. Rausch, O. Kohlbacher, *Nucleic Acids Res.* **2011**, *39*, 362–367.
- [18] P. J. Large, D. Peel, J. R. Quayle, *Biochem. J.* **1962**, *82*, 483–488.
- [19] S. G. Van Lanen, S. Lin, B. Shen, *Proc. Natl. Acad. Sci. USA.* **2008**, *105*, 494–499.
- [20] A. Ichiyama, *Proc. Jpn. Acad.*, **2011**, *87*, 274–286.